Bulletin 42

POLYPHASE METAMORPHISM

In the Canadian Shield of Northeastern Alberta

C.W. Langenberg
and
P.A. Nielsen

Alberta Geological Survey

Alberta
RESEARCH COUNCIL

Bulletin 42

POLYPHASE METAMORPHISM

In the Canadian Shield of Northeastern Alberta

C.W. Langenberg
and
P.A. Nielsen

Alberta Research Council
1982

PREFACE

The Canadian Shield of northeastern Alberta is a potential area for economic mineral deposits. For this reason, the Alberta Geological Survey conducts geological studies in this area. Knowledge about the conditions under which these complex rocks were formed is essential. In this publication, temperatures and pressures of formation of the rocks are presented. Based on these data, a theory about the genesis of these rocks is proposed.

ACKNOWLEDGMENTS

This study was suggested by Dr. J.D. Godfrey and we would like to express our appreciation for his encouragement and stimulating discussions. Drs. J. Krupička, R. St. J. Lambert, R.A. Burwash, and G.D. Mossop read the manuscript and suggested several improvements. The microprobe data were obtained by Dr. P.A. Nielsen during his tenure of a Visiting Fellowship at the Geological Survey of Canada.

Copies of this report
are available from:

Publication Sales
Alberta Research Council
5th Floor, Terrace Plaza
4445 Calgary Trail South
Edmonton, Alberta
T6H 5R7

TABLE OF CONTENTS

Abstract 1
Introduction 3
Location and accessibility 3
Methodology 3
Previous work 3
General geology 5
Petrography 6
Metasediments 6
High-grade metasediments 6
Low-grade metasediments 7
Granite gneisses 8
Granitoids 8
Slave Granitoids 9
Thesis Lake Granitoids 10
Wylie Lake Granitoids 11
Arch Lake Granitoids 11
Colin Lake Granitoids 12
Charles Lake Granitoids 12
Marguerite River Granitoids 12
Polyphase metamorphism 14
Metasediments 14
Orthopyroxene 14
Clinopyroxene 14
Sillimanite 14
Hercynite spinel 17
Corundum 17
Cordierite 17
Andalusite 19
Garnet 20
Amphibole 20
Biotite 20
Alkali-feldspar 21
Muscovite 21
Chlorite 21
Epidote 21
Tourmaline 21
Quartz 21
Plagioclase 21
Granitoids (north of Lake Athabasca) 21
Orthopyroxene 22
Clinopyroxene 22
Sillimanite 22
Hercynite spinel 22
Corundum 22
Cordierite 22
Andalusite 25
Garnet 25
Amphibole 25
Biotite 27
Alkali-feldspar 27

Muscovite 27
Chlorite and epidote 27
Quartz 27
Plagioclase 28
Granitoids (south of Lake Athabasca) 28
Metamorphic facies 28
South of Lake Athabasca 32
Fe-Mg cation exchange thermobarometry 32
Analytical methods 39
Garnet-biotite thermometry 39
Cordierite-garnet thermometry 39
Cordierite-garnet barometry 40
Discussion 40
Geological and metamorphic history: a summary 40
Archean 40
First cycle of metamorphism (M_1) 41
Aphebian 41
Second cycle of metamorphism (M_2) 41
References 44
Appendixes 47

LIST OF FIGURES

Figure 1. Location map showing the exposed Canadian Shield north and south of Lake Athabasca 2
Figure 2. Simplified geological map of the Canadian Shield of Alberta, north of Lake Athabasca 4
Figure 3. Simplified geological map of the Canadian Shield of Alberta, south of Lake Athabasca 5
Figure 4. Location of metasedimentary rock samples used with indication of the major outcrops of metasedimentary rocks 15
Figure 5. Orthopyroxene enclosed by light green amphibole 16
Figure 6. Orthopyroxene with preferred orientation partly replaced by dark green amphibole without preferred orientation 16
Figure 7. Flattened cordierite porphyroblast enclosing hercynite spinel and sillimanite needles 17
Figure 8. Detail of cordierite porphyroblast of figure 7, showing bundles of sillimanite needles and dark patches of hercynite spinel 18
Figure 9. Sillimanite prisms, hercynite spinel and quartz all enclosed by cordierite 18
Figure 10. Sillimanite prisms enclosed by andalusite 19
Figure 11. Corundum and minor hercynite spinel enclosed by andalusite porphyroblasts 20
Figure 12. Inclusions of platy quartz grains and sillimanite needles in garnet 22
Figure 13. Location of granitoid rock samples north of Lake Athabasca 23
Figure 14. Orthopyroxene partly replaced by biotite along rim 24
Figure 15. Zoned mineral relationships with a core of hercynite spinel surrounded by sillimanite in turn enclosed by biotite and garnet 24
Figure 16. Sillimanite concentrated in the finer grained parts of a mortar texture in between alkali-feldspar porphyroblasts 25
Figure 17. Cordierite porphyroblasts with characteristic twinning and pinite alteration 26
Figure 18. Flattened garnet crystal with parallel aligned hercynite spinel fragments 26
Figure 19. Late formed perthitic alkali-feldspar porphyroblast with inclusions of plagioclase and quartz 27
Figure 20. Lenses of platy quartz grains in a mortar texture of alkali-feldspar and quartz 38
Figure 21. Location of granitoid rock samples south of Lake Athabasca 29
Figure 22. Location of samples containing metamorphic minerals formed during the first cycle of metamorphism 30
Figure 23. Location of samples containing the more important metamorphic minerals formed during the second cycle of metamorphism 31
Figure 24. Metamorphic facies map of the Canadian Shield, north of Lake Athabasca 33
Figure 25. Metamorphic facies map of the Canadian Shield, south of Lake Athabasca 34
Figure 26. Calculated P-T values for the peak conditions of phase M_{2-1} as tabulated in table 3 35
Figure 27. Calculated P-T values for the peak conditions of phase M_{2-2} as tabulated in table 3 36
Figure 28. a. Metamorphic mineral assemblage of the moderate-pressure granulite facies event 37
b. Same view, crossed nicols 37
Figure 29. a. Metamorphic mineral assemblage of the low-pressure amphibolite facies event 38
b. Same view, crossed nicols 38
Figure 30. Path of metamorphism and related mineral growth in the Canadian Shield, north of Lake Athabsaca 40

LIST OF TABLES

Table 1. Chemical electron microprobe data on garnets from eight Slave Granitoid samples 10
Table 2 Wet chemical analyses of biotites from eight Colin Lake Granitoid samples 13
Table 3. Pressure and temperature conditions for M_2 mineral pairs 41

ABSTRACT

The Precambrian polymetamorphic complex of granitoids and metasediments in northeastern Alberta reveals two distinct cycles of metamorphism. During the Archean metamorphic cycle, metasediments were metamorphosed under high pressure granulite conditions (M_1). In a second cycle, probably related to remobilization during the Aphebian, the metasediments were subjected to conditions of granulite-amphibolite transitional facies retrogressing to greenschist facies metamorphism. Coexisting garnet-biotite and garnet-cordierite pairs in the metasediments allows estimation of P-T conditions during the granulite-amphibolite transitional facies, identifying a moderate-pressure granulite facies event ($M_{2.1}$) and a low-pressure amphibolite facies overprint ($M_{2.2}$). The widespread formation of granitoids by anatexis and ultrametamorphism during $M_{2.1}$ is indicated by their Aphebian ages and high initial strontium ratios. Some granitoids show minerals characteristic of both cycles of metamorphism, but others contain minerals characteristic of the second cycle only.

All rocks were subjected to a last retrograde phase under greenschist facies conditions ($M_{2.3}$), especially along mylonitic fault zones. Low-grade metasedimentary rocks underwent only greenschist facies metamorphism and are considered younger than the other metamorphic rocks. Unmetamorphosed Helikan sediments of the Athabasca Formation lie unconformably on the older crystalline rocks.

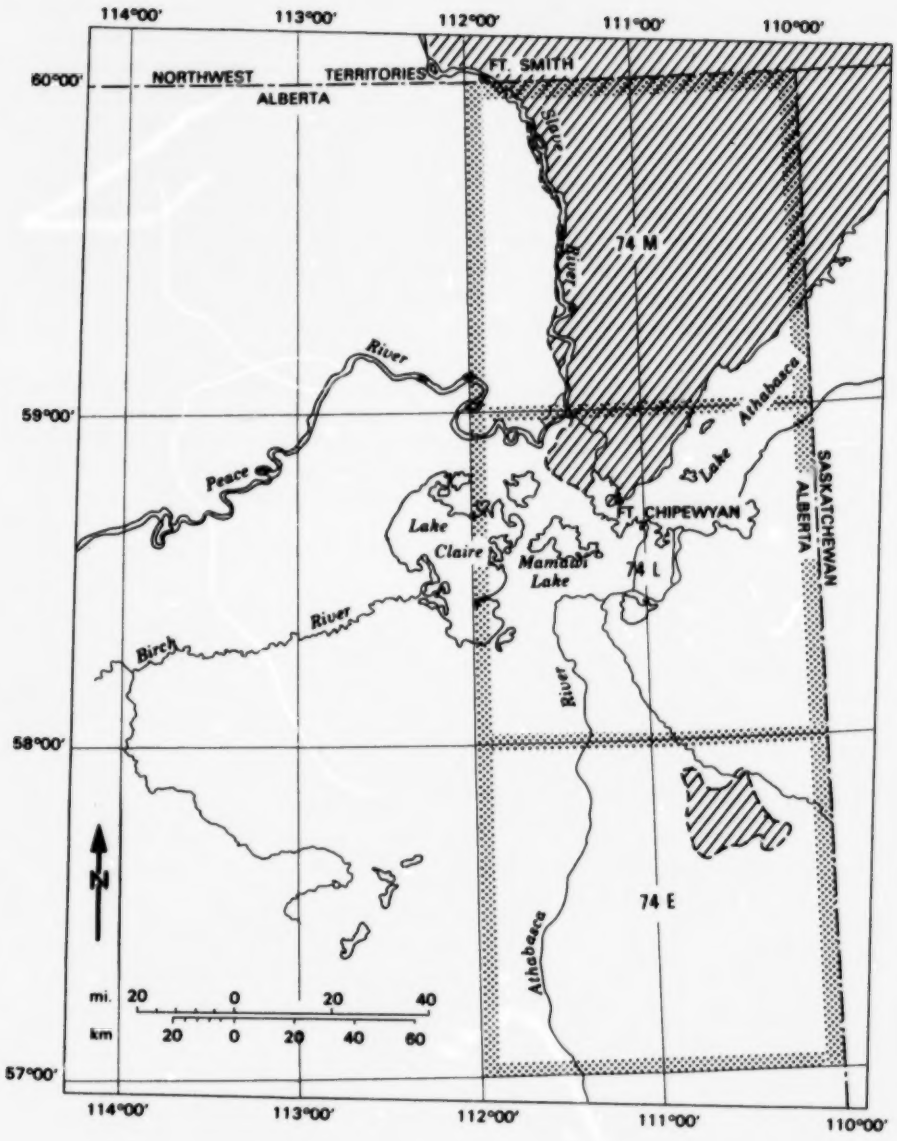

FIGURE 1. Location map showing the exposed Canadian Shield north and south of Lake Athabasca.

INTRODUCTION

This bulletin is one in a series of Alberta Research Council studies on the geology of the Canadian Shield in northeastern Alberta. Mapping started in 1957 and was finished in 1975. District geological maps have been published for parts of the area.

This study summarizes the metamorphic history of the exposed Canadian Shield of northeastern Alberta. Because of the presence of rocks of appropriate bulk compositions, and hence suitable mineral assemblages, an attempt is made to measure and record the pressures and temperatures of metamorphic equilibrations in the polymetamorphic rocks. Metamorphic minerals encountered in granitoid rocks provide insights into the genesis of these rocks, and are discussed here under 'Petrography'

LOCATION AND ACCESSIBILITY

The study area is located in northeastern Alberta, Canada, between latitudes 58°30', and 60°N, and longitudes 100° and 112°W. It forms parts of the Fitzgerald (NTS 74M) and Fort Chipewyan (NTS 74L) map sheets. Additional information is presented for the Marguerite River area of the McKay map sheet (NTS 74E). All locations are indicated on figure 1.

Access to the area can be obtained by regularly scheduled flights to both Fort Smith, N.W.T., and Fort Chipewyan.

METHODOLOGY

A simplified geological map of the area was prepared for this study, based on both published and unpublished district maps (figs. 2 and 3). Thin sections of 480 metasediment standard rock samples and 600 granitoid, granite gneiss, and amphibolite standard rock samples were studied. Modal and chemical analyses of these standard samples appear in reports accompanying district maps, and in Godfrey and Watanabe (1964). Inventories of metamorphic mineral assemblages in these samples are presented in appendixes A, B and C of this report. Critical observations were made of the relative times of crystallization of each mineral species.

Chemical analyses of cordierite, garnet, and biotite were obtained using the energy dispersive microprobe system at the Geological Survey of Canada, Ottawa. Paired garnet-biotite compositions were used to calculate temperatures by the methods of Nielsen (1977) and Ferry and Spear (1977). Paired cordierite-garnet compositions were used to calculate temperatures by the method of Nielsen (1977) and pressures were obtained by the methods of Hutcheon, *et al.* (1974) and Holdaway and Lee (1977).

PREVIOUS WORK

In 1957, the Alberta Research Council began systematic mapping of the Precambrian Shield in northeastern Alberta, and a number of district maps in this series have been published (Godfrey, 1961, 1963, 1966, 1970, 1980a, 1980b; Godfrey and Peikert, 1963, 1964). Geochronological studies have been published on those portions of the Shield initially mapped by the Alberta Research Council (Baadsgaard and Godfrey, 1967, 1972; Kuo, 1972; Day, 1975). Mineral showings encountered in the Andrew, Waugh and Johnson Lakes areas were reported by Godfrey (1958b). A structural interpretation of the Shield in Alberta, north of Lake Athabasca, was made by Godfrey (1958a), based on stereoscopic vertical air photographs.

In 1959, the Geological Survey of Canada conducted a reconnaissance geological survey of the Precambrian Shield in Alberta north of Lake Athabasca and published a map with marginal notes (Riley, 1960).

Peikert (1961, 1963) studied the petrogenesis of certain granitoid rocks in the Colin Lake area. Watanabe described metasediments of the Waugh Lake area (Watanabe, 1961) and cataclastic rocks of the Charles Lake area (Watanabe, 1965). Klewchuk (1972) reported on the petrogenesis of several granitoid rocks from the Fort Chipewyan district.

In 1977 the Alberta Research Council was invited to participate in a project to compile a metamorphic map of the Canadian Shield (GSC map 1475A), under the auspices of the Geological Survey of Canada. The symposium volume accompanying the metamorphic map includes a paper on the metamorphic history of the Shield in northeastern Alberta (Godfrey and Langenberg, 1978). Some preliminary results of temperature and pressure conditions of metamorphism were later reported by Nielsen (1979). A recent publication (Nielsen *et al.*, 1981) puts the crustal evolution of the area in a regional framework.

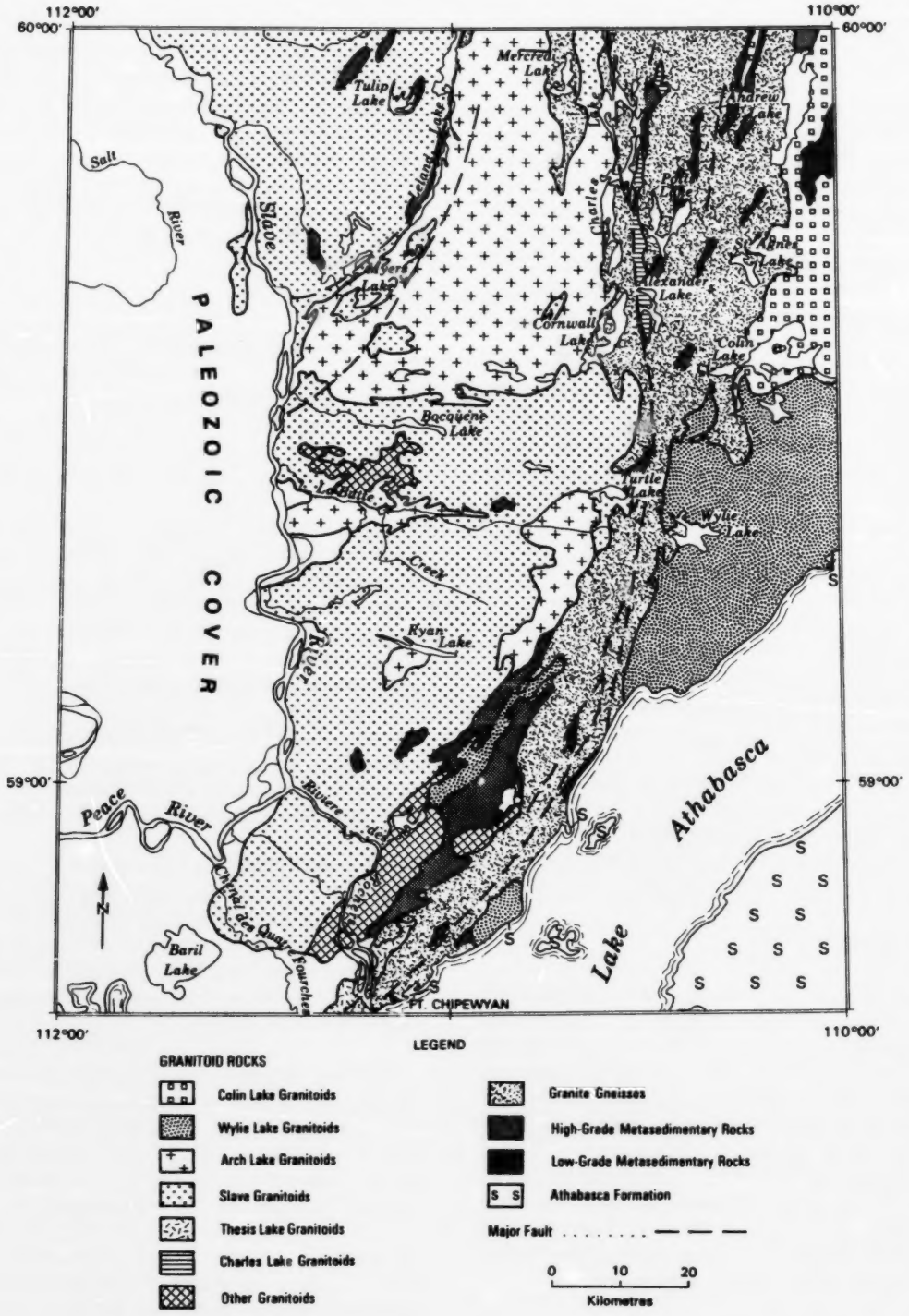

FIGURE 2. Simplified geological map of the Canadian Shield of Alberta, north of Lake Athabasca.

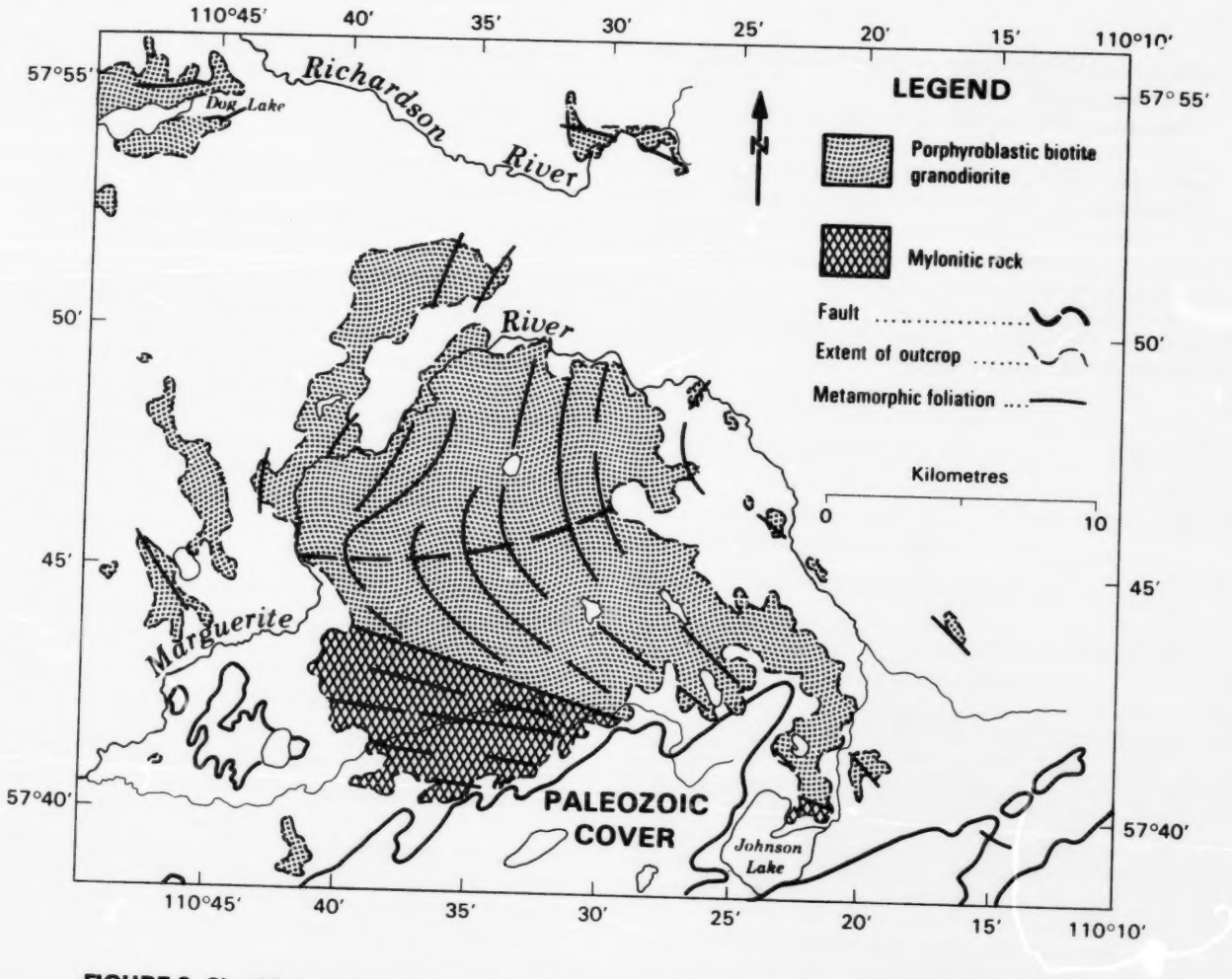

FIGURE 3. Simplified geological map of the Canadian Shield of Alberta, south of Lake Athabasca.

GENERAL GEOLOGY

The Precambrian Shield of northeastern Alberta consists of massive to foliated granitoids, banded granite gneisses, and layered to banded metasediments (fig. 2). It forms part of the Churchill Structural Province and is situated in the Athabasca Mobile Belt (Burwash and Culbert, 1976). The geological history involves sedimentation, deformation, metamorphism, and ultrametamorphism, accompanied by remobilization. These processes have operated during different orogenic periods, resulting in the formation of complex polymetamorphic rocks. From field contact relationships and bulk compositions, it is deduced that the migmatitic granite gneisses and high-grade metasediments were parent materials for several of the granitoid rocks (for example, see Klewchuk, 1972). Thus, the granitoids probably represent Archean basement remobilized during the Aphebian (see also Davidson, 1972).

Further evidence of multiple orogenic cycles is provided by geochronological studies of rocks from the area (Baadsgaard and Godfrey, 1967, 1972). This work reported on the Charles Lake, Andrew Lake and Colin Lake districts, and clearly identifies two distinct orogenic cycles. Rb-Sr whole rock isochrons on pegmatites within granitoids, gneisses and metasediments in the Charles Lake area show that these rocks have ages of about 2500 Ma. Because of this, they are considered to be part of an Archean basement.

Rb and Sr determinations on Colin Lake granitoids plot on a well-defined isochron with t = 1893 ± 6 Ma. A high initial $^{87}Sr/^{86}Sr$ ratio of 0.7083 ± 0.0002 may indicate derivation of these rocks by anatexis, or possibly ultrametamorphism, of pre-existing sedimentary rocks (Baadsgaard and Godfrey, 1972, p. 870). The immediate parent materials for the Colin Lake granitoids are probably the nearby Archean granite gneisses and high-grade metasedimentary rocks.

K-Ar determinations on muscovite, biotite and hornblende give a narrow distribution of ages. The average age of mica from many rock units is 1790 ± 40 Ma, which indicates that the K-Ar dates for all rocks within the region were effectively reset during the Hudsonian orogeny.

Thus, two Precambrian orogenic cycles for the Shield rocks of northeastern Alberta are firmly established.

Several (Hudsonian?) phases of deformation can be distinguished in the granitoid rocks. Some of the deformation can be explained by the process of gneissic, or diapiric, doming (Langenberg and Ramsden, 1980).

Low-grade metasedimentary rocks and metavolcanics show primary sedimentary and igneous structures respectively. An unconformity is suggested between the low-grade metasedimentary rocks and the underlying Archean high-grade granite gneisses and metasedimentary rocks. The age relationship between the low-grade metasedimentary rocks and the nearby Colin Lake granitoids is uncertain. Peikert (1961, 1963) postulates that the Colin Lake granitoids were formed by anatexis from the low-grade metasedimentary rocks. This explanation, however, seems improbable, because temperatures in the greenschist facies are too low for partial melting to occur (Koster and Baadsgaard, 1970). Therefore, it appears that the high-grade metasedimentary rocks and granite gneisses are the more likely parent materials for these and other granitoid bodies.

Major faults affect most of the rock units and are younger than the macroscopic fold structures in the granitoids. They are expressed as deformation zones characterized by mylonites (Watanabe, 1965). Breccias along some transverse faults may indicate still younger fault movements at higher crustal levels.

The Alberta Shield exposed south of Lake Athabasca, adjacent to the Marguerite River (fig. 3), consists mainly of granitoids, with mylonites in the southerly outcrops (Godfrey, 1969).

Glacial scouring during the Pleistocene left numerous fresh outcrops which greatly facilitate geologic studies in the area.

PETROGRAPHY

Rocks important in the metamorphic history of the Canadian Shield in northeastern Alberta can be grouped into three major units: metasediments, granite gneisses[1] and granitoids[2]. Some ideas on granitoid genesis are included because metamorphic minerals are present in granitoids.

Modal and chemical analyses of standard samples representing these rock units appear in reports accompanying district maps (for example, Godfrey, 1961).

METASEDIMENTS

Bands and lenses of biotite-quartz-feldspar rocks occur throughout the area. They grade locally into retrograde schist and phyllite. These rocks are interpreted as metasediments and they contain the highest proportion of metamorphic minerals. The metasediments can be divided into high-grade and low-grade bands.

High-grade Metasediments

High-grade metasedimentary rocks occur as bands and lenses, principally within the granite gneisses, but also in the granitoid rocks, such as the Slave Granitoids. They were distinguished in the field from the granite gneisses by the lack of gneissic banding. The long axes of these bands and lenses parallel local trends of the regional metamorphic foliation in the enclosing rocks (fig. 2).

The lithology of the metasediments is typically a biotite-quartz-feldspar rock, with minor amounts of retrograde schist and phyllite. Garnet is commonly seen in outcrop. The biotite-quartz-feldspar rocks are medium grained, sugary textured, and have layering and color banding of varied widths. The biotite foliation is parallel to the

---

[1]The term 'granite gneiss' is used for gneisses derived from sedimentary or igneous rock and having a granite mineralogy.

[2]The term 'granitoid' is used in its broadest sense to refer to medium- to coarse-grained crystalline rocks composed mainly of quartz and feldspar.

banding. Chemical analyses show that these rocks are peraluminous, since the molecular proportion of Al_2O_3 exceeds $CaO + Na_2O + K_2O$. The quartz-feldspar rocks grade into: impure quartzites by an increase in quartz; biotite gneiss by development of mineral banding; and sillimanite-granite-cordierite-feldspar-quartz rocks by an increase in cordierite and sillimanite.

Sillimanite-garnet-cordierite rocks have received interest in recent years because estimates of metamorphic P-T conditions can be obtained from this mineralogy (for example, Lee and Holdaway, 1977). The stability of co-existing minerals has been studied experimentally, theoretically and by observation of mineral assemblages in the field. The application of these methods to the sillimanite-garnet-cordierite rocks of northeastern Alberta is discussed under the heading "Fe-Mg cation exchange thermobarometry." These studies show that rocks containing garnet-cordierite-alkali-feldspar-plagioclase-quartz and either sillimanite or biotite may well be restites, left over from partial melting (Harris, 1976). This is especially likely if alkali-feldspar or plagioclase is depleted or missing, as was observed in several samples from the study area.

Small bodies of amphibolites and pyribolites within the high-grade metasedimentary bands may represent metaigneous components.

Polyphase deformation can give rise to mesoscopic interference patterns of folding. This type of folding was not encountered in the granitoids and the possibility remains that some of these folds in the high-grade metasediments are Archean structures. Granitoid materials cutting across folds show the migmatitic character of these rocks.

In thin section, quartz grains show undulatory extinction, alkali-feldspar grains are generally non-perthitic, and plagioclase forms subhedral crystals. Cordierite porphyroblasts lack a preferred orientation and grow over the existing fabric. This fabric is defined by elongate grains of garnet and green hercynite spinel, plus the preferred orientation of sillimanite and biotite. Andalusite forms unoriented porphyroblasts and corundum commonly accompanies green hercynite spinel. Orthopyroxene may show a preferred orientation, and is always found in rocks devoid of cordierite, sillimanite and green hercynite spinel. Orthopyroxene is replaced by green amphibole that lacks a preferred orientation.

Late stage deformation is indicated in many samples by mortar textures of quartz and alkali-feldspar. Cordierite porphyroblasts are flattened in this fabric, resulting in the formation of some augen. Feldspar and garnet porphyroclasts also form augen. Garnet is replaced by biotite and chlorite. Alkali-feldspar may be perthitic and plagioclase can show tapered twins. Plagioclase and cordierite are replaced by sericite. Biotite and sericite form along the deformational fabric, possibly in shear planes. These rocks grade into mylonites along minor and major fault zones.

Low-grade Metasediments

In the Waugh Lake area and along the shore of Lake Athabasca near Burntwood Island, relatively low-grade metasediments are found (fig. 2). In the Waugh Lake area these rocks are accompanied by metavolcanics. The principal metasedimentary rocks in this area are impure quartzites that show graded bedding and relict clastic sedimentary fabric. The coarse size fraction consists of largely subangular fine sand particles. The matrix is composed of a fine-grained aggregate of biotite, sericite, quartz, and feldspar. Among the impure quartzites, meta-graywackes and meta-siltstones can still be recognized. They may represent a graywacke suite from a deep water environment of sedimentation (Watanabe, 1961, p. 73). Accompanying the impure quartzites are schists (locally phyllonitic). The metavolcanics include basic to intermediate lavas as well as sills, tuffs and tufaceous metasediments.

In thin section, quartz locally shows undulatory extinction whereas metamorphic muscovite and biotite are oriented parallel to the bedding. These mica bands can be crenulated, with recrystallization of muscovite and biotite, parallel to the axial planes, thereby forming a crenulation cleavage. Chlorite replacing biotite is oriented parallel to the crenulation cleavage.

The schists show a higher percentage of phyllosilicates than the remainder of the metasediments. Deformation has played an important role in the history of these rocks as indicated by the recrystallization of lenses of deformed quartz grains. Some of the schists are probably mechanically degraded (phyllonitized) equivalents of coarser-grained parent rocks, that is, impure quartzites. Green amphibole (hornblende) and epidote are commonly encountered in the metavolcanic rocks.

The metasediments along the shore of Lake Athabasca form the Burntwood Group (Godfrey, 1980b). The principal rock types are meta-arkoses with minor pebble bands and slates. Primary bedding is recognized as alternating meta-arkose and slate layers and by graded layering in the meta-arkose. The well-developed cleavage of slates is formed by biotite and muscovite whereas coarser-grained pockets of biotite and chlorite lie between the cleavage planes. The slates grade into phyllites by an increase in grain size of the phyllosilicates.

The meta-arkose show angular (clastic) quartz and partly, to completely, sericitized feldspar grains in a matrix of phyllosilicates (mainly muscovite). The quartz grains are strongly undulose and some grains form mortar structures. An increase in deformation towards the west-northwest can be observed in metasediments of the Burntwood group expressed in the formation of mylonites. This deformation is related to a branch of the Allan Fault located just west of the Burntwood Group outcrops.

The metasediments of the Waugh Lake and Burntwood Groups are probably contemporaneous with those of the Thluicho Lake group in northern Saskatchewan (Scott, 1978) and of the Nonacho series in the Northwest Territories (Henderson, 1939).

GRANITE GNEISSES

These typically banded rocks consist of alternating mafic- and felsic-rich layers. The gneissic banding is better developed than in rocks mapped as high-grade metasediments. Where banding is irregular, the rocks assume a migmatitic character, and agmatites and chaotic folds are also found. Streaky, metamorphic foliation is formed by lenses of biotite and chlorite which parallel the gneissic banding. Amphibole is present locally. A regional band of granite gneiss crosses the area north of Lake Athabasca from north-northeast to south-southwest and includes lenses and bands of peraluminous metasedimentary rocks (fig. 2). The granite gneisses are probably largely derived from sedimentary rock. Based on geochronological data it is inferred that the granite gneisses and included metasediments comprise the oldest rocks in the area (Baadsgaard and Godfrey, 1972). The granite gneisses may have constituted the parent materials for several granitoids through anatexis (Klewchuk, 1972). Metamorphic minerals found in the gneisses are: biotite, amphibole, alkali-feldspar, plagioclase, quartz, chlorite (retrograde), epidote (retrograde) and muscovite (retrograde).

Quartz shows undulose extinction with typically serrated boundaries. In places, deformation was more intense and gave rise to mortar textures, and recrystallization has led to annealed aggregates. Alkali-feldspar is typically undulose, perthitic, and may show mortar textures. Plagioclase is commonly myrmekitic and may be slightly altered (sericitized and saussuritized). The granite gneisses show tight to isoclinal folding on meso- and microscopic scales. The folds are truncated by granitoid material. This type of fold is not encountered in the granitoids and it is possible that they are Archean structures.

Amphibolite bands and lenses are common in the granite gneisses. Green amphibole (hornblende) and plagioclase are the principal minerals, with minor biotite and chlorite. Veinlets of epidote and quartz may be present.

Mylonites were formed in the granite gneisses under retrograde metamorphic conditions along late stage major faults (Watanabe, 1965).

GRANITOIDS

The genesis of granitoid rocks has puzzled geologists since the days of Werner and Hutton. Granulites in Finland, which are similar to some of the granitoids in northeastern Alberta, were originally considered magmatic and later metamorphic in origin (Eskola, 1952, p. 168). Recent work has thrown new light on the genesis of granitoids (see for example, White and Chappell, 1977). Granitoid rocks are considered to have formed during ultrametamorphism at the climax of regional metamorphism (see also Carmichael, *et al.*, 1974, p. 595). Ultrametamorphism is regarded as that type of metamorphism within the crust where temperatures were high enough for rocks to begin to melt. The product of partial melting is a mixture of melt and solid residual material, the latter referred to as restite. In effect, the granitoid magma is a mixture of melt and solid material, where much of the latter is relict source material.

Many of the granitoid bodies of northeastern Alberta contain inclusions of residual metasedimentary material. The mineralogy of some of the metasediments

indicates that they are restites. Although the mineralogy of the metasediments is similar to that of the surrounding granitoids, the proportions are different. The minerals garnet, cordierite, sillimanite, green spinel, corundum, orthopyroxene, and some biotite, alkali-feldspar, plagioclase and quartz in the granitoid are also part of the residual source material. Consequently, they are metamorphic minerals. The rest of the feldspar, quartz and biotite is believed to have formed from the melted fraction, and therefore are magmatic minerals. Some cordierite and garnet may have formed by reaction between restite and melt. P-T curves supplied by Lee and Holdaway (1977) indicate that partial melting could occur in rocks containing garnet, cordierite, sillimanite, alkali-feldspar, biotite, plagioclase, and quartz.

Slave Granitoids

The Slave Granitoids form two large bodies along the Slave River (fig. 2). Part of the southern body was studied by Klewchuk (1972) and Godfrey (1980b). Slave Granitoids are mainly granitic in composition. The rock is typically medium- to coarse-grained, and whitish to pink in color. Locally, large feldspar megacrysts are present. The rock is commonly well foliated, as defined by elongated aggregates of platy quartz grains and biotite. Overall, it can be described as a leucogranite and has a mafic mineral content of about 4 percent. Locally, the mafic mineral content reaches 10 percent. Work in progress on geochemistry of these rocks shows that they have a Rb/Sr age of 1938 ± 28 Ma with an initial $^{87}Sr/^{86}Sr$ ratio of 0.710 ± 0.002. This isochron indicates that either contamination or derivation from metasediments occurred. (Nielsen *et al.*, 1981).

The larger quartz, alkali-feldspar, and plagioclase grains typically show undulatory extinction. The platy quartz grains are commonly arranged in lens-shaped aggregates, indicating that they are annealed, recrystallized grains following an earlier deformation. Alkali-feldspar is nearly always perthitic. It appears that deformation has contributed to the formation of perthite (Spry, 1969, p. 182). The larger alkali-feldspar grains are set in a matrix of smaller alkali-feldspar and plagioclase grains as a mortar texture. The fact that feldspars are more resistant to deformation than quartz (Spry, 1969, p. 234) shows that there are two deformations: an older deformation affecting the feldspars and a later one that produced undulose extinction of quartz. If the deformation was of a single age the quartz should show at least a mortar structure. Plagioclase grains locally show tapered or curved twins; another indication that deformation played a role in its history. Myrmekite occurs commonly and may have formed as a result of simultaneous recrystallization of crushed quartz and feldspar following deformation (Spry, 1969, p. 104).

Garnet, although a minor constituent, occurs commonly. Compositions of some garnets are given in table 1. Garnets are typically flattened and elongated up to ratios of 1:10. Minor sillimanite can be concentrated between fine-grained feldspar in mortar structures. Minor cordierite forms porphyroblasts. Orthopyroxene is sparse and may be enclosed in biotite. Green hercynite spinel is present in most samples that contain garnet, cordierite or sillimanite. In a few cases it is accompanied by corundum. All samples contain biotite. Garnet, cordierite and biotite are locally altered to chlorite, muscovite or epidote.

Lenses of mafic-rich mineral concentrations are interpreted as metasedimentary rock relics, as indicated by their mineralogy. They are found throughout the Slave granitoids and range in size from hand specimens to mappable areas. In the latter case they form a separate map unit.

This information, combined with the high initial $^{87}Sr/^{86}Sr$ ratio, points to formation of these granitoids by anatexis and ultrametamorphism of pre-existing peraluminous metasediments. The distribution of Fe and Mg between coexisting garnet and biotite is consistent with conditions of high-grade metamorphism (Klewchuk, 1972). Rocks of similar mineralogy and texture from Finland were described by Eskola (1952, p. 138) as granitic granulites and light (leucocratic) massive to foliated granulites. Eskola was the first to suggest that some granulites could be formed by partial melting of pre-existing rocks (Eskola, 1952, p. 169).

Similar rocks are reported by Reinhardt (1969) just south of the east arm of Great Slave Lake. He describes a quartz monzonite and granite (rock unit 7) with biotite, garnet, cordierite, sillimanite, andalusite and/or green spinel. He concluded that these rocks originated because "the more refractory parts of the original host rocks resisted complete melting whereas the less refractory parts were incorporated in the granitic melt" (Reinhardt, 1969, p. 14). He further suggests that emplacement of the granitoids contributed to the high-grade regional metamorphism of the sediments. Ideas expressed by White and Chappell (1977) suggest that

TABLE 1.
Chemical electron microprobe data on garnets from eight Slave Granitoid samples
(Klewchuk, 1972, table 14)

	A	B	C	D	E	F	G	H
	Percent oxides (average of a minimum of 3 analyzed grains per sample)							
SiO_2	37.40	37.49	37.38	37.64	38.18	37.92	37.24	37.61
Al_2O_3	21.07	21.18	21.14	21.14	21.48	21.31	20.77	21.16
FeO*	33.71	33.19	32.50	31.43	32.63	33.82	34.52	33.11
MnO	0.76	0.57	0.78	1.27	0.69	0.67	0.89	0.80
MgO	5.45	5.77	6.59	6.76	6.98	6.07	4.19	5.97
CaO	0.86	0.78	0.58	1.05	1.00	0.87	1.29	0.92
Total	99.25	98.98	98.97	99.29	100.96	100.66	98.90	99.57
	Percentage composition in terms of garnet end-member molecules							
Almandine	74.43	73.69	71.00	68.15	69.33	72.83	77.51	72.42
Pyrope	21.42	22.83	25.64	26.12	26.40	23.28	16.75	23.21
Spessartine	1.71	1.28	1.73	2.80	1.51	1.47	2.03	1.79
Grossularite	2.44	2.20	1.63	2.93	2.77	2.43	3.71	2.58
Total	100.00	100.00	100.00	100.00	100.01	100.01	100.00	100.00

*all iron is reported as ferrous iron

high-grade metamorphism may have contributed to the formation of the granitoids. Similar rocks in the English River gneissic belt of Ontario are described as homogenous diatexites (Breaks, *et al.*, 1978).

The Slave Granitoids were subjected to several phases of deformation, and gneissic doming has occurred (Langenberg and Ramsden, 1980). The metamorphic foliation in the granitoids must have formed before or during doming. The undulose extinction of quartz is related to one of the last phases of deformation. Along fault zones this deformation was more intense and mylonites were formed. Mylonitization was accompanied by neocrystallization of chlorite, muscovite, biotite, and epidote.

Thesis Lake Granitoids

The Thesis Lake Granitoids are named after a small lake within the rock body, 7 km north of Fort Chipewyan (fig. 2). These granitoids formed the subject of a study by Klewchuk (1972). The composition ranges from granite to granodiorite (Godfrey, 1980b).

Texturally, the rock is characterized by augen-shaped alkali-feldspar megacrysts, aligned with lens-shaped quartz aggregates and biotite. Together, these elements define the foliation. Locally, where alkali-feldspar megacrysts show a more random orientation, the strings of quartz grains and biotite determine the foliation.

The large quartz grains show undulose extinction. They are typically partly recrystallized at grain margins, giving the rock a mortar texture. Other quartz lenses show a granoblastic polygonal network of annealed grains, indicative of complete recrystallization.

Crystals of plagioclase are smaller than those of alkali-feldspar. Twinning is common, myrmekite is present, and plagioclase is partly altered to sericite.

Biotite is the most common mafic mineral. It is typically fresh-looking, but can be altered to chlorite. In one thin section, orthopyroxene was seen to be rimmed by biotite. Green amphibole is present in a few samples. Thesis Lake Granitoids are characterized by leucocratic granitoid material as dykes, veins or pods. The leucocratic material is generally of granitic composition and it grades into aplite dykes and pegmatites. It shows the migmatitic character of the granitoids.

Along fault zones, the deformation is more intense and the granitoids form mylonites. Klewchuk (1972) compared the bulk composition of different phases of the Thesis Lake Granitoids with experimental data. This comparison points to the formation of the granitoids by anatexis of pre-existing rocks, possibly from the granite gneisses which surround the granitoids. This mode of formation is compatible with ultrametramorphism as described by White and Chappell (1977).

Wylie Lake Granitoids

The Wylie Lake Granitoids are typical of the Wylie Lake region (fig. 2). Several rock units can be mapped within these granitoids (Godfrey, 1980a). Their composition ranges from granite to tonalite. The contact with Colin Lake Granitoids south of Colin Lake is gradational, indicating that these rocks are genetically related. The main difference between rocks of the two regions is the generally lower proportion of porphyroblastic textures in the Wylie Lake Granitoids. Megacrysts include both alkali-feldspar and plagioclase. The Wylie Lake Granodiorites have a slightly higher biotite content and as a result show a greenish to brownish-red color in outcrop. Another conspicuous feature of the Wylie Lake Granitoids is the abundance of leucocractic granite intermixed with other lithologies, giving the assemblage a migmatitic character.

Isolated patches of metasediments and granite gneisses are present within the granitoids. Two occurrences of garnet are reported in Wylie Lake leucogranites (appendix B). All of these features point to an origin by ultrametamorphism of pre-existing supracrustal rocks.

Foliation produced by planar orientation of the major minerals is generally present, although in places the rock is massive. In places of intense deformation the rocks are mylonitic and commonly contain chlorite and epidote. A structural analysis of orientation data shows a dome and basin structure in the granitoids around Wylie Lake (Langenberg, in preparation). Doming may have resulted from the ultrametamorphism and remobilization of pre-existing rocks.

Arch Lake Granitoids

Arch Lake Granitoids occupy a large area between Charles Lake and Leland Lakes. The name was introduced by Hicks (1932) because these rocks crop out on the shore of Arch Lake, 1 km west of Charles Lake (Godfrey, 1966). Isolated patches of Arch Lake Granitoids are found south of the main body, where they are enclosed by Slave Granitoids. Although most Arch Lake Granitoids have a granitic composition, granodiorites are also present.

Arch Lake Granitoids are texturally distinctive, with elongate feldspar megacrysts commonly aligned in a foliated matrix (augen texture).

Lenses of well layered granite gneiss and massive amphibolite occur within the granitoids. Contact with granite gneisses to the east is normally a mixed zone of gneisses and granitoids. Several occurrences of garnet are reported from the Arch Lake Granitoids (appendix B). These features point to an origin by ultrametamorphism of pre-existing paragneisses. Pegmatite and aplite dykes are found in the Arch Lake Granitoids. The aplite dykes are very similar to fine-grained Slave Granitoids and may represent remobilized Slave Granitoid material.

Deformation has played an important role in the history of these rocks. Feldspar megacrysts (mainly perthitic alkali-feldspar) are rounded and lens-shaped with shadowy extinction and fractures, giving the rock an augen texture. Euhedral, zoned plagioclase crystals and undeformed quartz crystals are included in the alkali-feldspar megacrysts. In some cases, the inclusions show a linear arrangement. Quartz outside the feldspar megacrysts is arranged in lens-shaped aggregates with mortar textures. Although the megacrysts may have

started growing in a stress field that imposed an initial preferred orientation on them, the main deformation took place after the megacrysts were formed. This temporal relationship is clearly indicated by the difference in degrees of deformation of inclusions in the megacrysts and the same minerals in the matrix. The grain size in the matrix is tectonically reduced in many places. Recrystallization continued after deformation as shown by annealed quartz and undeformed fresh biotite. The megacrysts are set in a foliated matrix of plagioclase, quartz, microcline and biotite.

The main Arch Lake Granitoid body shows a large scale synform, which may be a refolded, older antiform (Langenberg and Ramsden, 1980). In areas affected by major fault zones, deformational textures are more prevalent and mylonites were formed during a late stage of the Precambrian history (Watanabe, 1965). Deformation was accompanied by neocrystallization of chlorite, biotite, and epidote.

Colin Lake Granitoids

The Colin Lake Granitoids crop out in the area of Colin Lake and straddle the Alberta-Saskatchewan border (fig. 2). This rock unit encompasses several rock units mapped by Godfrey (1961, 1963) and Godfrey and Pelkert (1963, 1964) and is roughly equivalent to the Colin Granite-granodiorite Complex of Koster (1971) in Saskatchewan.

The composition of Colin Lake Granitoids ranges from granite to tonalite. The typically porphyroblastic texture has alkali-feldspar megacrysts, though more equigranular textures are also present. The rocks are foliated; the foliation is defined by preferred orientation of tabular alkali-feldspar megacrysts and biotite. Small lenses of basic material are present throughout the rock body, as are pegmatite and aplite dykes. The basic lenses probably represent residual parent material. In the northern part of the area these granitoids are bordered by metasediments and one isolated body is completely enclosed by metasediments. Garnet is recorded from the northern area (sample 12, appendix B). Detailed study of the alkali-feldspar megacrysts in thin section suggests that they formed in place during a relatively late stage in the history of the rocks, and thus may be termed porphyroblasts (Pelkert, 1961, 1963). Biotite compositional variations within and around the granitoids is consistent with the interpretation that these rocks were derived from metasediments and metavolcanics (Pelkert, 1963). Chemical analyses of biotites from the Colin Lake Granitoids are presented in table 2. Isotopic data supplied by Baadsgaard and Godfrey (1972) show that the Colin Lake Granitoids had an initial $^{87}Sr/^{86}Sr$ ratio of 0.7083. This high ratio indicates derivation of the granitoids by ultrametamorphism from metasedimentary (pelitic) sources and they classify as S-type granitoids (White and Chappell, 1977).

The foliation is a result of crystallization under stress. The rocks typically show a mortar texture. In places where deformation was more intense, the rocks are mylonitic. The mylonitization is usually accompanied by neocrystallization of chlorite and epidote.

Charles Lake Granitoids

A narrow elongate body of granitoid rocks that crops out along Charles Lake is similar to one phase of the Colin Lake Granitoids (fig. 2). Rb/Sr dating, however, shows that the Charles Lake Granitoids are Archean (Baadsgaard and Godfrey, 1972) and thus they cannot be correlated with the Colin Lake Granitoids. The Charles Lake Granitoids form part of the Archean basement, which consists mainly of migmatitic granite gneisses and metasediments.

The Charles Lake Granitoids are mainly granodioritic in composition. The texture is typically porphyroblastic with alkali-feldspar megacrysts. The rocks are characteristically foliated with tabular alkali-feldspar megacrysts and oriented biotite. Garnet is widely observed in these rocks. The granitoid body is elongated parallel to a major fault (Allan Fault) and grades into mylonites in the fault zone. This late-stage deformation is characterized by mortar textures, undulose quartz, bent twin lamellae in plagioclase and altered minerals. Garnet is altered to chlorite, biotite and sericite. Biotite is altered to chlorite, and feldspars show sericitization.

Marguerite River Granitoids

Precambrian rock outcrops south of Lake Athabasca in Alberta were mapped by Godfrey (1970). The main concentration of outcrops lies south of the Marguerite River (figs. 1 and 3). The rocks are largely granitoids, with minor leucocratic phases and with compositions that span the granite to granodiorite fields. The rocks are generally medium grained with slightly larger feldspar crystals up to 2 cm in diameter.

TABLE 2.
Wet chemical analyses of biotites from eight Colin Lake Granitoid samples
(Peikert, 1983, table 7)

	A	B	C	D	E	F	G	H
SiO_2	38.12	36.51	37.41	38.00	38.12	36.91	36.08	33.59
TiO_2	2.26	2.00	2.33	2.02	2.55	2.34	2.84	3.22
Al_2O_3	15.47	15.54	15.29	14.69	16.59	15.54	15.54	14.96
Fe_2O_3	5.12	3.53	4.85	(5.08)	3.94	5.38	5.40	6.66
FeO	14.47	15.26	15.22	(15.00)	17.79	16.42	18.00	25.39
MgO	9.10	11.07	10.06	10.02	7.74	9.78	8.10	3.76
CaO	1.85	1.95	2.04	2.38	1.14	1.04	1.49	1.56
Na_2O	0.34	0.21	0.20	0.31	0.43	0.20	0.23	0.14
K_2O	7.73	8.14	7.78	7.26	7.15	8.71	8.31	6.81
P_2O_5	1.00	1.10	1.03	0.62	0.81	0.75	1.03	0.89
L.O.I.	2.59	2.67	2.28	2.34	2.54	1.86	1.62	2.33
Total	98.03	97.98	98.35	97.72	98.80	99.03	98.64	99.31
				Cations to 22 Oxygen				
Si	5.64	5.49	5.57	5.66	5.70	5.47	5.44	5.32
Al (IV)	2.36	2.51	2.43	2.34	2.30	2.53	2.56	2.68
Al (VI)	0.35	0.24	0.24	0.25	0.61	0.20	0.18	0.10
Ti	0.25	0.21	0.26	0.23	0.28	0.20	0.33	0.37
Fe^{+++}	0.57	0.40	0.55		0.44	0.60	0.61	0.63
Fe^{++}	1.78	1.92	1.90		2.21	2.13	2.29	3.33
Mg	2.02	2.50	2.25	2.24	1.71	2.16	1.83	0.89
Ca	0.30	0.32	0.32	0.38	0.18	0.17	0.25	0.26
Na	0.10	0.06	0.06	0.09	0.12	0.06	0.06	0.05
K	1.47	1.56	1.54	1.37	1.35	1.65	1.58	1.38
P	0.12	0.12	0.12	0.08	0.10	0.09	0.12	0.12
N	1.624	1.630	1.634	1.637	1.641	1.644	1.652	1.663
Fe^{++}/Mg	0.882	0.768	0.845		1.292	0.986	1.250	3.742

( ) based on estimated FeO: Fe_2O_3 ratio

The rocks are characteristically foliated as a result of deformational processes, and larger grains in a matrix of smaller grain size produce a mortar structure. Biotite tends to be recrystallized along the foliation planes and garnet, altered to chlorite, is common in the granitoids. Ortho- and clinopyroxene are present locally.

A two-mile-wide zone in the southern part of the area is more intensely deformed, resulting in the formation of mylonites. Garnet, orthopyroxene and feldspar porphyroclasts are preserved between recrystrallized quartz and feldspar zones. Although no suitable parent material is directly evident in the exposed area, it seems probable that these granitoids were formed by ultrametamorphism of pre-existing rocks.

POLYPHASE METAMORPHISM

Most of the insight into the metamorphic history comes from the high-grade metasediments, which contain the highest proportion of metamorphic minerals. Additional information is obtained from residual metasedimentary material in granitoids. The history of the granite gneisses is limited to information from biotite and amphibole, therefore its metamorphic conditions are extrapolated from included metasedimentary bands. In the following discussion, a distinction is made between metamorphic minerals from metasediments and those from granitoids.

In the course of study of thin sections, critical note was taken of age relationships between different minerals and between mineral growth and deformation. The textural criteria used to decipher these age relationships have been applied successfully in other orogenic belts. These studies have been particularly suited to medium-grade, fine-grained metasediments as, for example, in the Pyrenees (Zwart, 1960) and Beltic Cordilleras (Langenberg, 1972) in Spain. It is more difficult to work out age relationships in coarser-grained metasediments of granulite to amphibolite grade, as found in northeastern Alberta (Brown *et al.*, 1969, p. 532).

Some of the age relationship criteria are summarized by Spry (1969, p. 305) as follows:

Minerals which crystallized at the *same time* may:

1. show no alteration or reaction of mutual contacts,
2. be intimately intergrown,
3. have related preferred orientation fabrics,
4. show similar alteration to another mineral or minerals.

Minerals which crystallized at *different times* may:

5. show replacement, reaction or some special mutual texture,
6. have significant differences in fabric of preferred orientation,
7. be known to be stable under different physical conditions,
8. be enclosed, one within the other, where inclusions are probably older than the host (armoured relicts).

Of all these criteria, only the seventh is conclusive: the others are only indications. The age relationships established in this chapter are further substantitated under the heading 'Fe-Mg cation exchange thermobarometry.'

METASEDIMENTS

All metamorphic minerals in the metasediments are discussed systematically below. Sample numbers refer to the inventory (appendix A), and locations are given in figure 4. Quartz and plagioclase, which are present in all samples, and retrograde minerals, have been omitted from this list. The low-grade metasedimentary rocks included in the list are represented by samples M-11, M-12, and M-69.

Orthopyroxene

Orthopyroxene is present in several of the metasedimentary rock bands. In most cases, the orthopyroxene appears to be hypersthene ($-2V \approx 60°$). In some cases, enstatite ($+2V$ large) is present. The pyroxene can be surrounded by green amphibole (fig. 5), or biotite. Occasionally, oriented orthopyroxene is partly replaced by green amphibole that lacks a preferred orientation (fig. 6). These textural features indicate that orthopyroxene formed before amphibole and biotite.

Clinopyroxene

Clinopyroxene is commonly found with orthopyroxene, and similarly with amphibole and biotite. It is concluded that clinopyroxene formed more or less contemporaneously with orthopyroxene.

Sillimanite

Sillimanite occurs in most high-grade metasedimentary bands. It may be present either as fine needles, usually enclosed in garnet and cordierite porphyroblasts (figs. 7

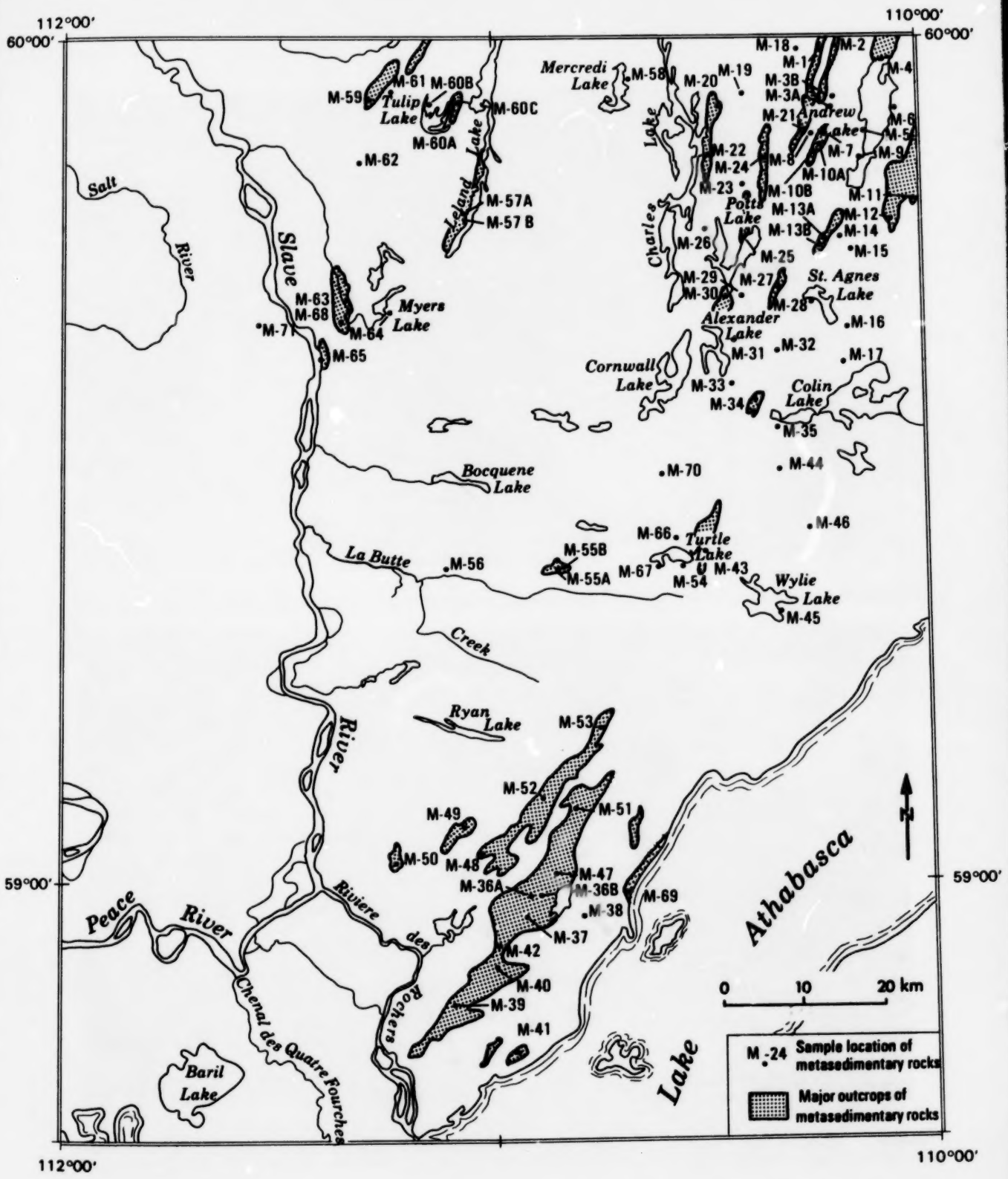

FIGURE 4. Location of metasedimentary rock samples used in this study, with indication of the major outcrops of metasedimentary rocks.

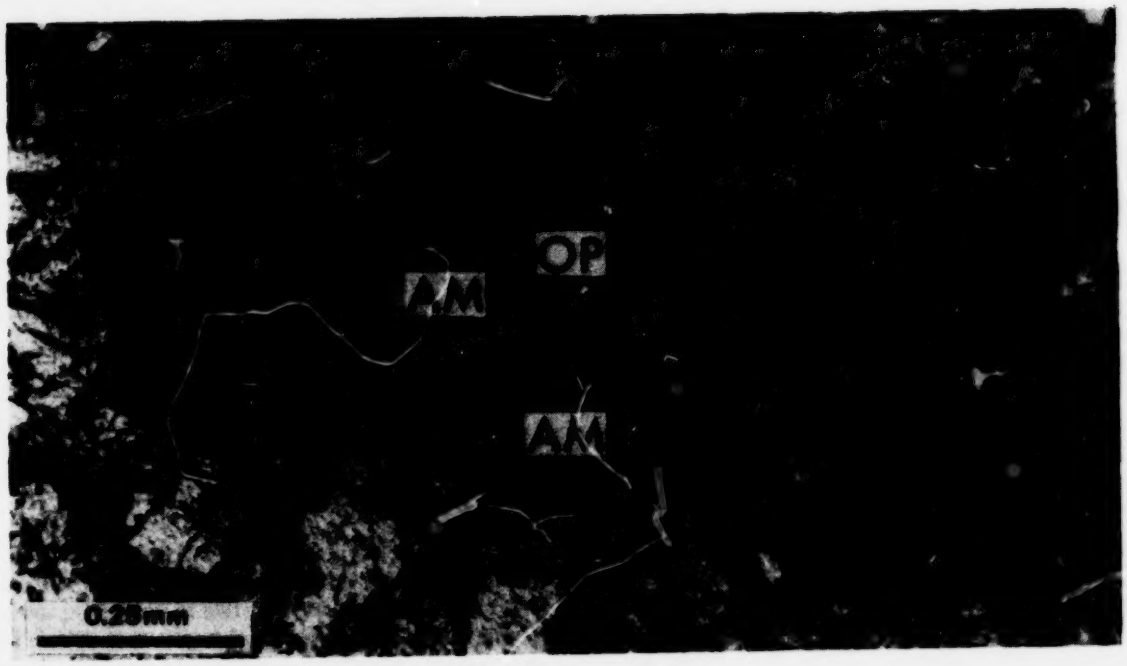

FIGURE 5. Orthopyroxene (OP) enclosed by light green amphibole (AM). Plane polarized light (Sample M-64).

FIGURE 6. Orthopyroxene (OP) with preferred orientation partly replaced by dark green amphibole (AM) without preferred orientation. Plane polarized light. (Sample M-70).

and 8), or as larger prismatic crystals. Though much less common, the larger crystals may also be enclosed by cordierite (fig. 9) and garnet. Sample M-4 shows sillimanite to be affected by two phases of folding, whereas biotite was only folded during the second phase. Andalusite encloses sillimanite and therefore is probably younger (fig. 10). Using age relationship criterion 8, it is inferred from these observations that most sillimanite formed early in the history of these rocks, before crystallization of garnet and cordierite. Some sillimanite may have developed at a later stage, concurrently with the formation of garnet and cordierite.

Hercynite Spinel

Hercynite spinel is present in many rocks which also contain cordierite and sillimanite. These rocks are generally located west of the Allan Fault zone. The only occurrences of spinel east of the Allan Fault relate to minor grains found in metasedimentary samples M-3A, M-24 and M-25. Here, the spinel is a green-brown variety as compared to the dark green spinel in the west. The textural relationships of hercynite spinel are very similar to those of sillimanite in that it can be enclosed by cordierite (figs. 7 and 9) or garnet. Hercynite spinel is flattened in those rocks where garnet is flattened. The conclusion is that hercynite spinel must be contemporaneous with sillimanite (age relationship criteria 1 and 2) and older than cordierite and garnet.

Corundum

Corundum is present in a few metasedimentary bands, in the area west of the Allan Fault. Such restricted distribution suggests slightly different metamorphic conditions existed in the western part of the area during early phases of the metamorphic history. Corundum is typically in close contact with, and in some cases completely surrounded by, hercynite spinel. This relationship may indicate that corundum is older. Cordierite commonly encloses both corundum and hercynite spinel. Sample M-55B shows corundum and minor hercynite spinel enclosed by andalusite porphyroblasts (fig. 11).

It is concluded that corundum formed approximately contemporaneously with sillimanite and hercynite spinel.

Cordierite

Cordierite, encountered in the majority of the metasedimentary bands, forms porphyroblasts that

FIGURE 7. Flattened cordierite (CD) porphyroblast enclosing hercynite spinel (SP) and sillimanite (SI) needles. Crossed nicols. (Sample M-48).

FIGURE 8. Detail of cordierite porphyroblast of figure 7, showing bundles of silimanite needles and dark patches of hercynite spinel. Plane polarized light. (Sample M-48).

FIGURE 9. Sillimanite (SI) prisms, hercynite spinel (SP) and quartz (QU) all enclosed by cordierite (CD). Plane polarized light. (Sample M-57A).

FIGURE 10. Sillimanite (SI) prisms enclosed by andalusite (AN). Plane polarized light. (Sample M-62).

enclose pre-existing minerals, including sillimanite, hercynite spinel and corundum. In samples that show late-stage deformation with mortar textures of quartz and feldspar, the cordierite porphyroblasts show flattening and form augen (fig. 7). Cordierite commonly shows well-developed sector twinning and varied amounts of pinite alteration. Cordierite is typically intimately intergrown with garnet. Using the age relationship criteria it is concluded that cordierite is younger than hercynite spinel, corundum and most sillimanite, and is contemporaneous with garnet. Chemical analyses reveal the presence of two cordierite varieties with different Mg/Mg + Fe ratios, hence, cordierite grew during two stages. In the first stage, it grew together with garnet and possibly with sillimanite. In a second stage, it grew with garnet of a different composition (see also under the heading "Fe-Mg cation exchange thermobarometry").

Andalusite

Andalusite is present in several of the metasedimentary bands, in both the eastern and western parts of the area. Although it is not found south of 59°15' in the Ryan Lake and Fort Chipewyan districts, it is present in a granitoid sample (373) from near Ryan Lake.

Andalusite encloses corundum, hercynite spinel, (fig. 11) and sillimanite (fig. 10). It always forms porphyroblasts (locally poikiloblastic) but they are never extensively affected by deformation. The porphyroblasts may enclose biotite and appear to nucleate on these grains. Sample M-138 shows andalusite with cordierite, which are in places intergrown.

Andalusite grew at a fairly late stage in the history of the metasediments, probably during the second stage of cordierite growth and possibly extending beyond the period of cordierite crystallization. Andalusite grew under low-pressure conditions, as indicated by the absence of deformational effects on andalusite. The absence of andalusite in the southern part of the area indicates that temperatures in this area were a little lower during the later phases of metamorphism. This absence suggests that the southern area represented either a higher crustal level at that time, or alternatively, that a lower geothermal gradient existed.

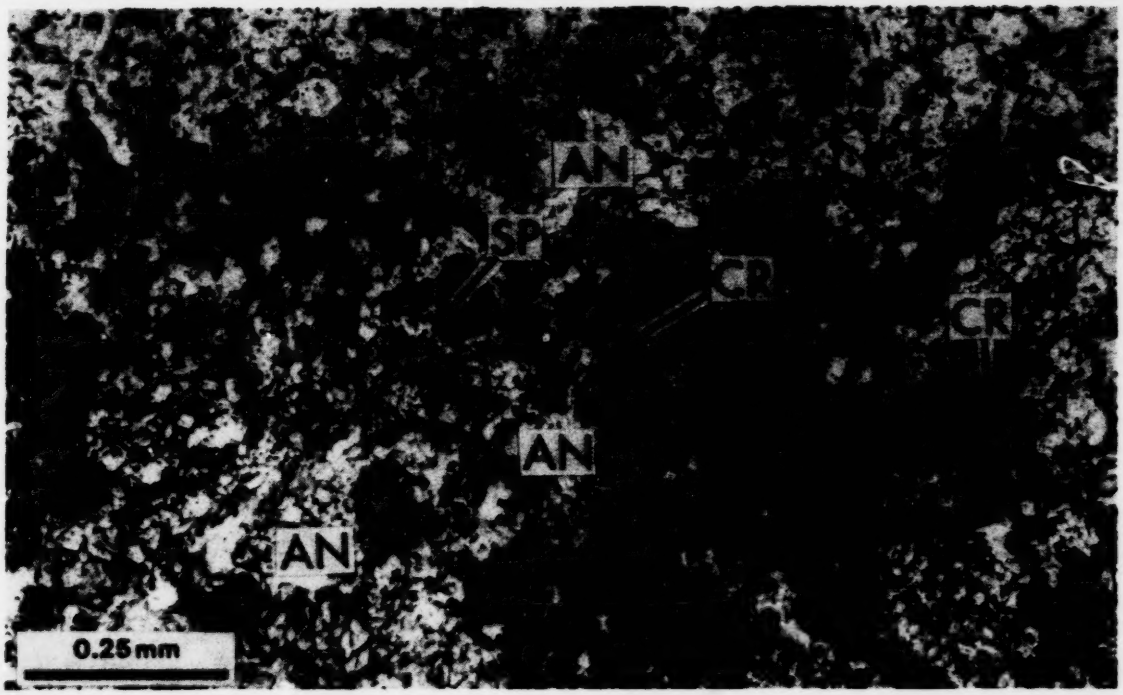

FIGURE 11. Corundum (CR) and minor hercynite spinel (SP)enclosed by andalusite (AN) porphyroblasts. Plane polarized light. (Sample M-55B).

Garnet

Garnet of almandine composition (appendix D) is present in most high-grade metasedimentary bands. Garnet commonly has inclusions of quartz, sillimanite, hercynite spinel and biotite. In many samples, garnet is closely associated with cordierite and shows no alteration or reaction from the contact. It is concluded that garnet is younger than sillimanite, hercynite spinel and corundum, and is contemporaneous with cordierite. Microprobe analyses show the presence of two varieties of garnet having different Fe/Fe + Mg ratios. The lower Fe/Fe + Mg ratio variety typically has sillimanite inclusions and may be rimmed by the higher Fe/Fe + Mg ratio variety of garnet (see under heading "Fe-Mg cation exchange barometry"). Sample M-3A shows garnet to contain inclusions of fine sillimanite needles, quartz and biotite. Sillimanite is preferentially found in more elongated garnet crystals. These elongated, flattened crystals probably represent an older generation of garnet than the more equant crystals.

These observations suggest that garnet was formed during two stages. In the first stage, it grew together with cordierite and possibly sillimanite; in the second, it grew with cordierite of a different composition.

Amphibole

Amphibole is not found in the metapelitic rocks with garnet, cordierite, or sillimanite, but occurs in the more basic phases of the metasedimentary bands. Both light and dark green varieties are present. Amphibole is commonly found in rocks containing pyroxene, which it replaces along the edges or overgrows (figs. 5 and 6).

It is assumed that amphibole grew after pyroxene under distinctly different P-T conditions. An amphibole from metasediments, dated by Baadsgaard and Godfrey (1972, table 1, sample 68-3-2A) gave an age of 1820 million years.

Biotite

Biotite is present in almost all metasedimentary rocks of the area. It exhibits a wide variety of textural relationships and forms inclusions in the older variety of garnet.

Where the rock is tectonically flattened, some biotite is folded, whereas other crystals form porphyroblasts that cut across the foliation or form polygonic arcs. These textural relationships indicate both pre- and post-tectonic origins. Biotite is also found in the low-grade metasedimentary rocks. Biotite and muscovite from a variety of rocks, including the metasediments, give an average K/Ar age of 1790 ± 40 million years (Baadsgaard and Godfrey, 1972). The small age scatter in samples from all rock units indicates that the micas were reset during a last thermal event The low-grade metasediments were affected by the same event, as shown by an age of 1760 million years for biotite from metavolcanic rocks of the Waugh Lake band (Baadsgaard and Godfrey, 1972, table 1, sample 68-98-2).

Alkali-feldspar

Alkali-feldspar forms porphyroblasts that enclose garnet, sillimanite, biotite, quartz and plagioclase. It can be poikiloblastic. Late deformation caused flattening of these crystals. The conclusion is that the majority of the alkali-feldspar co-crystallized with the younger growth phases of cordierite and garnet. The alkali-feldspar forms porphyroclasts in mylonites, and it also crystallized with epidote along late-stage cracks.

Muscovite

Muscovite is found both as fine-grained sericite and as larger crystals. It may replace feldspar and cordierite, and it is commonly found along late-stage fault zones in mylonites. These textural and structural relationships clearly indicate the retrograde character of muscovite. Muscovite appears as a primary metamorphic mineral in the low-grade metasediments of the Waugh Lake and Burntwood Groups, where it forms the cleavage in slates and phyllites.

Chlorite

Chlorite is present both as a retrograde replacement of garnet and biotite, and as a primary mineral in the low-grade metasediments.

Epidote

Epidote appears in a metamorphic retrograde role, both as a replacement of garnet and biotite and also along cracks together with alkali-feldspar. In the low-grade metasediments, epidote is probably a primary metamorphic mineral.

Tourmaline

Tourmaline was found in the Waugh Lake group metasediments near the southeast corner of Waugh Lake (Sample M-11). Boron metasomatism is believed to be responsible for this abnormal concentration of tourmaline (Watanabe, 1961, p. 71).

Quartz

Quartz is present in most samples. It is stable over a wide range of P-T conditions and is omitted from the metamorphic mineral inventory (appendix A). However, microstructures of quartz and other minerals give detailed information about the deformational history of rocks (see Hobbs, *et al.*, 1976). For example, the observation that quartz forms elongated lenses within the metamorphic foliation is important. This type of platy quartz fabric has been described from many granulite facies terrains (Brown *et al.*, 1969; Winkler, 1967, p. 135). It is a type of blastomylonitic structure because the quartz completely recrystallized after the deformation that gave rise to the lenses. These structures are assumed to have formed by the process of dislocation creep (Kerrich and Allison, 1978). This deformation is early, as indicated by inclusions of platy quartz and sillimanite in garnet (fig. 12). The garnet is elongated, which indicates that it was also flattened. Late-stage deformation results in undulose extinction and mortar structures. This deformation is extreme along late-stage fault zones, resulting in mylonites with flaser structures of completely annealed quartz.

Plagioclase

Plagioclase is present in most samples and is excluded from the metamorphic mineral inventory.

GRANITOIDS (NORTH OF LAKE ATHABASCA)

As stated under "Petrography," most of the characteristic metamorphic minerals are present in the Slave Granitoids. Most of the following descriptions are from these rocks. Some additional information came from the Thesis Lake Granitoids (orthopyroxene and biotite), Colin Lake Granitoids (garnet, alkali-feldspar and biotite), Wylie Lake Granitoids (garnet, alkali-

FIGURE 12. Inclusions of platy quartz (QU) grains and sillimanite (SI) needles in garnet. Crossed nicols. (Sample M-60A).

feldspar and biotite), and Arch Lake Granitoids (garnet, alkali-feldspar and biotite). All samples with metamorphic minerals are listed in appendix B; their locations are given in figure 13.

Orthopyroxene

Orthopyroxene is present in a few granitoid samples, and optical determinations show it to be hypersthene ($-2V \approx 60°$). Hypersthene is replaced along the rims by biotite (fig. 14), indicating a lower metamorphic grade at a later stage.

Clinopyroxene

Clinopyroxene coexists with orthopyroxene, indicating that they are contemporaneous.

Sillimanite

Sillimanite is a common minor constituent of the Slave Granitoids. Sample 444 shows sillimanite surrounded by garnet and biotite (fig. 15). In some cases it is concentrated in the finer grained parts of mortar textures (fig. 16). It is concluded that granitoid sillimanite is contemporaneous with the sillimanite found in the metasediments.

Hercynite Spinel

Hercynite spinel is another minor constituent that is typical of the Slave Granitoids. In some cases it is surrounded by sillimanite, garnet, and biotite (fig. 15), indicating that spinel is formed earlier. It is probably contemporaneous with hercynite spinel in metasediments.

Corundum

Corundum has been observed in a few samples, but only in Slave Granitoids. It can be completely enclosed by hercynite spinel. Corundum in the Slave Granitoids is assumed to be the same age as that in the metasediments.

Cordierite

Cordierite is typical of the Slave Granitoids, especially where sillimanite and hercynite spinel are also present.

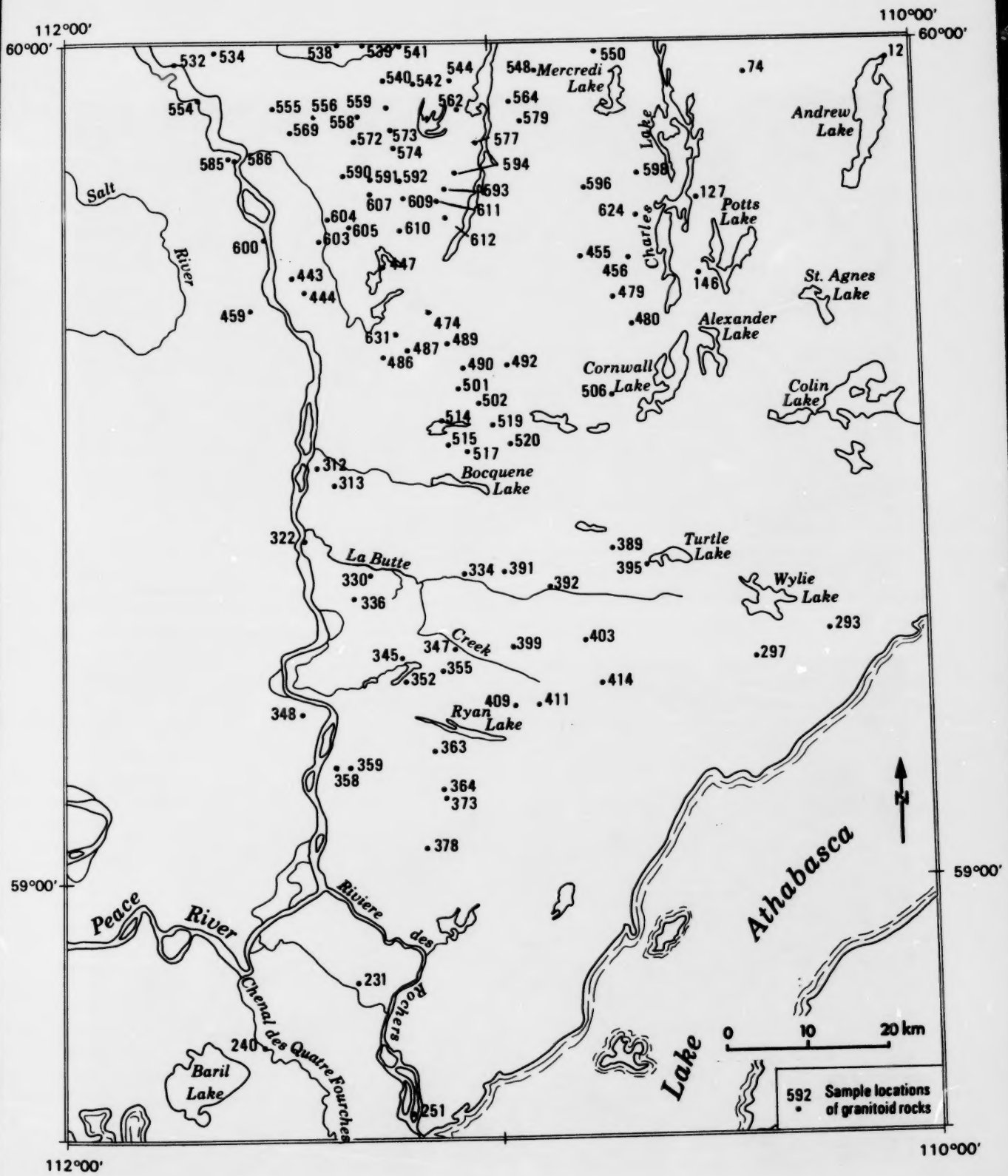

FIGURE 13. Location of granitoid rock samples north of Lake Athabasca.

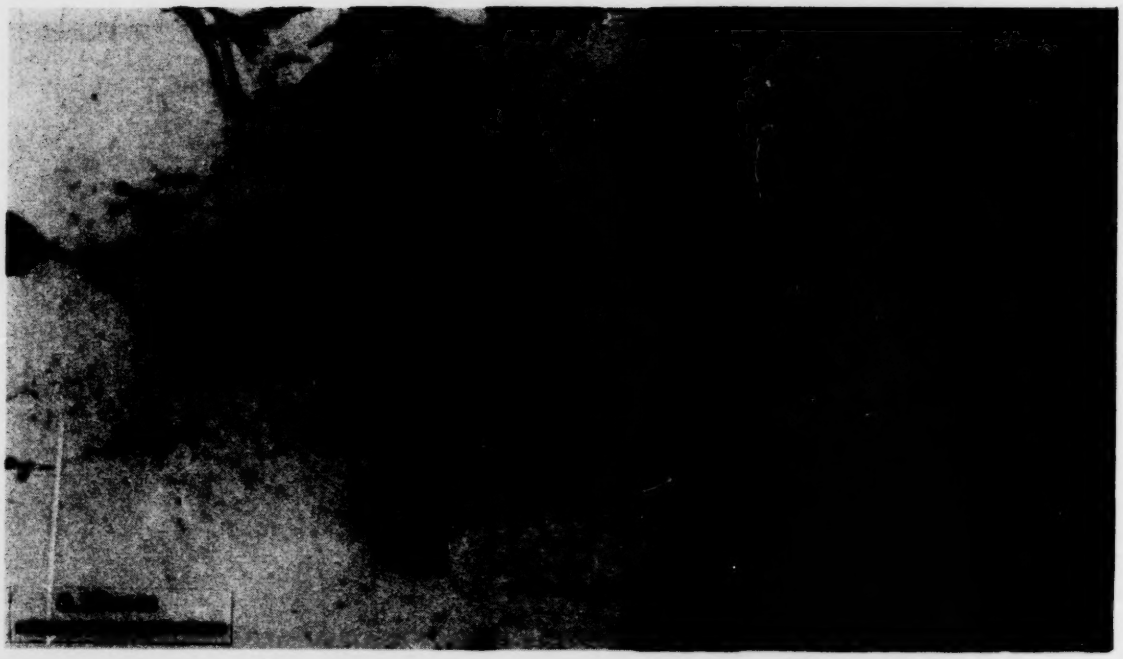

FIGURE 14. Orthopyroxene (OP), partly replaced by biotite (BI) along rim. Plane polarized light. (Slave Granitoid, sample 389).

FIGURE 15. Zoned mineral relationships with a core of hercynite spinel (SP) surrounded by sillimanite (SI) in turn enclosed by biotite (BI) and garnet (GA). Plane polarized light. (Slave Granitoid, sample 444).

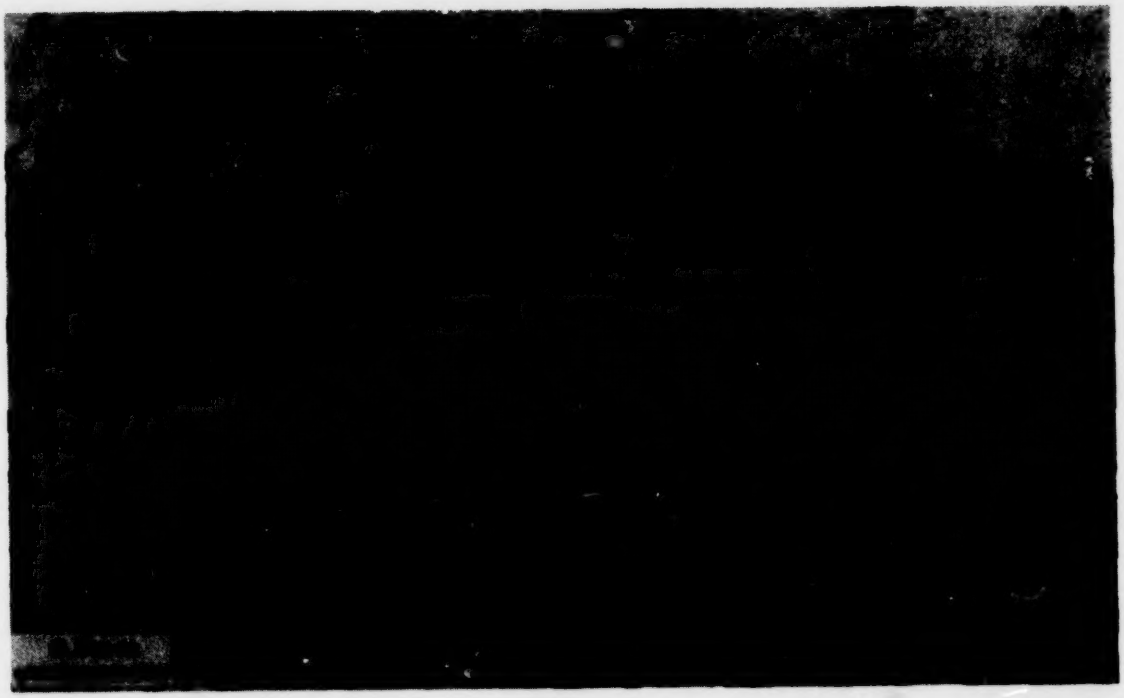

FIGURE 16. Sillimanite concentrated in the finer grained parts of a mortar texture in between alkali-feldspar porphyroblasts. Plane polarized light. (Slave Granitoid, sample 607).

A small metasedimentary inclusion, 2 x 10 cm, at location 586, contains cordierite, sillimanite, hercynite spinel, biotite, and garnet. The enclosing granitoid shows scattered sillimanite, cordierite, and hercynite spinel. These mineral occurrences provide good evidence as to the residual character of cordierite, garnet, sillimanite and hercynite spinel in the granitoid. Some cordierite grains form equant porphyroblasts. (fig. 17), whereas others have a pronounced flattening. The evidence suggests that granitoid cordierite is contemporaneous with cordierite in metasedimentary rocks.

Andalusite

Undeformed andalusite is present in two Slave Granitoid samples. It is assumed to have formed together with andalusite of the metasediments.

Garnet

Garnet is present in a range of granitoid rocks, but it is most common in the Slave Granitoids. Microprobe analyses of garnets from the Slave Granitoids show them to be almandine (table 1). Inclusions in garnet most commonly consist of quartz and biotite but occasionally are sillimanite and hercynite spinel (fig. 15). Some of the biotite may be formed by the breakdown of garnet. Garnet forms either equant porphyroblasts or is flattened in the platy quartz foliation. The considerable extent of this flattening is indicated by garnets with axial ratios close to 1 to 10 (fig. 18).

These observations indicate that garnets in Slave Granitoids and in metasediments within the Slave Granitoids are of the same age. Garnets in other granitoids are more difficult to correlate because of the lack of diagnostic metamorphic minerals in both the granitoids and their closely associated metasediments.

Amphibole

Amphibole is present in several of the granitoid bodies. However, it always lacks an association with other diagnostic metamorphic minerals. Consequently, none of the amphibole-bearing localities are included in the metamorphic mineral inventory (appendix B).

FIGURE 17. Cordierite porphyroblasts with characteristic twinning and pinite alteration. Crossed nicols. (Slave Granitoid, sample 568).

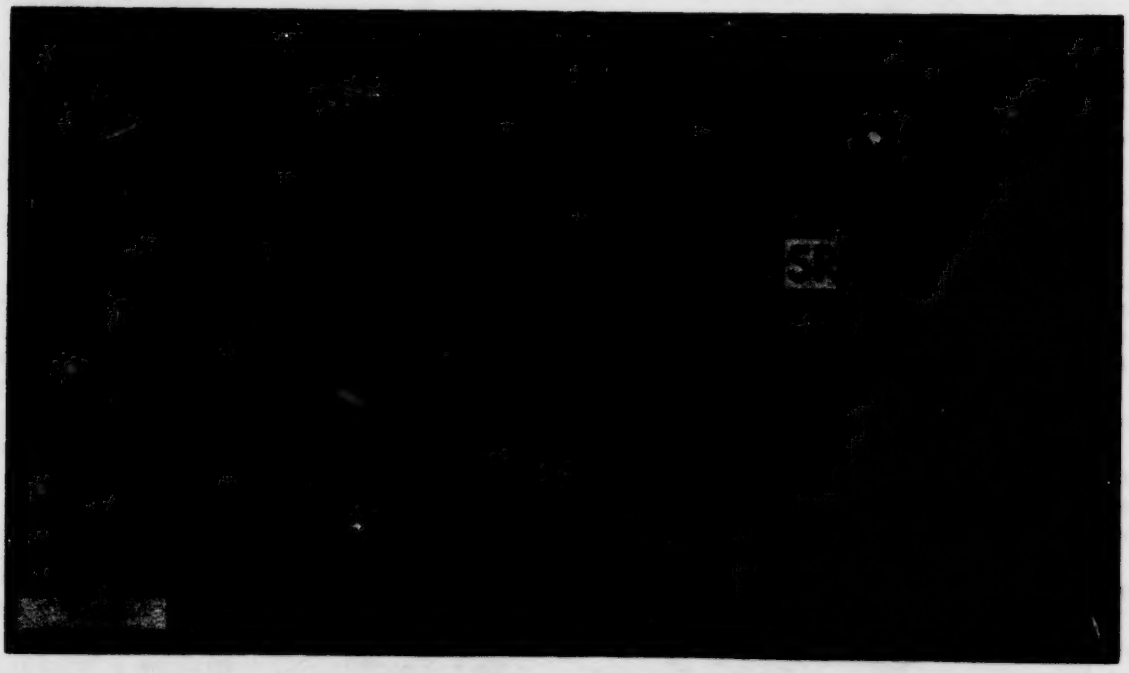

FIGURE 18. Flattened garnet (GA) crystal with parallel aligned hercynite spinel (SP) fragments. Plane polarized light. (Slave Granitoid, sample 352).

FIGURE 19. Late formed perthitic alkali-feldspar porphyroblast with inclusions of plagioclase and quartz. Crossed nicols. (Arch Lake Granitoid, sample 550).

Biotite

Biotite is present in almost all granitoids. It shows a variety of textural relationships, indicating both pre- and post-kinematic origins. Biotites from granitoids dated by Baadsgaard and Godfrey (1972) clearly give reset ages of 1790 ± 40 million years.

Alkali-feldspar

Alkali-feldspar is common to all granitoids, typically as megacrysts. Peikert (1963) showed that they are porphyroblasts in the Colin Lake Granitoids and they are likewise assumed to be porphyroblasts in other granitoids. Typical inclusions in the porphyroblasts are plagioclase (zoned in part) and quartz (fig. 19). Alkali-feldspar in the Slave Granitoids also encloses sillimanite. The alkali-feldspar megacrysts are typically aligned in the foliation. These data indicate that alkali-feldspar in the granitoids grew contemporaneously with alkali-feldspar in the metasediments, during the younger crystallization phase.

Muscovite

Muscovite is present in all granitoids, either as fine-grained sericite or as larger crystals, and is clearly retrograde.

Chlorite and Epidote

Chlorite and epidote occur only as retrograde minerals in the granitoids.

Quartz

Quartz is a constituent of all granitoids and is omitted from the inventory (appendix B). Lenses of platy quartz grains are found that are similar to those in the metasediments (fig. 20). This structure is especially common in the Slave Granitoids and helps to define the foliation. According to Kerrich and Allison (1978) these structures form by the process of dislocation creep under high temperature and pressure. The foliation, which is partly defined by the quartz lenses, forms

FIGURE 20. Lenses of platy quartz grains in a mortar texture of alkali-feldspar and quartz. Crossed nicols. (Slave Granitoid, sample 569).

macroscopic fold structures (Langenberg and Ramsden, 1980). This relationship indicates that the quartz lenses are older than the fold structures, although the possibility that they are the same age cannot be excluded. The latter would be the case where quartz lenses formed as a result of stress fields during the formation of the macroscopic structures, as in the experiments by Dixon (1975). Major faults cutting across the macroscopic folds are considered to be younger. They are accompanied by mylonites, characterized by highly sheared and recrystallized flaser structures of quartz.

Plagioclase

Plagioclase is present in most samples and is omitted from the metamorphic minerals inventory. In some cases it forms porphyroclasts.

GRANITOIDS (SOUTH OF LAKE ATHABASCA)

Several metamorphic minerals are present in the granitoid rocks of the Marguerite River area (appendix C). The location of these samples is shown in figure 21. They include: pyroxene, amphibole and garnet. In sample 6, the pyroxenes, including orthopyroxene, are surrounded by younger amphibole. Muscovite and some of the biotite are of retrograde origin.

METAMORPHIC FACIES

The critical age relationships between the metamorphic minerals permit several phases of metamorphism to be distinguished (Godfrey and Langenberg, 1978). The data from the granitoids are consistent with the age relationships in the metasediments and the polymetamorphic history is adequately recorded by the high-grade metasediments. Most data on Fe-Mg cation exchange thermobarometry, presented under the next heading, are from these rocks.

The peraluminous sillimanite-garnet-cordierite-feldspar-quartz rocks provide the following information. The oldest metamorphic phase is characterized by the minerals, sillimanite, hercynite spinel and corundum.

Pyroxene-bearing rocks (devoid of cordierite and sillimanite) show that ortho- and clinopyroxene formed

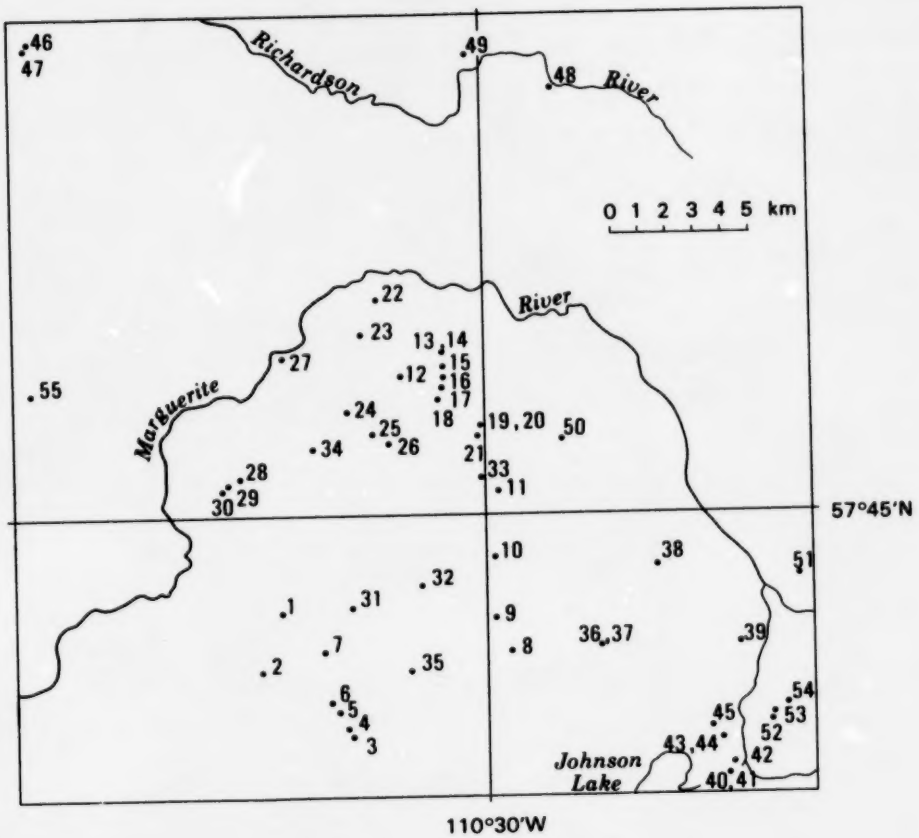

FIGURE 21. Location of granitoid rock samples south of Lake Athabasca.

at an early stage, followed by amphibole and biotite. This early stage is tentatively correlated with the first phase of metamorphism in the sillimanite-garnet-cordierite rocks.

Thus, we arrive at a first phase (M_1) characterized by the minerals orthopyroxene (hypersthene), clinopyroxene, sillimanite, hercynite spinel and corundum. This mineral assemblage is indicative of granulite facies conditions (Turner, 1968). Because the metasediments are considered to be part of an Archean basement (see under heading "General geology"), M_1 is tentatively assigned to the Archean. The locations of samples containing M_1 minerals are indicated in figure 22.

A second cycle of metamorphism (M_2) is found in the metasediments. These sillimanite-garnet-cordierite rocks contain minerals that are younger than M_1. They are indicative of amphibolite-granulite transitional facies conditions (Turner, 1968). Amphibole from rocks lacking cordierite and garnet is tentatively correlated with this transitional phase. The locations of the samples containing the more important M_2 minerals are shown in figure 23.

Textural relationships and microprobe studies (under the next heading) indicate that cordierite and garnet grew during two stages. A moderate-pressure granulite facies event ($M_{2.1}$) can be distinguished from a younger low-pressure amphibolite facies overprint ($M_{2.2}$).

All of the rock units show, in places, a last retrograde stage of metamorphism ($M_{2.3}$) that is characterized by the minerals muscovite, chlorite, biotite, and epidote, which are indicative of greenschist facies conditions (Turner, 1968). These retrograde minerals are also

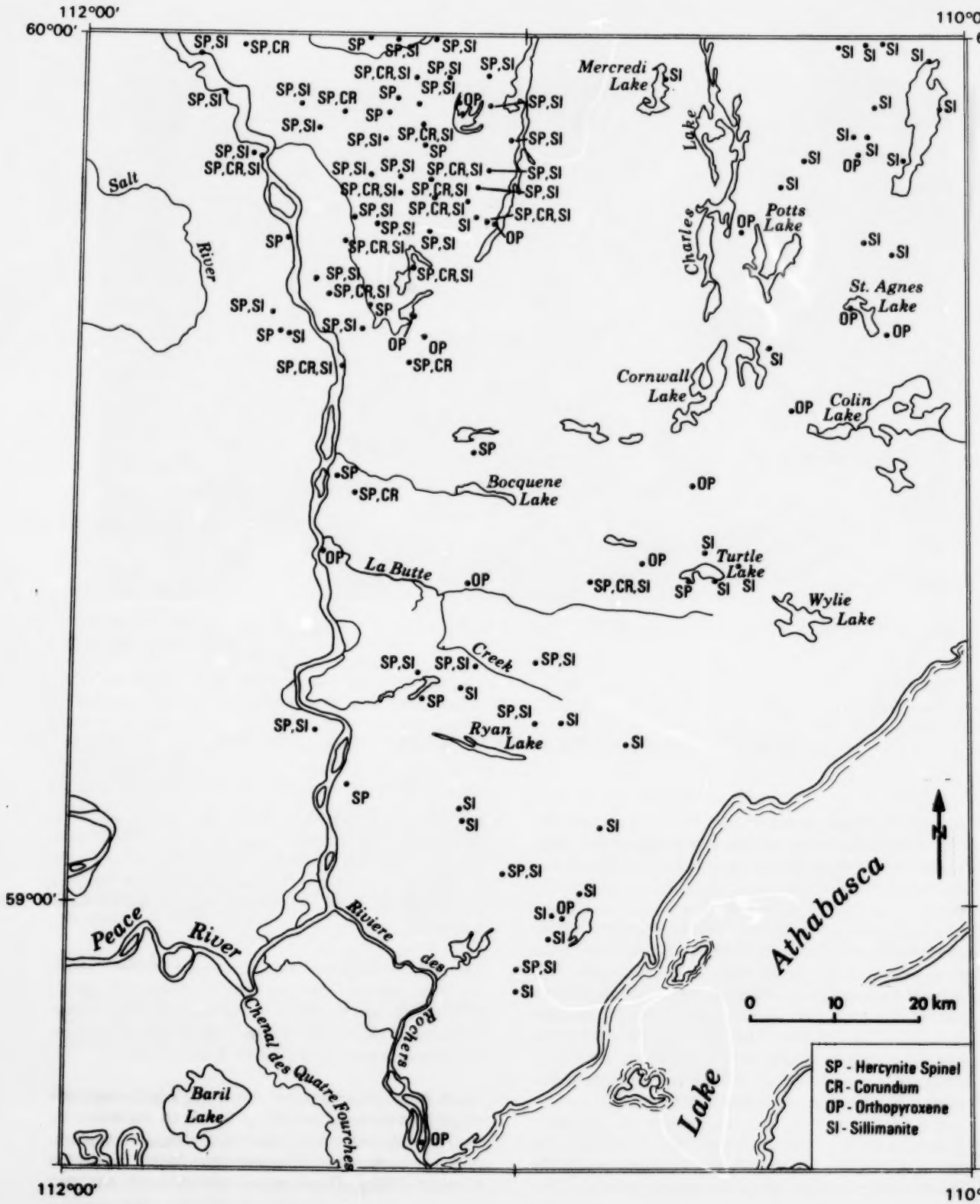

FIGURE 22. Location of samples containing metamorphic minerals formed during the first cycle of metamorphism (M_1). Note that some of the sillimanite may be formed during the second cycle of metamorphism.

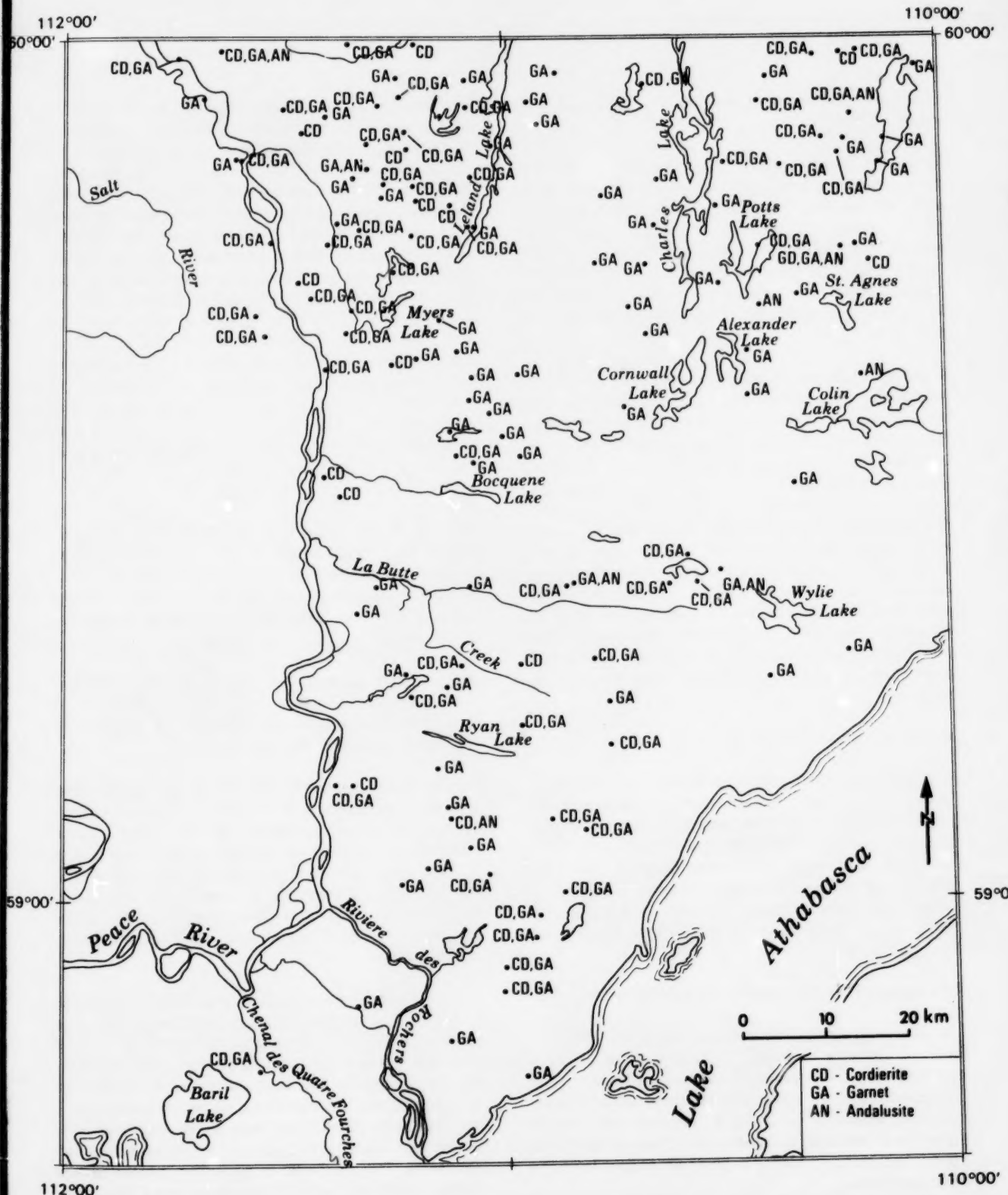

FIGURE 23. Location of samples containing the more important metamorphic minerals formed during the second cycle of metamorphism (M_2).

found in mylonitic rocks developed along major fault zones.

Muscovite, chlorite, biotite and epidote are primary metamorphic minerals in the low-grade metasediments and indicate that the Waugh Lake and Burntwood groups attained only greenschist facies conditions. Amphibole is found in the metavolcanics of the Waugh Lake Group. The greenschist facies of the low-grade metasediments is tentatively correlated with the retrograde greenschist facies ($M_{2\text{-}3}$) of the higher grade rock units.

A metamorphic facies map can be constructed after establishing the different phases of metamorphism and the distribution of diagnostic metamorphic minerals. High-grade metasediments, Slave Granitoids and Thesis Lake Granitoids show the effects of the granulite facies (M_1) and M_2 overprint. Other rock units, including Colin Lake Granitoids, Wylie Lake Granitoids, Arch Lake Granitoids and some minor granitoid bodies, show only an M_2 mineral assemblage. In the granite gneisses only biotite, amphibole and alkali-feldspar are present, but because of the large number of included high-grade metasedimentary bands, they are assumed to have experienced the same metamorphic history as these metasediments. The map of figure 24 was constructed from these observations (Godfrey and Langenberg, 1978; fig. 5).

South of Lake Athabasca

Orthopyroxene in the Marguerite River Granitoids indicates that granulite facies conditions prevailed in the early geologic history. The amphibole surrounding orthopyroxene further establishes an amphibolite facies overprint. Most rocks in the area, however, show the assemblage biotite-garnet-alkali-feldspar, indicative of amphibolite facies conditions only. A metamorphic facies map of the area was produced from these observations (fig. 25).

Fe-Mg CATION EXCHANGE THERMOBAROMETRY

As discussed earlier, the Precambrian Shield in northeastern Alberta consists of massive to foliated granitoids, granite gneisses and metasediments. The metasediments are commonly observed as rafts or inclusions within or as belts in contact with S-type granites as defined by White and Chappell (1977). In these occurrences, biotite is generally absent from the metasediments.

The S-type granites are characterized by the presence of relict spinel, garnet and cordierite or any combination of these. Rb/Sr studies suggest an age of 1938 ± 29 Ma (Nielsen *et al.*, 1981). The high $^{87}Sr/^{86}Sr$ initial ratio (0.710 ± 0.002) coupled with the relict aluminous metasedimentary phases strongly suggests that these granitoids were formed by anatexis and ultrametamorphism of a pre-existing basement gneiss complex. Cordierite-garnet pairs from metasediments coeval with these S-type granites consistently indicate a relatively dry metamorphic fluid ($X_{H_2O} < 0.4$) at P = 5.0 ± 0.7 kbar and T = 740 ± 30°C during the $M_{2.1}$ phase of metamorphism (fig. 26). The effects of regional uplift and erosion are evident subsequent to attaining these peak metamorphic conditions. Phase $M_{2.2}$ is recorded by both biotite-garnet and cordierite-garnet pairs in all areas. Metamorphic conditions during phase $M_{2.2}$ were P = 3.0 ± 0.3 kbar and T = 550 ± 55°C with $X_{H_2O} > 0.4$ (fig. 27).

The last phase, $M_{2\text{-}3}$, is recorded by K-Ar dating of biotites from a wide range of rock types, which yield an age of 1790 ± 40 Ma (Baadsgaard and Godfrey, 1972). Rocks yielding this younger age are typically chloritized or sericitized, suggesting lower greenschist facies conditions ($M_{2.3}$).

This section analyzes coexisting biotite-garnet and cordierite-garnet pairs and the pressures and temperatures of equilibration resulting from applied Fe-Mg cation exchange thermobarometry.

The samples chosen for this study are mainly peraluminous metasediments and contain varied proportions of sillimanite, cordierite, garnet, biotite, quartz, plagioclase, and (perthitic) alkali-feldspar. Minor phases include magnetite, hercynite spinel, monazite and ilmenite. Detailed petrographic examination resulted in the identification of two stages of equilibration, based on textural relationships and equilibrium mineral assemblages.

These textures and assemblages are shown in figures 28 and 29. The earlier formed assemblage ($M_{2.1}$) is cordierite-garnet-sillimanite-quartz. This critical assemblage is accompanied by perthitic alkali-feldspar, plagioclase, quartz and subordinate biotite in the surrounding matrix. Cordierite and garnet commonly contain inclusions of relict hercynite spinel and magnetite. Garnet also contains inclusions of quartz and prismatic sillimanite. The cordierite is generally untwinned and shows varied amounts of late-stage pinite alteration.

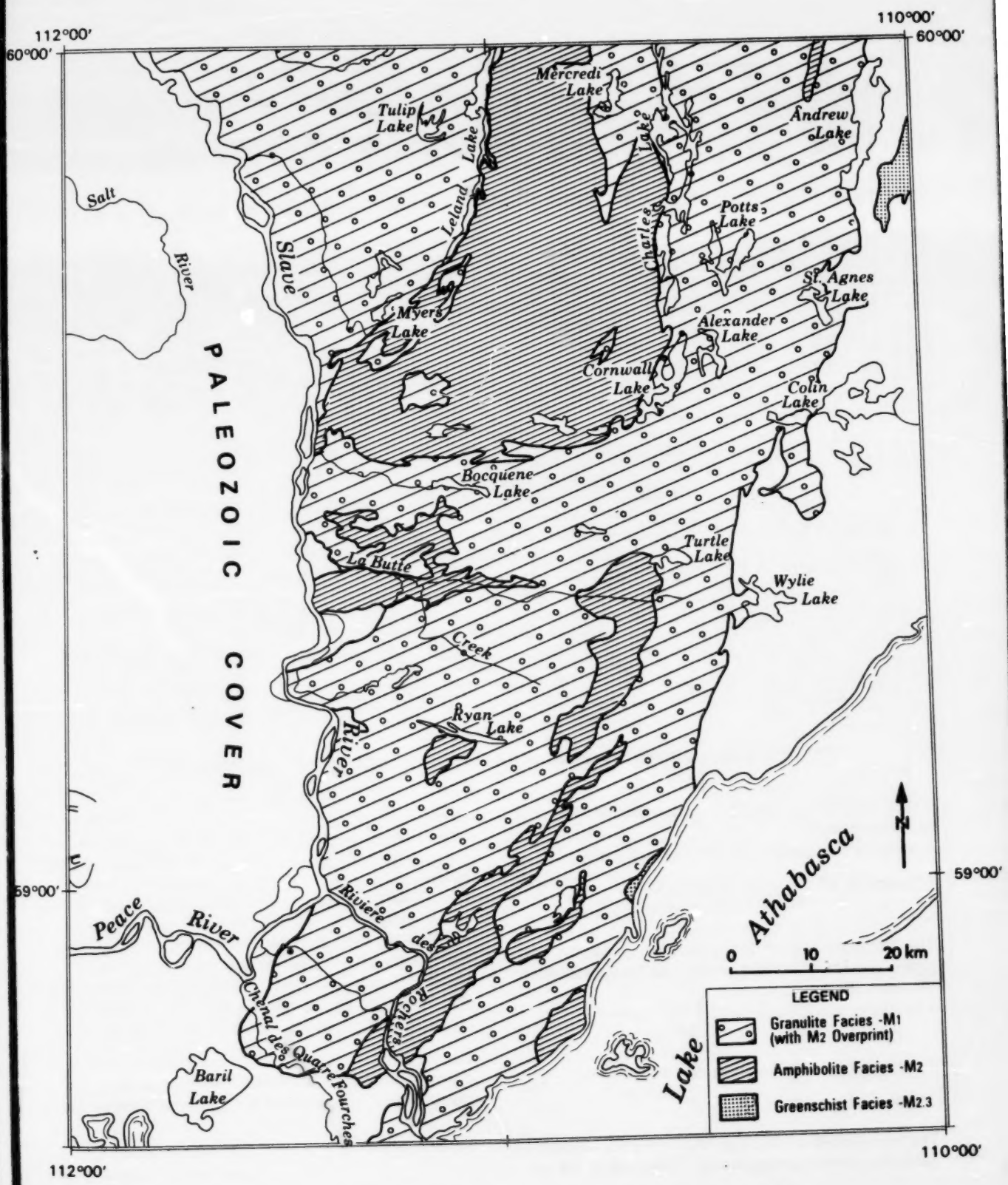

FIGURE 24. Metamorphic facies map of the Canadian Shield, north of Lake Athabasca.

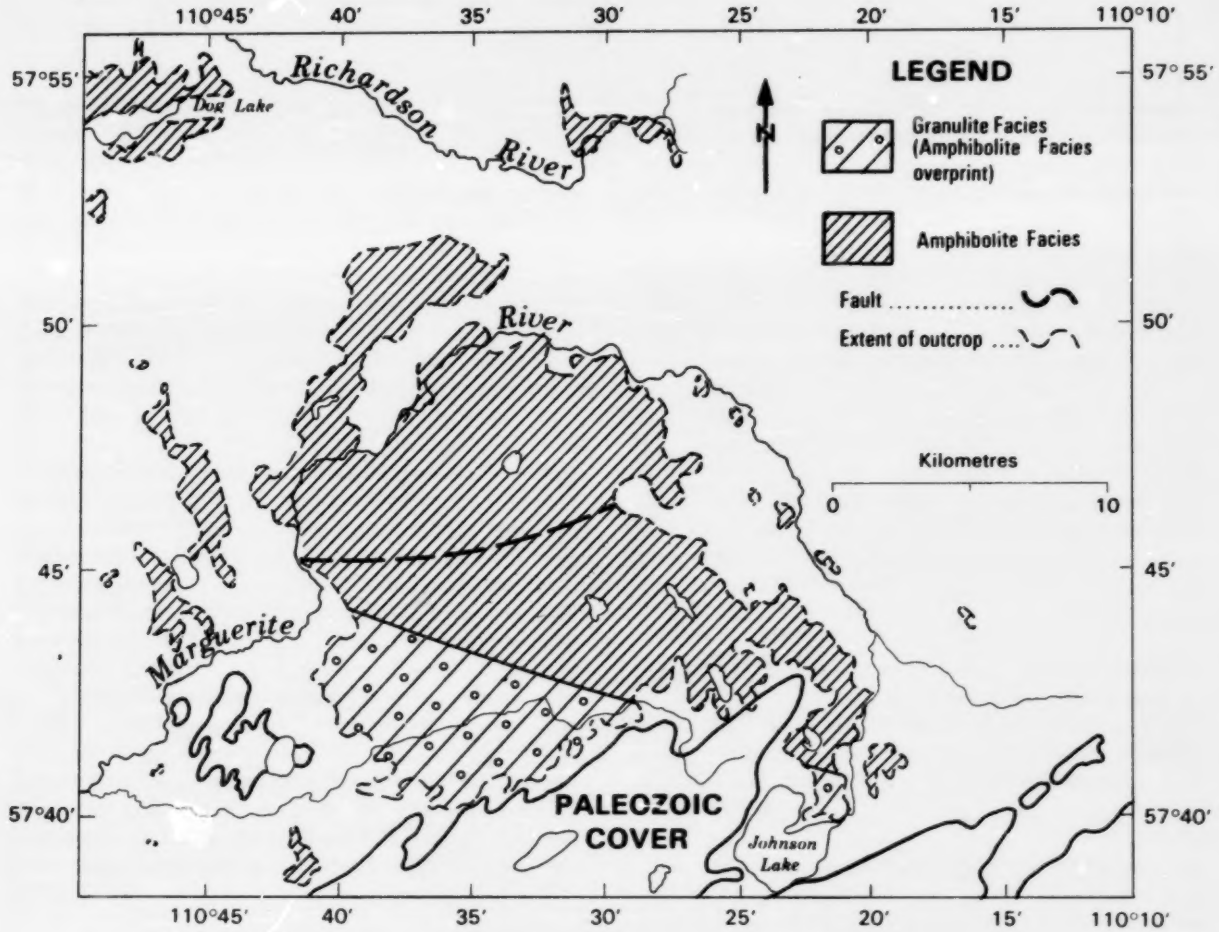

FIGURE 25. Metamorphic facies map of the Canadian Shield, south of Lake Athabasca.

The following reaction (R.1) produced the observed $M_{2.1}$ assemblage:

3 cordierite ⇌ 2 garnet + 4 sillimanite + 5 quartz

$$3(FeMg)_2Al_4Si_4O_{18} \rightleftharpoons 2(FeMg)_3Al_2Si_3O_{12} + 4Al_2SiO_5 + 5SiO_2 \quad \text{(R.1)}$$

The compositions of the coexisting cordierite and garnet were modified by a continuous Fe-Mg exchange (Reaction 2):

3 Fe cordierite + 2 Mg garnet ⇌ 3 Mg cordierite + 2 Fe garnet

$$3Fe_2Al_4Si_5O_{18} + 2Mg_3Al_2Si_3O_{12} \rightleftharpoons 3Mg_2Al_4Si_5O_{18} + Fe_3Al_2Si_3O_{12} \quad \text{(R.2)}$$

The later-formed assemblage ($M_{2.2}$) contains cordierite-garnet-biotite-plagioclase-biotite. Sillimanite is still present in most rock samples, but it is not found in contact with biotite or garnet and quartz. It is found primarily in the quartzo-feldspathic matrix or as inclusions in the newly formed cordierite. Cordierite from $M_{2.2}$ generally displays well-developed sector twinning, with little or no pinite alteration. $M_{2.2}$ cordierite has a higher Mg/Fe + Mg ratio than $M_{2.1}$ cordierite. $M_{2.2}$ garnet is free of sillimanite inclusions, and has a higher Fe/Fe + Mg ratio than $M_{2.1}$ garnet. It is found as small subhedral porphyroblasts and as rims on $M_{2.1}$ garnet. Both $M_{2.2}$ cordierite and garnet are in contact with alkali-feldspar.

Based on the observed mineral associations, the following reaction (R.3) produced the observed assemblage:

Biotite + sillimanite + quartz ⇌ cordierite + garnet + alkali-feldspar + vapor (R.3)

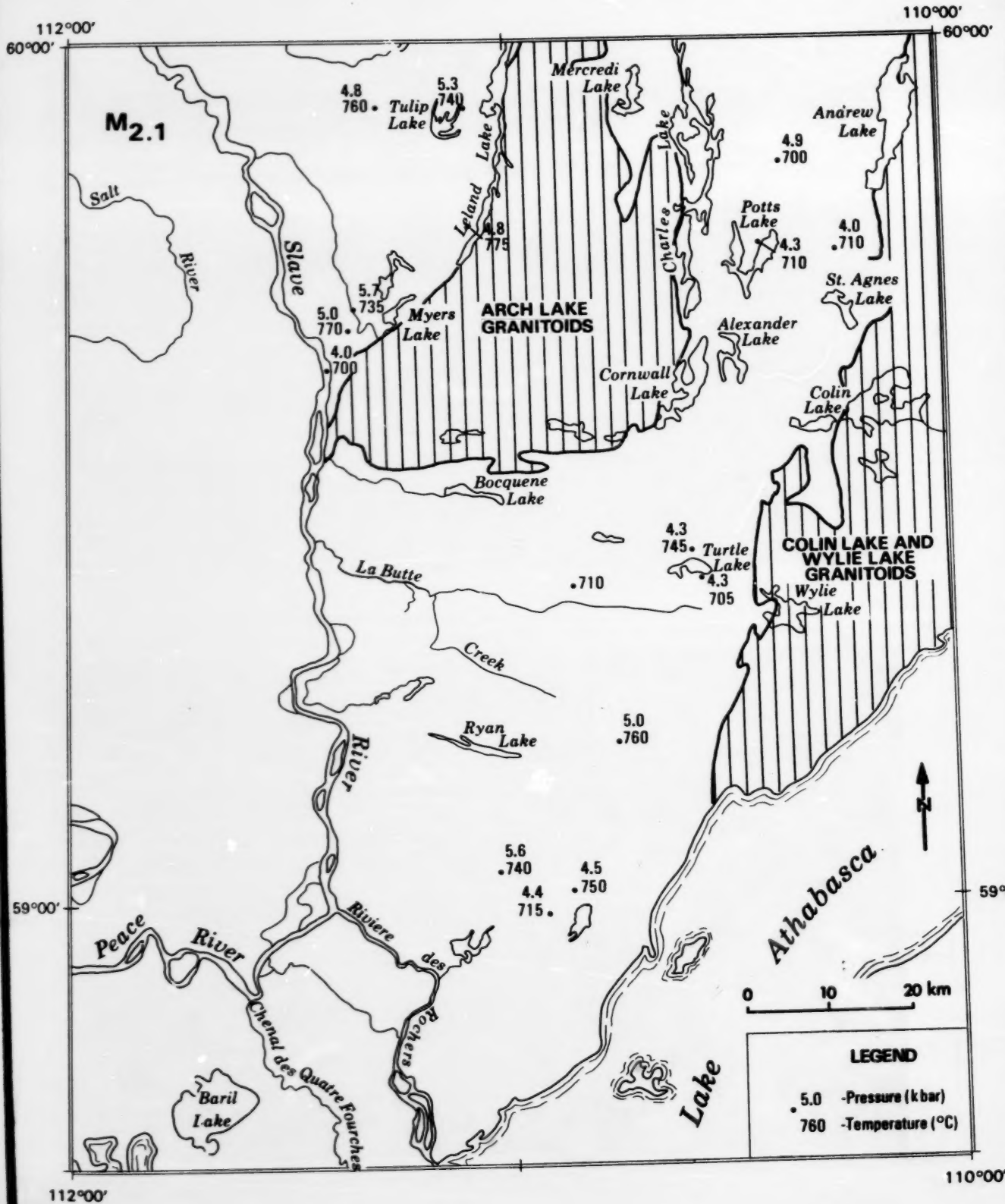

FIGURE 28. Calculated P-T values for the peak conditions of phase $M_{2.1}$ as tabulated in table 3.

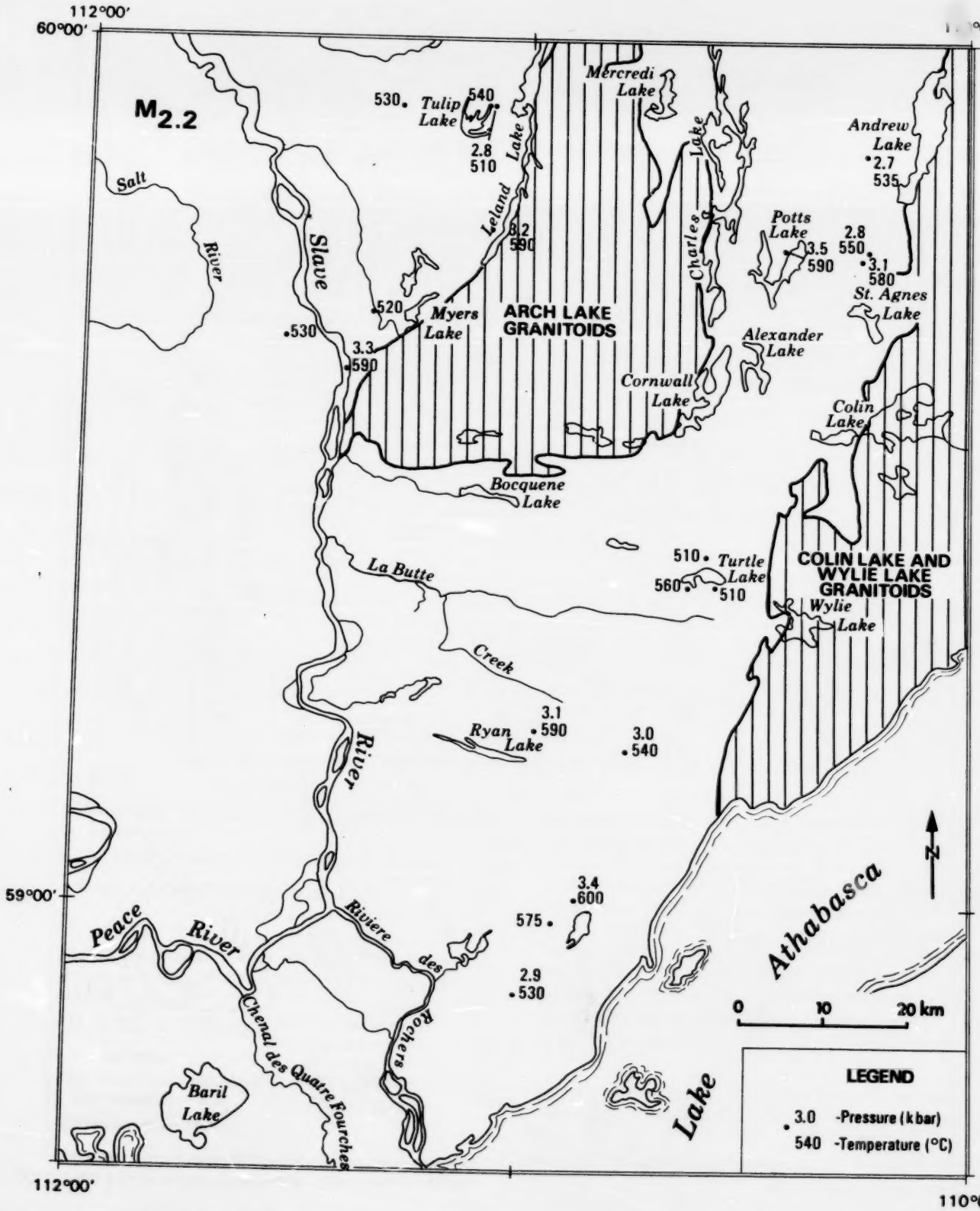

FIGURE 27. Calculated P-T values for the peak conditions of phase $M_{2.2}$ as tabulated in table 3.

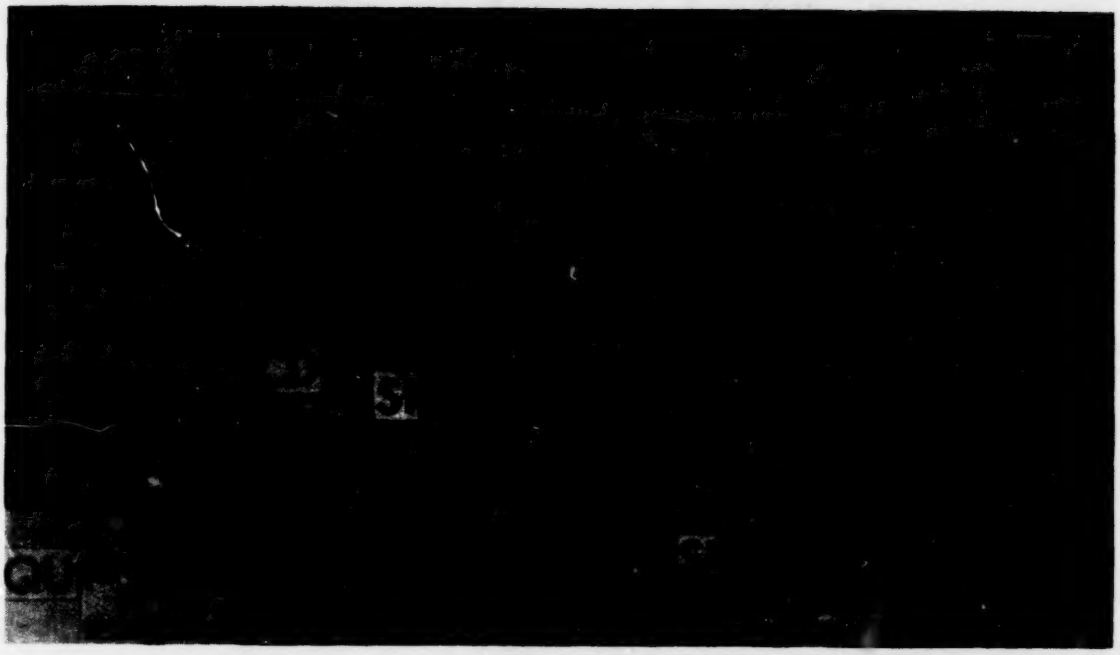

FIGURE 28. A. Metamorphic mineral assemblage of the moderate pressure granulite facies event ($M_{2.1}$); CD - cordierite, GA - garnet, SI - sillimanite, BI - biotite, QU - quartz, FS - feldspar. Sample M-25. Plane polarized light.

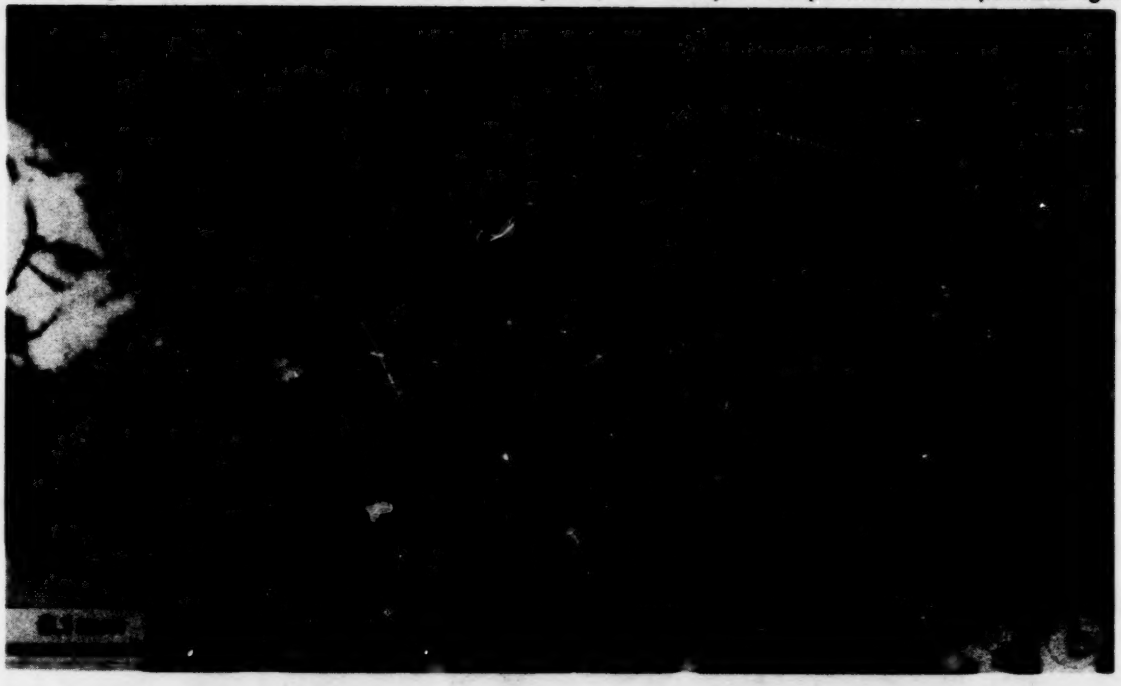

B. Same view, crossed nicols.

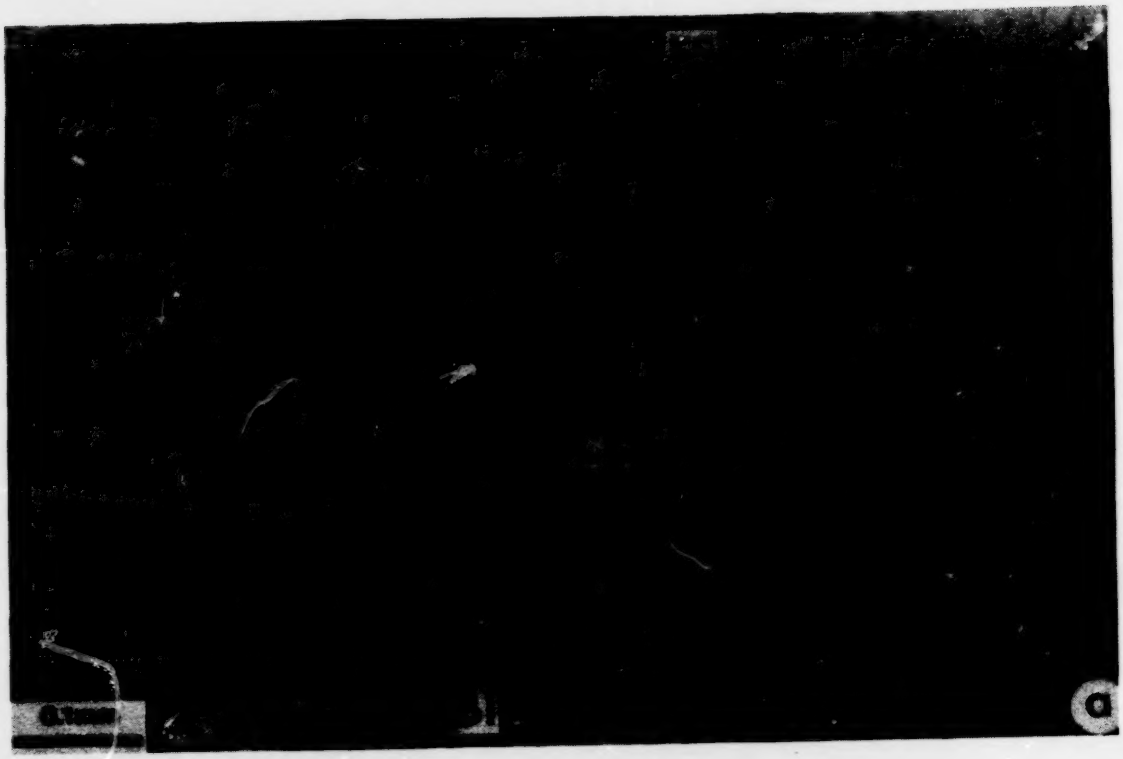

FIGURE 29. a. Metamorphic mineral assemblage of the low pressure amphibolite facies event ($M_{2.2}$). Symbols as in figure 28. Plane polarized light.

B. Same view, crossed nicols.

As was observed for $M_{2.1}$, a series of 3 Fe-Mg cation exchange reactions also proceeded at this time (R.2, R.4, R.5):

Fe biotite + Mg garnet ⇌ Mg biotite + Fe garnet (R.4)

Fe cordierite + Mg biotite ⇌ Mg cordierite + Fe biotite (R.5)

ANALYTICAL METHODS

Four hundred mineral analyses were collected at the microprobe laboratory at the Geological Survey of Canada using an energy dispersive system and a modified Bence-Albee data reduction program. Data were collected for the elements Si, Ti, Al, Fe, Cr, Mg, Mn, Ca, Na, and K. These elements were converted to oxides and structural formulae were calculated for biotite, cordierite, and garnet analyses (22, 18, and 24 oxygens respectively). Average analyses for the investigated minerals are presented in appendix D.

Based on the structural formulae, distribution coefficients (K_D's) for Fe, Mg, and Mn were calculated for coexisting biotite-garnet and cordierite-garnet pairs. Fe-Mg distribution data for biotite-garnet pairs were used to calculate the temperature of equilibration using the data and equation of Ferry and Spear (1978) and Nielsen (1977). Cordierite-garnet Fe-Mg distribution data were used to calculate temperature (Nielsen, 1977 and Hutcheon *et al.*, 1974) and pressure of equilibration using the data of Holdaway and Lee (1977) and the equations of Hutcheon *et al.*, (1974). The results of these calculations are presented in appendix D.

Garnet-Biotite Thermometry

Method 1 - Ferry and Spear (1978)

$$T°K = \frac{13390 + 0.057\,P}{5.723 - 5.962\,\ln K_D}$$

$$K_D = \left(\frac{Mg}{Fe}\right)_{gt} \cdot \left(\frac{Fe}{Mg}\right)_{Bi}$$

Successful application of this thermometer requires an estimate of pressure in bars, usually available from cordierite-garnet barometry. The major limitation is that this thermometer is based on experiments in the pure Fe-Mg system. Examination of the biotite and garnet compositions from northeastern Alberta shows moderate contents of TiO_2 in biotite and up to 2.5 percent combined MnO and CaO in garnet. The presence of these elements implies lower actual temperatures than those calculated by this method.

Temperatures calculated by this method for the $M_{2.1}$ event are not reliable above about 700°C because these temperatures are higher than the best equilibrium experimental data presented by Ferry and Spear (1978).

Method 2 - Nielsen (1977)

$$T°K = (3.644 \times 10^{-4} \ln K_D + 5.637 \times 10^{-4})^{-1}$$

$$K_D = \left(\frac{Fe}{Mg}\right)_{gt} \cdot \left(\frac{Mg}{Fe}\right)_{Bi}$$

This thermometer is a modification of Thompson's (1976) empirical data based on naturally occurring biotite-garnet pairs. Thus the presence of TiO_2 in biotite and CaO and MnO in low concentrations in garnet are taken into account by the presence of these elements in the naturally occurring minerals used in Thompson's study.

As can be seen in appendix D, there is a close correspondence between biotite-garnet temperatures calculated by method 2 and cordierite-garnet temperatures calculated using the equation of Nielsen (1977). Biotite-garnet temperatures calculated by method 2 are generally 30 to 50° lower than those from method 1 for $M_{2.1}$ and 10 to 50° lower than for $M_{2.2}$.

Cordierite-Garnet Thermometry

Method 1 - Nielsen (1977)

$$T°K = (3.841 \times 10^{-4} \ln K_D + 2.936 \times 10^{-4})^{-1}$$

$$KD = \left(\frac{Mg}{Fe}\right)_{cd} \cdot \left(\frac{Fe}{Mg}\right)_{gt}$$

As with method 2 biotite-garnet thermometry, this thermometer is based on Thompson's (1976) empirical equation using naturally occurring cordierite-garnet pairs and the relevant high-pressure-temperature data of Hensen and Green (1973).

Method 2 - Hutcheon *et al.* (1974)

$$T°K = \frac{58141.126}{3.648 \times (R \ln K_2 - 22.95) - 3.8252 \times (R \ln K_1 - 18)}$$

where

$$K_1 = \frac{\left(\frac{Fe}{Fe+Mg+Mn}\right)^6_{cd}}{\left(\frac{Fe}{Fe+Mg+Mn+Ca}\right)^6_{gt}} \qquad K_2 = \frac{\left(\frac{Mg}{Fe+Mg+Mn}\right)^6_{cd}}{\left(\frac{Mg}{Fe+Mg+Mn+Ca}\right)^6_{gt}}$$

and R is the universal gas constant.

The expression was derived from thermodynamic data for the pure Mg and Fe end member garnet and cordierite compositions for reaction R.1. If this reaction has not occurred, or if there has been Fe-Mg cation exchange between garnet and cordierite during cooling and uplift, this expression yields incorrect and anomalously low values. This method is used only on the few samples where method 1 yielded unreasonably high ($>$ 800°C) temperatures.

Cordierite-Garnet Barometry

Method 1 - Hutcheon *et al.*, (1974)

$$P = \frac{(R \ln K_2 - 22.95) \times 6682.35 - [(R \ln K_1 - 18) \times (-9035.73)]}{3.825 \times (R \ln K_1 - 18) - 3.648 \times (R \ln K_2 - 22.95)}$$

where K_1 and K_2 are as in cordierite-garnet thermometry method 2 and R is the universal gas constant.

The equation presented here provides results which compare favorably with pressure limits estimated from other methods (such as recalculated stratigraphic thicknesses). This is true in spite of the fact that this method is based on thermodynamic data for reaction R.1 only. (It requires the assemblage garnet-cordierite-sillimanite-quartz.) Though the exact reasons are not clear at this time, this method appears to work as an Fe-Mg cation exchange barometer for any cordierite-garnet assemblage, whether or not sillimanite is part of the equilibrium assemblage. All of the pressures listed in table 3 and shown in figures 26 and 27 were calculated from this expression.

Method 2 - Holdaway and Lee (1977)

This data set allows the simultaneous derivation of P_{load}, X_{H_2O} and T based on the composition of cordierite in the presence of a total assemblage cordierite-garnet-biotite-sillimanite-quartz-plagioclase-alkali feldspar-melt. In assemblages where one or more of these phases is absent, an estimate of X_{H_2O} and T are required in order to interpolate P_{load}. See Holdaway and Lee (1977) and Lee and Holdaway (1977) for further discussion.

Pressures obtained by these methods generally agree within 300 bars for $M_{2.1}$. This method is not applicable to $M_{2.2}$, because the reactions which occurred were not those studied by Holdaway and Lee (1977).

DISCUSSION

The temperatures shown in appendix D were calculated using biotite-garnet and cordierite-garnet. Pressures were calculated using cordierite-garnet data only. The presented analyses are averages of a number of analyses (the number used is in parentheses), making the pressures and temperatures average values as well. In the case of sample M-59, the temperature of $M_{2.1}$ is based on selected individual mineral pairs because of a large spread in the data and the resulting difficulty in averaging.

The data, presented in table 3 in the first two columns of $M_{2.1}$ and $M_{2.2}$ respectively, represent best estimates for peak temperatures and pressures. Data in the second two columns for each event are values recorded by averaged data and represent P and T intermediate between $M_{2.1}$ and $M_{2.2}$ or $M_{2.2}$ and $M_{2.3}$.

Based on this, peak conditions for $M_{2.1}$ were 740 $\pm$ 30°C, 5.0 $\pm$ 0.7 kbar and $X_{H_2O} \leq 0.4$. Many samples yield P and T values intermediate between the peak $M_{2.1}$ and $M_{2.2}$ conditions, reflecting slow continuous Fe-Mg exchange between biotite, cordierite and garnet. $M_{2.2}$ is defined as the closure of Fe-Mg exchange between cordierite and garnet at P = 3.0 $\pm$ 0.3 kbar, T = 555 $\pm$ 55°C, $X_{H_2O} \geq 0.4$. Biotite and garnet continued to re-equilibrate and exchange Fe-Mg to temperatures as low as 380°C, conditions intermediate between $M_{2.2}$ and $M_{2.3}$ (where $M_{2.3}$ is defined by closure of Ar loss in biotite). The exact P-T conditions associated with $M_{2.3}$ are unknown, because they are also a function of f_{Ar} in the metamorphic fluid. Estimates for the closure temperature range from 225°C to 300°C (Harrison *et al.*, 1979). The temporal framework for $M_{2.1}$ - $M_{2.3}$ is shown schematically in figure 30.

GEOLOGICAL AND METAMORPHIC HISTORY: A SUMMARY

The geological history of the area can be divided into two principal episodes, Archean and Aphebian. These episodes are correlated with metamorphic events. Two cycles of metamorphism can be distinguished. The second cycle can be further subdivided into three stages in certain areas.

ARCHEAN

Field relationships show that the granite gneisses and associated (partly pelitic) metasediments are the oldest rocks in the area. The relative antiquity of these rocks is further substantiated by geochronological work in the Charles Lake area, which proved the existence of an Archean basement complex of gneisses, metasedi-

TABLE 3.
Pressure (kbar) and Temperature (°C) conditions for M_2 mineral pairs based on chemical data and calculations presented in appendix D

Sample Number	$M_{2.1}$				$M_{2.2}$			
	T	P	T	P	T	P	T	P
409	-	-	-	-	580	3.1	380	-
M-10A	-	-	-	-	535	2.7	-	-
M-13A	-	-	630	3.3	550	2.8	-	-
M-13B	710	4.0	620	-	580	3.1	-	-
M-24	700	4.9	630	3.5	-	-	400	-
M-25	710	4.3	-	-	590	3.5	-	-
M-36A	715	4.4	620	3.6	575	-	-	-
M-40	-	-	670	4.0	530	2.9	-	-
M-47	750	4.5	-	-	600	3.4	-	-
M-48	740	5.6	670	-	-	-	-	-
M-53	760	5.0	-	-	540	3.0	490	
M-54	705	4.3	625	3.7	510	-	-	-
M-55A	710	-	615	-	-	-	-	-
M-57A	775	4.8	-	-	590	3.2	-	-
M-59	760	4.8	680	4.2	530	-	420	-
M-60A	740	5.3	-	4.6	540	-	440	-
M-60C	-	-	640	3.7	510	2.8	460	-
M-63	735	5.7	700	4.6	520	-	-	-
M-65	700	4.0	625	-	590	3.3	-	-
M-66	745	4.3	680	3.7	510	-	-	-
M-67	-	-	-	-	580	-	-	-
M-68	770	5.0	615	3.9	-	-	-	-
M-71	-	-	630	3.9	530	-	-	-

ments and granitoids (Baadsgaard and Godfrey, 1972). This information indicates that even in Archean times, distinction can be made between an infrastructure and a superstructure. The relatively low initial $^{87}Sr/^{86}Sr$ ratio (0.7030) of the pegmatites points to I-type granitoids (White and Chappell, 1977) which were derived from igneous source rocks, and may also include original upper mantle material.

First Cycle of Metamorphism (M_1)

The Archean basement complex of northeastern Alberta was extensively remobilized and metamorphosed during the Aphebian. Only a few probable Archean minerals can be recognized in metasediments, Slave Granitoids, and Thesis Lake Granitoids. The M_1 phase of metamorphism in the granulite facies, characterized by the relict minerals hypersthene, sillimanite, green spinel, and corundum, is tentatively assigned to the Archean. Temperature and pressure estimates for this mineral assemblage are 900 ± 100°C and 7.5 ± 2 kbar (Hensen and Green, 1973; Ganguly, 1972). The hypothesis that a subsequent moderate pressure granulite event, that produced cordierite, garnet, sillimanite, and quartz, is of Archean age (Nielsen, 1979) can no longer be maintained. This modification is indicated by a whole rock Rb/Sr date of 1938 Ma for the Slave granitoids in the Tulip Lake area. (Nielsen *et al.*, 1981). This age dates the formation of the Slave Granitoids by ultrametamorphism, and consequently also dates the metamorphism of the metasediments enclosed by the granitoids. It follows that the moderate pressure granulite facies event which was the main phase of metamorphism in the Tulip Lake area is not Archean.

APHEBIAN

The Aphebian is characterized by widespread metamorphism and remobilization of the basement which resulted in the formation of granitoids by ultrametamorphism. These granitoid bodies were subsequently emplaced higher in the crust as illustrated by the process of diapiric doming in the Tulip Lake and Wylie Lake areas.

Second Cycle of Metamorphism (M_2)

The metasediments provide the best record of the metamorphic history. They show a gradual cooling and release of pressure during Aphebian times. This

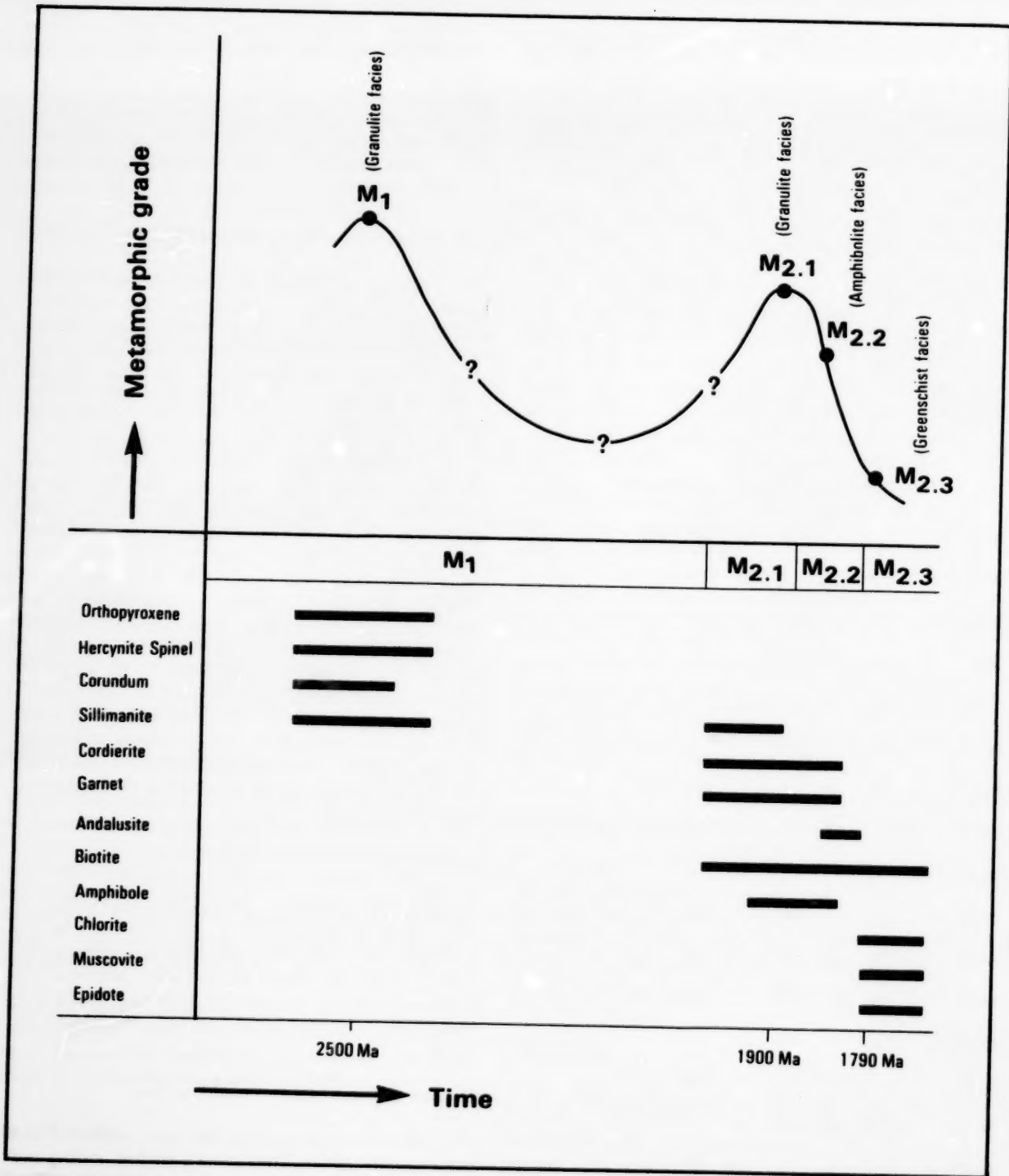

FIGURE 30. Path of metamorphism and related mineral growth in the Canadian Shield, north of Lake Athabasca. Phase M_1, $M_{2.1}$ and $M_{2.3}$ are fixed by isotope dating techniques. The age of phase $M_{2.2}$ is estimated at 30 to 40 million years after $M_{2.1}$.

retrograde path of metamorphism is probably related to uplift and erosion. Temperature and pressure estimates for phase $M_{2.1}$ are T = 740 ± 30°C and P = 5.0 ± 0.7 kbar and for phase $M_{2.2}$ T = 550 ± 55°C and P = 3.0 ± 0.3 kbar.

The uplift has not been uniform over the whole area, as indicated by diapiric doming structures and the slightly higher temperatures and pressures during $M_{2.1}$ in the Tulip Lake area. The Tulip Lake area may well represent an originally deeper crustal level. This could also explain why there are generally more supracrustal gneisses and metasediments in the eastern than in the western part of the area (fig. 2).

The sediments of the Waugh Lake and Burntwood Groups may have been derived from this possible differential uplift. It is uncertain what happened between the Archean high pressure granulite facies (M_1) and the Aphebian moderate pressure granulite facies ($M_{2.1}$). It is plausible to suggest that $M_{2.1}$ is a second cycle of metamorphism within the Aphebian Athabasca mobile belt. Most of the high-grade metasediments of the area, and possibly also the granitoids, show a three stage cooling ($M_{2.1} \rightarrow M_{2.2} \rightarrow M_{2.3}$). The slightly higher grade of metamorphism in the Tulip Lake area can be explained by a more rapid uplift during doming.

The high P-T conditions calculated for $M_{2.1}$ were sufficient to generate anatectic granitoids, such as the Slave Granitoids on a large scale. The Slave Granitoids give a Rb/Sr whole rock age of 1938 ± 28 Ma with an initial $^{87}Sr/^{86}Sr$ ratio of 0710 ± 0.002. Scatter around the isochron indicates that complete homogeneity was not obtained. In this case, the data over-estimates the age of formation of these granitoids slightly (H. Baadsgaard, pers. comm.). The formation of the Slave Granitoids is now estimated to have occurred about 1900 Ma ago (Nielsen *et al.*, 1981). This provides a maximum age for the $M_{2.1}$ event recorded by the enclosed metasediments. The age of phase $M_{2.2}$ is estimated at 30 to 40 million years after $M_{2.1}$. Because of the equivalent age relationships of metamorphic minerals in the Slave Granitoids and the metasediments, the Slave Granitoids are assumed to have undergone the same retrograde path of metamorphism. All other granitoids in northeastern Alberta lack the characteristic mineralogy of the Slave Granitoids. The presence of garnet and amphibole, and high initial Sr ratios (for example, 0.7083 for the Colin Lake Granitoids), indicate that the other granitoids were also formed by ultrametamorphism of supercrustal material. The temperature and pressure constraints suggest that they were formed during $M_{2.1}$. Doming in the Wylie Lake area was probably active during this event.

The domes have elliptical outcrop patterns and are elongated in a NNE — SSW direction. Some macroscopic folds have similar trends and may be genetically related to the doming (Langenberg and Ramsden, 1980). Such elongation indicates an ESE — WNW directed compressional deformation during M_2.

Continued uplift and erosion resulted in a retrograde shift to greenschist facies conditions ($M_{2.3}$). The degree of equilibration was varied. Mylonites, formed along fault zones, were completely retrogressed to greenschist facies. In other areas with less deformation, the rocks were less affected by this metamorphism. The K-Ar systems of all micas were reset during this $M_{2.3}$ event, as indicated by the average date of many mica samples of 1790 ± 40 Ma. This data spread is only slightly greater than if a single mica sample had been run repeatedly (Baadsgaard and Godfrey, 1972, p. 889). The path of metamorphism and related mineral growth is represented schematically in figure 30.

Metasediments and metavolcanics of the Waugh Lake and Burntwood Groups show metamorphic minerals characteristic of greenschist facies conditions. An unconformity has to be assumed between these low-grade metasediments and the adjacent higher-grade rocks. The continued uplift in the areas of sedimentation must have ended temporarily and subsidence must have taken place in order to explain the prograde nature of the greenschist facies in the low-grade metasediments. A K/Ar age of 1760 Ma for biotite from a metavolcanic rock of the Waugh Lake band correlates the prograde greenschist facies with the retrograde greenschist facies elsewhere in the area.

Dynamo-metamorphic effects are also evident in the low-grade metasediments where phyllites, schists and mylonites have been derived from impure quartzites and meta-arkoses.

The K-Ar dating, combined with the field observations noted above, identifies the period of large scale faulting and accompanying mylonitization as Late Hudsonian. This faulting ties in with collision tectonics between the Slave and Churchill cratonic blocks (Gibb, 1978).

During continued uplift and erosion, continental conditions of sedimentation prevailed, and sandstones of the Helikian Athabasca Formation now lie unconformably on the older crystalline basement rocks.

REFERENCES

Baadsgaard, H., and J.D. Godfrey (1967): Geochronology of the Canadian Shield in northeastern Alberta, I. Andrew Lake area; Canadian Journal of Earth Sciences, Vol. 4, p. 541-563.

Baadsgaard, H., and J.D. Godfrey (1972): Geochronology of the Canadian Shield in northeastern Alberta, II: Charles-Andrew-Colin Lakes area; Canadian Journal of Earth Sciences, Vol. 9, p. 863-881.

Breaks, F.W., W.D. Bond, J.R. Bartlett, and F. Facca (1978): The English River Subprovince, an Archean gneissic belt; Toronto '78 — Joint annual meeting of the Geological Association of Canada and the Geological Society of America, Field Trips Guidebook, p. 220 - 236.

Brown, R.L., I.W.D. Dalziel and B.R. Rust (1969): The structure, metamorphism, and development of the Boothia Arch, Arctic Canada; Canadian Journal of Earth Sciences, Vol. 6, p. 525-543.

Burwash, R.A., and R.R. Culbert (1976): Multivariate geochemical and mineral patterns in the Precambrian basement of western Canada; Canadian Journal of Earth Sciences, Vol. 13, p. 1-18.

Carmichael, I.S.E., F.J. Turner and J. Verhoogen (1974): Igneous petrology; McGraw-Hill, 739 pages.

Davidson, A. (1972): The Churchill Province; *in* Variations in tectonic styles in Canada, The Geological Association of Canada, Special Paper 11, p. 381-434.

Day, W. (1975): Zircon geochronology in northeastern Alberta; unpublished M.Sc. thesis, University of Alberta, 72 pages.

Dixon, J.M. (1975): Finite strain and progressive deformation in models of diapiric structures; Tectonophysics,Vol. 38, p. 89-124.

Eskola, P. (1952): On the granulites of Lapland; American Journal of Science, Bowen Volume, p. 133-171.

Ferry, J.M., and F.S. Spear (1978): Experimental calibration of the partitioning of Fe and Mg between biotite and garnet; Contributions to Mineralogy and Petrology, Vol. 66, p. 113-117.

Ganguly, J. (1972): Staurolite stability and related parageneses: theory, experiments and applications; Journal of Petrology, Vol. 13, p. 335-365.

Gibb, R.A. (1979): Slave-Churchill collision tectonics; Nature , 271, p. 50-52.

Godfrey, J.D. (1958a): Aerial photographic interpretation of Precambrian structures, north of Lake Athabasca; Research Council of Alberta, Bulletin 1, 19 pages.

———(1958b): Mineralization in the Andrew, Waugh and Johnson Lakes area, northeastern Alberta; Research Council of Alberta, Preliminary Report 58-4, 17 pages.

———(1961): Geology of the Andrew Lake, north district, Alberta; Research Council of Alberta, Preliminary Report 58-3, 32 pages.

———(1963): Geology of the Andrew Lake, south district, Alberta; Research Council of Alberta, Preliminary Report 61-2, 30 pages.

———(1966): Geology of the Bayonet, Ashton, Potts, and Charles Lake districts, Alberta; Research Council of Alberta, Preliminary Report 65-6, 45 pages.

———(1970): Geology of the Marguerite River district, Alberta; Alberta Research Council Map (scale 1 inch to 1 mile).

———(1980a): Geology of the Alexander-Wylie Lakes district; Alberta Research Council, Earth Sciences Report 78-1, 26 pages.

———(1980b): Geology of the Fort Chipewyan district; Alberta Research Council, Earth Sciences Report 77-3, 20 pages.

Godfrey, J.D., and C.W. Langenberg (1979): Metamorphism in the Canadian Shield of northeastern Alberta; *in* Metamorphism of the Canadian Shield; Geological Survey of Canada, Paper 78-10, p. 129-138.

Godfrey, J.D., and E.W. Peikert (1963): Geology of the St. Agnes district, Alberta; Research Council of Alberta, Preliminary Report 62-1, 31 pages.

———(1964): Geology of the Colin Lake district, Alberta; Research Council of Alberta, Preliminary Report 62-2, 28 pages.

Godfrey, J.D., and R.Y. Watanabe (1973): The mineralogical composition of an area of Precambrian Shield in northeastern Alberta, Canada; Proceedings 22nd International Geological Congress, New Delhi 1964, part 16, p. 300-328.

Harris, N.B.W. (1976): The significance of garnet and cordierite from the Sioux Lookout region, English River gneiss belt, northern Ontario; Contributions to Mineralogy and Petrology, Vol. 55, p. 91-104.

Harrison, T.M., R.L. Armstrong, C.W. Naeser and J.E. Harakal (1979): Geochronology and thermal history of the Coast Plutonic Complex, near Prince Rupert, British Columbia; Canadian Journal of Earth Sciences, Vol. 16, p. 400-410.

Henderson, J.F. (1939): Nonacho Lake; Geological Survey of Canada, Map 526A (scale 1 inch to 4 miles).

Hensen, B.J. and D.H. Green (1973): Experimental study of the stability of cordierite and garnet in pelitic compositions at high temperatures and pressures, Part III. Synthesis of experimental data and geological applications; Contributions to Mineralogy and Petrology, Vol. 38, p. 151-166.

Hicks, H.S. (1932): The geology of the Fitzgerald and northern portion of the Chipewyan map areas, northern Alberta, Canada; unpublished Ph.D. thesis, University of Minnesota, 82 pages.

Hobbs, B.E., W.D. Means and P.F. Williams (1976): An outline of structural geology; John Wiley and Sons, 571 pages.

Holdaway, M.J., and S.M. Lee (1977): Fe-Mg cordierite stability in high-grade pelitic rocks based on experimental, theoretical, and natural observations; Contributions to Mineralogy and Petrology, Vol. 63, p. 175-198.

Hutcheon, I., E. Froese and T.M. Gordon (1974): The assemblage quartz-sillimanite-garnet-cordierite as an indicator of metamorphic conditions in the Daly Bay Complex, N.W.T.: Contributions to Mineralogy and Petrology, Vol. 44, p. 29-34.

Kerrich, R., and I. Allison (1978): Flow mechanisms in rocks; Geoscience Canada, Vol. 5, p. 109-118.

Klewchuk, P. (1972): Mineralogy and petrology of some granitic rocks in the Canadian Shield north of Fort Chipewyan, Alberta; unpublished M.Sc. thesis, University of Calgary, 134 pages.

Koster, F. (1971): Geological investigations in the Tazin Lake region, northwest Saskatchewan, Canada; Proceedings of the Koninkliike Nederlandse Akademie van Wetenschappen, Series B, Physical Sciences, Vol. 74, p. 63-92.

Koster, F., and H. Baadsgaard (1970): On the geology and geochronology of northwestern Saskatchewan. I. Tazin Lake region; Canadian Journal of Earth Sciences, Vol. 7, p. 919-930.

Kuo, S.L. (1972): Uranium-lead geocronology in the Charles Lake area; unpublished M.Sc. thesis, University of Alberta, 126 pages.

Langenberg, C.W. (1972): Polyphase deformation in the eastern Sierra de los Filabres north of Lubrin, SE Spain; GUA Papers of Geology, Series 1, No. 2, 81 pages.

———(in preparation): Polyphase deformation in the Canadian Shield of northeastern Alberta; Alberta Research Council Bulletin.

Langenberg, C.W., and J. Ramsden (1980): The geometry of folds in granitoid rocks of northeastern Alberta; Tectonophysics, Vol. 66, p. 269-285.

Lee, S.M., and M.J. Holdaway (1977): Significance of Fe-Mg cordierite stability relations on temperature, pressure, and water pressure in cordierite granulites; Geophysical Monographs 20, American Geophysical Union, p. 79-94.

Nielsen, P.A. (1977): Mineralogy and metamorphic petrology of the Arseno Lake area, N.W.T.; unpublished Ph.D. thesis, University of Alberta, 227 pages.

Nielsen, P.A. (1979): Fe-Mg cation exchange thermobarometry of polymetamorphic rocks from the Precambrian Shield of northeastern Alberta; Current Research, Part A, Geological Survey of Canada, Paper 79-1A, p. 133-137.

Nielsen, P.A., C.W. Langenberg, H. Baadsgaard and J.D. Godfrey (1981): Precambrian metamorphic conditions and crustal evolution, northeastern Alberta, Canada; Precambrian Research, Vol. 16, p. 171-193.

Peikert, E.W. (1961): Petrological study of a group of porphyroblastic rocks in the Precambrian of northeastern Alberta; unpublished Pn.D. thesis, University of Illinois, 151 pages.

———(1963): Biotite variation as a guide to petrogenesis of granitic rocks in the Precambrian of northeastern Alberta; Journal of Petrology, Vol. 4, p. 432-459.

Reinhardt, E.W. (1969): Geology of the Precambrian rocks of Thubun Lakes map-area in relationship to the McDonald Fault System, District of Mackenzie; Geological Survey of Canada, Paper 69-21, 29 pages.

Riley, G.C. (1960): Geology, Fort Fitzgerald, Alberta; Geological Survey of Canada, Map 12-1960 (scale 1 inch to 4 miles).

Scott, B.P. (1978): The geology of an area east o Thluicho Lake, Saskatchewan; Saskatchewa Department of Mineral Resources, Report 167, 5 pages.

Spry, A. (1969): Metamorphic textures; Pergamon Press, 350 pages.

Thompson, A.B. (1976): Mineral reactions in pelitic rocks. II. Calculation of some P-T-X (Fe-Mg) phase relations; American Journal of Science, Vol. 276, p. 285-308.

Turner, F.J. (1968): Metamorphic petrology; McGraw-Hill, 403 pages.

Watanabe, R.Y. (1961): Geology of the Waugh Lake metasedimentary complex, northeastern Alberta; unpublished M.Sc. thesis, University of Alberta, 89 pages.

———(1965): Petrology of cataclastic rocks of north eastern Alberta; unpublished Ph.D. thesis, University of Alberta, 219 pages.

White, A.J.R., and B.W. Chappell (1977): Ultrametamorphism and granitoids genesis; Tectonophysics, Vol. 43, p. 7-22.

Winkler, H.G.F. (1967): Petrogenesis of metamorphic rocks; 2nd edition, Springer-Verlag, 237 pages.

Zwart, H.J. (1960): Relations between folding and metamorphism in the central Pyrenees, and their chronological succession; Geologic en Mijnbouw, Vol. 22, p. 163-180.

APPENDIXES A, B and C

ABBREVIATION CODES:

Minerals:

AM - Amphibole
AN - Andalusite
BI - Biotite
CD - Cordierite
CL - Chlorite
CP - Clinopyroxene
CR - Corundum
EP - Epidote
GA - Garnet
KF - Alkali-feldspar
MU - Muscovite
OP - Orthopyroxene
SI - Sillimanite
SP - Spinel
TO - Tourmaline

Rock Units:

100 - Slave Granitoids
110 - Thesis Lake Granitoids
120 - Colin Lake Granitoids
130 - Wylie Lake Granitoids
160 - Arch Lake Granitoids
170 - Charles Lake Granitoids

APPENDIX A

Inventory of Metamorphic Minerals in Metasediments (North of Lake Athabasca)
See figure 4 for locations

Sample Number	Metamorphic Minerals													
	OP	CP	SP	CR	SI	GA	CD	AM	AN	KF	BI	MU	CL	E
M-1	-	-	-	-	x	-	x	-	-	x	x	x	-	
M-2	-	-	-	-	x	x	x	-	-	-	-	x	-	
M-3A	-	-	x	-	x	x	x	-	x	x	x	x	-	
M-3B	-	-	-	-	-	-	-	x	-	x	x	x	x	x
M-4	-	-	-	-	x	-	-	-	-	x	x	x	-	
M-5	-	-	-	-	-	x	-	-	-	x	x	x	x	
M-6	-	-	-	-	x	-	-	-	-	x	x	x	x	
M-7	-	-	-	-	x	x	-	-	-	-	x	x	x	
M-8	-	-	-	-	x	-	-	-	-	-	x	x	x	x
M-9	-	-	-	-	x	x	-	-	-	-	x	-	-	
M-10A	-	-	-	-	-	x	x	-	-	-	x	x	x	
M-10B	x	-	-	-	-	-	-	-	-	x	x	-	-	
M-11	-	-	-	-	-	-	-	-	-	-	-	x	x	x
M-12	-	-	-	-	-	-	-	x	-	x	x	-	x	x
M-13A	-	-	-	-	x	x	x	-	x	x	x	x	-	
M-13B	-	-	-	-	x	x	x	-	x	-	x	x	x	
M-14	-	-	-	-	-	x	-	x	-	x	x	-	x	x
M-15	-	-	-	-	x	x	x	-	-	-	x	x	-	
M-16	x	-	-	-	-	-	-	x	-	-	x	x	-	
M-17	-	-	-	-	-	-	-	-	x	-	x	x	x	
M-18	-	-	-	-	x	x	x	-	-	x	x	x	x	
M-19	-	-	-	-	-	x	x	-	-	x	x	x	x	
M-20	-	-	-	-	-	-	x	-	x	x	-	-	x	
M-21	-	-	-	-	-	-	x	x	-	-	x	x	-	x

Sample Number	Metamorphic Minerals													
	OP	CP	SP	CR	SI	GA	CD	AM	AN	KF	BI	MU	CL	EP
M-22	-	-	-	-	-	x	x	-	-	x	x	x	x	-
M-23	-	-	-	-	x	-	-	-	-	-	x	x	x	-
M-24	-	-	x	-	x	x	x	-	-	x	x	x	-	-
M-25	-	-	x	-	-	x	x	-	-	x	x	-	x	-
M-26	x	-	-	-	-	-	-	-	-	x	x	-	-	-
M-27	-	-	-	-	-	x	-	-	-	x	x	x	x	-
M-28	x	x	-	-	-	-	-	x	-	-	x	x	-	-
M-29	-	-	-	-	-	-	-	-	x	-	x	x	x	-
M-30	-	-	-	-	-	-	-	x	-	x	x	-	x	-
M-31	-	-	-	-	x	x	-	-	-	x	x	-	-	-
M-32	-	-	-	-	-	-	-	x	-	x	x	-	-	-
M-33	-	-	-	-	-	x	-	x	-	-	-	-	-	-
M-34	x	x	-	-	-	-	-	x	-	-	x	-	-	-
M-35	-	-	-	-	-	-	-	x	-	-	x	-	-	-
M-36A	-	-	-	-	x	x	x	-	-	x	x	-	-	-
M-36B	x	-	-	-	-	-	-	-	-	-	-	x	x	x
M-37	-	-	-	-	x	x	x	-	-	x	x	x	x	x
M-38	-	-	-	-	-	-	-	-	-	x	x	-	x	x
M-39	-	-	-	-	-	x	-	-	-	-	x	x	x	-
M-40	-	-	-	-	x	x	x	-	-	x	x	x	x	-
M-41	-	-	-	-	-	x	-	-	-	x	x	x	x	-
M-42	-	-	x	-	x	x	x	-	-	x	x	x	x	-
M-43	-	-	-	-	x	x	-	-	x	x	x	x	-	-
M-44	-	-	-	-	-	x	-	-	-	x	x	x	-	-
M-45	-	-	-	-	-	-	-	-	-	x	x	x	x	-

APPENDIX A (continued)

Sample Number	Metamorphic Minerals													
	OP	CP	SP	CR	SI	GA	CD	AM	AN	KF	BI	MU	CL	EP
M-46	-	-	-	-	-	-	-	x	-	x	x	x	x	-
M-47	-	-	-	-	x	x	x	-	-	x	x	-	-	-
M-48	-	-	x	-	x	x	x	-	-	x	x	x	-	-
M-49	-	-	-	-	-	x	-	-	-	x	x	-	x	-
M-50	-	-	-	-	-	x	-	-	-	x	x	x	x	-
M-51	-	-	-	-	x	x	x	-	-	x	x	x	-	-
M-52	-	-	-	-	-	x	x	-	-	x	x	x	-	-
M-53	-	-	-	-	x	x	x	-	-	x	x	x	-	-
M-54	-	-	-	-	x	x	x	-	-	x	x	x	x	-
M-55A	-	-	-	-	-	x	x	-	-	x	x	-	-	-
M-55B	-	-	x	x	x	x	-	-	x	x	x	x	-	-
M-56	x	-	-	-	-	-	-	-	-	x	x	-	-	-
M-57A	-	-	x	x	x	x	x	-	-	x	x	x	x	-
M-57B	x	-	-	-	-	x	-	-	-	x	x	x	x	-
M-58	-	-	-	-	x	x	x	-	-	x	x	x	-	-
M-59	-	-	x	-	-	x	x	-	-	x	x	-	-	-
M-60A	-	-	x	-	x	x	x	-	-	x	x	-	-	-
M-60B	x	-	-	-	-	-	-	-	-	-	x	x	-	-
M-60C	-	-	x	-	x	x	x	-	-	x	x	x	-	-
M-61	-	-	x	-	x	x	x	-	-	x	x	-	-	-
M-62	-	-	-	-	x	x	-	-	x	-	x	-	-	-
M-63	-	-	x	-	-	x	x	-	-	x	x	-	-	-
M-64	x	-	-	-	-	-	-	x	-	x	x	x	-	-
M-65	-	-	x	x	x	x	x	-	-	-	x	x	-	-
M-66	-	-	-	-	x	x	x	-	-	x	x	-	x	x

Sample Number	Metamorphic Minerals													
	OP	CP	SP	CR	SI	GA	CD	AM	AN	KF	BI	MU	CL	EP
M-67	-	-	x	-	-	x	x	-	-	x	x	x	-	-
M-68	-	-	x	-	x	x	x	-	-	x	-	-	-	-
M-69	-	-	-	-	-	-	-	-	-	-	x	x	x	-
M-70	x	x	-	-	-	-	-	x	-	-	x	-	x	-
M-71	-	-	x	-	x	x	x	-	-	x	x	-	-	-

APPENDIX B

Inventory of Metamorphic Minerals in Granitoids (North of Lake Athabasca)
See figure 13 for locations

Sample Number	Metamorphic Minerals											Rock Unit
	OP	CP	SP	CR	SI	GA	CD	AM	AN	KF	BI	
12	-	-	-	-	-	x	-	-	-	x	-	120
74	-	-	-	-	-	x	-	-	-	x	x	170
127	-	-	-	-	-	x	-	-	-	x	x	170
146	-	-	-	-	-	x	-	-	-	x	x	170
231	-	-	-	-	-	x	-	-	-	x	x	100
240	-	-	-	-	-	x	x	-	-	x	x	100
251	x	x	-	-	-	-	-	-	-	x	x	110
293	-	-	-	-	-	x	-	-	-	x	x	130
297	-	-	-	-	-	x	-	-	-	x	-	130
312	-	-	x	-	-	-	x	-	-	x	-	100
313	-	-	x	x	-	-	x	-	-	x	x	100
322	x	-	-	-	-	-	-	-	-	x	x	100
330	-	-	-	-	-	x	-	-	-	x	x	160

APPENDIX B (continued)

Sample Number	Metamorphic Minerals											Rock Unit
	OP	CP	SP	CR	SI	GA	CD	AM	AN	KF	BI	
334	-	-	-	-	-	x	-	-	-	x	x	160
336	-	-	-	-	-	x	-	-	-	x	x	160
345	-	-	x	-	x	x	-	-	-	x	x	100
347	-	-	x	-	x	x	x	-	-	x	x	100
348	-	-	x	-	x	-	-	-	-	x	x	100
352	-	-	x	-	-	x	x	-	-	x	-	100
355	-	-	-	-	x	x	-	-	-	x	x	100
358	-	-	x	-	-	x	x	-	-	x	x	100
359	-	-	-	-	-	-	x	-	-	x	-	100
363	-	-	-	-	-	x	-	-	-	x	x	100
364	-	-	-	-	x	x	-	-	-	x	x	100
373	-	-	x	-	x	-	x	-	x	x	-	100
378	-	-	-	-	-	x	-	-	-	x	x	160
389	x	-	-	-	-	-	-	-	-	x	x	100
391	-	x	-	-	-	-	-	x	-	x	x	100
392	-	-	-	-	-	x	-	-	-	x	x	160
395	-	-	-	-	-	x	-	-	-	x	x	160
399	-	-	x	x	x	-	x	-	-	x	x	100
403	-	-	-	-	-	x	x	-	-	x	x	100
409	-	-	x	-	x	x	x	-	-	x	x	100
411	-	-	-	-	x	-	-	-	-	x	x	100
414	-	-	-	-	-	x	-	-	-	x	x	160
443	-	-	x	-	x	-	x	-	-	x	x	100
444	-	-	x	x	x	x	x	-	-	x	x	100
447	-	-	x	x	x	x	x	-	-	x	x	100

Sample Number	Metamorphic Minerals											Rock Unit
	OP	CP	SP	CR	SI	GA	CD	AM	AN	KF	BI	
455	-	-	-	-	-	x	-	-	-	x	x	160
456	-	-	-	-	-	x	-	-	-	x	x	160
459	-	-	x	-	x	x	x	-	-	x	x	100
474	-	-	-	-	-	x	-	-	-	x	x	160
479	-	-	-	-	-	x	-	-	-	x	x	160
480	-	-	-	-	-	x	-	-	-	x	x	160
486	-	-	x	x	-	-	x	-	-	x	x	100
487	-	-	-	-	-	x	-	-	-	x	x	160
489	-	-	-	-	-	x	-	-	-	x	x	160
490	-	-	-	-	-	x	-	-	-	x	x	160
492	-	-	-	-	-	x	-	-	-	x	x	160
501	-	-	-	-	-	x	-	-	-	x	x	160
502	-	-	-	-	-	x	-	-	-	x	x	160
506	-	-	-	-	-	x	-	-	-	x	x	160
514	-	-	-	-	-	x	-	-	-	x	x	160
515	-	-	x	-	-	x	x	-	-	x	x	100
517	-	-	-	-	-	x	-	-	-	x	x	160
519	-	-	-	-	-	x	-	-	-	x	x	160
520	-	-	-	-	-	x	-	-	-	x	x	100
532	-	-	x	-	x	x	x	-	-	x	x	100
534	-	-	x	x	-	x	x	-	x	x	x	100
538	-	-	x	-	-	x	x	-	-	x	x	100
539	-	-	x	-	x	-	-	-	-	x	x	100
540	-	-	x	x	x	x	-	-	-	x	x	100
541	-	-	x	-	x	-	x	-	-	x	x	100

APPENDIX B (continued)

Sample Number	Metamorphic Minerals											Rock Unit
	OP	CP	SP	CR	SI	GA	CD	AM	AN	KF	BI	
542	-	-	x	-	x	x	x	-	-	x	x	100
544	-	-	x	-	x	x	-	-	-	x	x	100
548	-	-	-	-	-	x	-	-	-	x	x	160
554	-	-	x	-	x	x	-	-	-	x	x	100
555	-	-	x	-	x	x	x	-	-	x	x	100
556	-	-	-	x	x	x	-	-	-	x	x	100
558	-	-	x	-	-	x	x	-	-	x	x	100
559	-	-	x	-	x	x	x	-	-	x	x	100
562	-	-	x	-	x	x	x	-	-	x	x	100
564	-	-	-	-	-	x	-	-	-	x	x	160
569	-	-	x	-	x	-	x	-	-	x	-	100
572	-	-	x	-	x	x	x	-	-	x	x	100
573	-	-	x	x	x	x	x	-	-	x	x	100
574	-	-	x	-	-	-	x	-	-	x	x	100
577	-	-	x	-	x	x	-	-	-	x	x	100
579	-	-	-	-	-	x	-	-	-	x	x	160
585	-	-	x	-	x	x	-	-	-	x	x	100
586	-	-	x	x	x	x	x	-	-	x	x	100
590	-	-	x	-	x	x	-	-	-	x	x	100
591	-	-	x	-	x	x	x	-	-	x	x	100
592	-	-	x	x	x	x	x	-	-	x	x	100
593	-	-	x	-	x	-	-	-	-	x	x	100
594	-	-	x	-	x	x	x	-	-	x	x	100
596	-	-	-	-	-	x	-	-	-	x	x	160
598	-	-	-	-	-	x	-	-	-	x	x	160

Sample Number	Metamorphic Minerals											Rock Unit
	OP	CP	SP	CR	SI	GA	CD	AM	AN	KF	BI	
600	-	-	x	-	-	x	x	-	-	x	x	100
603	-	-	x	x	x	x	x	-	-	x	x	100
604	-	-	x	-	x	x	-	-	-	x	x	100
605	-	-	x	-	x	x	x	-	-	x	x	100
607	-	-	x	x	x	x	-	-	-	x	x	100
609	-	-	x	x	x	-	x	-	-	x	x	100
610	-	-	x	-	x	x	x	-	-	x	x	100
611	-	-	x	x	x	-	x	-	-	x	x	100
612	-	-	-	-	x	x	x	-	-	x	x	100
624	-	-	-	-	-	x	-	-	-	x	x	160
631	x	-	-	-	-	-	-	-	-	x	x	100

APPENDIX C

Inventory of Metamorphic Minerals in Granitoid Rocks (South of Lake Athabasca)
(see figure 21 for locations)

Sample Number	Metamorphic Minerals					
	OP	CP	GA	AM	KF	BI
1	-	-	x	-	x	x
2	-	-	-	x	x	x
3	-	-	x	-	x	x
4	x	-	-	-	x	x
5	x	-	-	-	x	x
6	x	x	-	x	-	-
7	-	-	x	-	x	-
8	-	-	x	-	x	-
9	-	-	x	-	x	x
10	-	-	x	-	x	x
11	-	-	x	-	-	x
12	-	-	x	-	x	-
13	-	-	x	-	-	x
14	-	-	x	-	x	x
15	-	-	x	-	x	-

APPENDIX C (continued)

Sample Number	Metamorphic Minerals					
	OP	CP	GA	AM	KF	BI
16	-	-	x	-	x	x
17	-	-	x	-	x	x
18	-	-	x	-	x	-
19	-	-	x	-	x	x
20	-	-	x	-	x	-
21	-	-	x	-	x	-
22	-	-	x	-	x	x
23	-	-	x	-	-	x
24	-	-	x	-	x	x
25	-	-	x	-	x	x
26	-	-	x	-	x	x
27	-	-	x	-	x	x
28	-	-	-	x	-	x
29	-	-	-	x	x	x
30	-	-	-	x	-	x
31	x	-	-	-	-	x
32	-	-	x	-	x	x
33	-	-	x	-	x	x
34	-	-	x	-	x	x
35	-	-	x	-	x	-
36	-	-	x	-	x	x
37	-	-	x	-	x	x
38	-	-	x		x	x
39	-	-	x	-	x	x
40	-	-	x	-	x	x
41	-	-	x	-	x	x
42	-	-	x	-	x	-
43	-	-	x	-	x	-
44	-	-	x	-	x	x
45	x	-	-	-	-	x
46	-	-	x	-	-	x
47	-	-	x	-	x	-
48	-	-	x	-	x	x
49	-	-	-	x	x	x
50	-	-	x	-	x	-
51	x	x	-	-	-	x
52	-	-	x	-	x	x
53	-	-	x	-	x	x
54	-	-	x	-	x	-
55	-	-	x	-	x	-

APPENDIX D

Chemical Analyses, Structural Formulae and
Fe-Mg Cation Exchange Thermometry and Barometry

Abbreviations Codes:

GA(9) average chemical composition of nine analyzed garnet grains

CD(3) average chemical composition of three analyzed cordierite grains

BI(4) average chemical composition of four analyzed biotite grains

T_{HU}
P_{HU} Temperature (°C) and pressure (kbar) estimated from cordierite-garnet pairs according to Hutcheon *et al.* (1974)

$T_{N\text{-}CG}$ Temperature (°C) estimate from cordierite-garnet pairs based on Nielsen (1977)

$T_{N\text{-}BG}$ Temperature (°C) estimate from biotite-garnet pairs following Nielsen (1977)

$T_{F\text{-}BG}$ Temperature (°C) estimate from biotite-garnet pairs following Ferry and Spear (1978)

Sample: 409

mineral index-number	1	2	3	4	5
	GA(9)	CD(2)	BI(4)	GA(1)	BI(4)
SiO_2	38.410	48.650	35.940	37.660	37.750
TiO_2	0.000	0.000	2.490	0.000	2.150
Al_2O_3	21.690	33.280	19.380	20.570	16.090
FeO	38.380	10.030	20.220	38.770	16.260
MnO	1.730	0.140	0.000	1.570	0.000
MgO	3.130	7.800	9.110	2.500	12.770
CaO	0.570	0.000	0.000	0.320	0.000
K_2O	0.000	0.000	9.430	0.000	9.950
Total	103.910	99.900	96.570	101.390	94.970
Si^{4+}	5.986	4.968	5.401	6.045	5.682
Ti	0.000	0.000	0.281	0.000	0.243
Al^{3+}	3.984	4.079	3.433	3.892	2.854
Fe^{2+}	5.002	0.857	2.541	5.204	2.047
Mn	0.230	0.012	0.000	0.215	0.000
Mg	0.727	1.187	2.041	0.549	2.865
Ca	0.095	0.000	0.000	0.055	0.000
K	0.000	0.000	1.808	0.000	1.911
#of anions	24.000	18.000	22.000	24.000	22.000

	mineral pair:		mineral pair:	
R ln K_1	1, 2	-8.158		
R ln K_2	1, 2	18.723		
P_{HU}	1, 2	3.12 kbar		
T_{N-CG}	1, 2	590°		
T_{N-BG}	1, 3	570°	4, 5	391°
T_{F-BG}	1, 3	579°	4, 5	369°

Sample: M-10A

mineral index-number	1	2	3
	GA(4)	CD(2)	BI(3)
SiO_2	36.490	48.470	34.720
TiO_2	0.000	0.000	2.710
Al_2O_3	19.620	31.040	17.230
FeO	36.340	9.790	19.380
MnO	2.400	0.150	0.000
MgO	2.470	7.670	8.480
CaO	0.930	0.000	0.000
K_2O	0.000	0.000	9.160
Total	98.250	97.120	91.680
Si^{4+}	6.049	5.085	5.508
Ti^{4+}	0.000	0.000	0.323
Al	3.883	3.838	3.222
Fe^{2+}	5.038	0.859	2.571
Mn^{2+}	0.339	0.013	0.000
Mg	0.610	1.199	2.005
Ca	0.165	0.000	0.000
K	0.000	0.000	1.854
#of anions	24.000	18.000	22.000

	mineral pair:	
R ln K_1	1, 2	-8.111
R ln K_2	1, 2	21.04
P_{HU}	1, 2	2.68 kbar
$T_{N\text{-}CG}$	1, 2	538°
$T_{N\text{-}BG}$	1, 3	532°
$T_{F\text{-}BG}$	1, 3	532°

Sample: M-13A

mineral index-number	1	2	3	4	5	6
	GA(3)	CD(3)	BI(2)	GA(7)	CD(2)	BI(6)
SiO_2	36.720	46.430	33.810	36.910	47.170	33.830
TiO_2	0.000	0.000	3.170	0.000	0.000	2.920
Al_2O_3	20.520	30.980	17.490	20.610	31.780	17.270
FeO	36.770	10.140	21.350	37.310	9.570	20.540
MnO	1.080	0.080	0.000	1.260	0.060	0.000
MgO	3.070	7.070	8.300	2.640	7.390	8.500
CaO	0.970	0.000	0.000	0.940	0.000	0.000
K_2O	0.000	0.000	9.510	0.000	0.000	9.410
Total	99.130	94.700	93.630	95.970	95.970	92.470
Si^{4+}	5.995	5.013	5.328	6.007	5.006	5.376
Ti^{4+}	0.000	0.000	0.376	0.000	0.000	0.349
Al	3.948	3.942	3.249	3.953	3.975	3.235
Fe^{2+}	5.020	0.916	2.841	5.078	0.849	2.730
Mn^{2+}	0.150	0.007	0.000	0.175	0.005	0.000
Mg	0.747	1.138	1.950	0.640	1.169	2.013
Ca	0.170	0.000	0.000	0.164	0.000	0.000
K	0.000	0.000	1.912	0.000	0.000	1.908
#of anions	24.000	18.000	22.000	24.000	18.000	22.000

	mineral pair:		mineral pair:	
R ln K_1	1, 2	-7.371	4, 5	-8.251
R ln K_2	1, 2	17.933	4, 5	20.259
P_{HU}	1, 2	3.33 kbar	4, 5	2.81 kbar
$T_{N\text{-}CG}$	1, 2	629°	4, 5	552°
$T_{N\text{-}BG}$	1, 3	616°	4, 6	555°
$T_{F\text{-}BG}$	1, 3	639°	4, 6	560°

Sample: M-13B

mineral index-number	1	2	3	4	5	6
	GA(2)	CD(1)	BI(2)	GA(6)	CD(3)	BI(2)
SiO_2	37.560	46.760	33.920	37.490	47.250	34.900
TiO_2	0.000	0.000	3.000	0.000	0.000	2.480
Al_2O_3	21.600	32.100	18.350	21.650	32.350	19.040
FeO	36.890	10.320	21.710	37.650	9.570	21.470
MnO	0.910	0.080	0.000	1.250	0.060	0.000
MgO	3.830	7.000	7.500	3.100	7.730	8.300
CaO	0.880	0.000	0.000	0.900	0.000	0.000
K_2O	0.000	0.000	9.570	0.000	0.000	9.650
Total	101.670	96.260	94.050	102.040	96.960	96.200
Si^{4+}	5.947	4.969	5.321	5.943	4.966	5.324
Ti^{4+}	0.000	0.000	0.354	0.000	0.000	0.326
Al	4.031	4.020	3.393	4.045	4.007	3.423
Fe^{2+}	4.885	0.917	2.848	4.992	0.841	2.739
Mn^{2+}	0.123	0.007	0.000	0.169	0.005	0.000
Mg	0.904	1.109	1.754	0.733	1.211	1.887
Ca	0.149	0.000	0.000	0.153	0.000	0.000
K	0.000	0.000	1.915	0.000	0.000	1.878
#of anions	24.000	18.000	22.000	24.000	18.000	22.000

	mineral pair:		mineral pair:	
R ln K_1	1, 2	-6.921	4, 5	-8.379
R ln K_2	1, 2	15.462	4, 5	18.844
P_{HU}	1, 2	4.04 kbar	4, 5	3.09 kbar
$T_{N\text{-}CG}$	1, 2	712°	4, 5	581°
$T_{N\text{-}BG}$	1, 3	725°	4, 5	581°
$T_{F\text{-}BG}$	1, 3	783°	4, 6	635°

Sample: M-24

mineral index-number	1	2	3	4	5	6
	GA(3)	CD(2)	BI(3)	GA(2)	CD(4)	BI(1)
SiO_2	38.520	48.050	35.790	38.210	48.240	37.360
TiO_2	0.000	0.000	2.570	0.000	0.000	0.930
Al_2O_3	22.380	33.040	19.920	22.220	33.220	19.730
FeO	35.690	9.720	19.170	37.860	9.630	12.900
MnO	0.580	0.030	0.000	0.740	0.020	0.000
MgO	5.210	7.760	9.030	3.770	7.920	14.970
CaO	0.830	0.000	0.000	0.890	0.000	0.000
K_2O	0.000	0.000	9.650	0.000	0.000	8.830
Sum	103.210	98.600	96.130	103.690	99.030	94.72
Si^{4+}	5.941	4.964	5.382	5.933	4.959	5.489
Ti^{4+}	0.000	0.000	0.291	0.000	0.000	0.103
Al	4.068	4.023	3.530	4.066	4.025	3.417
Fe^{2+}	4.604	0.840	2.411	4.916	0.828	1.585
Mn^{2+}	0.076	0.003	0.000	0.098	0.002	0.000
Mg	1.198	1.195	2.024	0.873	1.214	3.278
Ca	0.137	0.000	0.000	0.148	0.000	0.000
K	0.000	0.000	1.851	0.000	0.000	0.000
#of anions	24.000	18.000	22.000	24.000	18.000	22.000

	mineral pair:		mineral pair:	
R ln K	1, 2	-7.381	4, 5	-8.33
R ln K_x	1, 2	12.875	4, 5	16.841
P_{HU}	1, 2	4.90 kbar	4, 5	3.55 kbar
T_{HU}	1, 2	700°		
$T_{N\text{-}CG}$			4, 5	632°
$T_{N\text{-}BG}$	1, 3	738°	4, 6	413°
$T_{F\text{-}BG}$			4, 6	394°

Sample: M-25

mineral index-number	1	2	3	4	5	6
	GA(4)	CD(4)	BI(8)	GA(2)	CD(2)	BI(1)
SiO_2	37.670	45.980	35.810	37.730	47.690	35.200
TiO_2	0.000	0.000	3.150	0.000	0.000	2.640
Al_2O_3	21.780	31.560	17.380	21.700	32.790	17.170
FeO	35.400	8.970	18.400	35.920	7.990	17.440
MnO	0.700	0.030	0.000	0.650	0.030	0.000
MgO	4.660	7.760	9.950	4.170	8.810	10.200
CaO	1.280	0.000	0.000	1.300	0.000	0.000
K_2O	0.000	0.000	9.540	0.000	9.270	
Total	101.490	94.300	94.230	101.470	97.310	91.920
Si^{4+}	5.934	4.960	5.494	5.956	4.957	5.515
Ti^{4+}	0.000	0.000	0.363	0.000	0.000	0.311
Al	4.043	4.013	3.143	4.038	4.017	3.170
Fe^{2+}	4.663	0.809	2.361	4.742	0.694	2.285
Mn^{2+}	0.094	0.003	0.000	0.087	0.003	0.000
Mg	1.094	1.248	2.275	0.981	1.365	2.382
Ca	0.216	0.000	0.000	0.220	0.000	0.000
K	0.000	0.000	1.867	0.000	0.000	1.853
#of anions	24.000	18.000	22.000	24.000	18.000	22.000

	mineral pair:		mineral pair:	
R ln K_1	1, 2	-8.006	4, 5	-10.119
R ln K_2	1, 2	14.450	4, 5	16.734
P_{HU}	1, 2	4.25 kbar	4, 5	3.48 kbar
$T_{N\text{-}CG}$	1, 2	710°	4, 5	590°
$T_{N\text{-}BG}$	1, 3	654°	4, 6	594°
$T_{F\text{-}BG}$	1, 3	691°	4, 6	610°

Sample: M-36A

mineral index-number	1	2	3	4	5	6
	GA(9)	CD(9)	BI(11)	GA(4)	CD(3)	BI(2)
SiO_2	37.650	47.280	34.900	37.260	47.860	35.270
TiO_2	0.000	0.000	3.200	0.000	0.000	3.380
Al_2O_3	20.960	31.560	17.760	21.150	32.690	17.680
FeO	35.080	8.830	19.040	36.390	8.670	17.850
MnO	0.830	0.070	0.000	1.000	0.070	0.000
MgO	4.950	8.050	9.260	3.980	8.180	10.590
CaO	0.830	0.000	0.000	0.840	0.000	0.000
K_2O	0.000	0.000	9.670	0.000	0.000	9.690
Total	100.300	95.790	93.830	100.620	97.470	94.460
Si^{4+}	5.997	5.012	5.411	5.961	4.979	5.397
Ti^{4+}	0.000	0.000	0.373	0.000	0.000	0.389
Al	3.935	3.943	3.245	3.988	4.008	3.189
Fe^{2+}	4.673	0.783	2.469	4.868	0.754	2.284
Mn^{2+}	0.113	0.006	0.000	0.136	0.006	0.000
Mg	1.175	1.272	2.140	0.949	1.268	2.415
Ca	0.142	0.000	0.000	0.144	0.000	0.000
K	0.000	0.000	1.912	0.000	0.000	1.891
#of anions	24.000	18.000	22.000	24.000	18.000	22.000

	mineral pair:		mineral pair:	
R ln K_1	1, 2	-8.357	4, 5	-9.113
R ln K_2	1, 2	13.89	4, 5	16.58
P_{HU}	1, 2	4.40 kbar	4, 5	3.57 kbar
$T_{N\text{-}CG}$	1, 2	717°	4, 5	619°
$T_{N\text{-}BG}$	1, 3	712°	4, 6	574°
$T_{F\text{-}BG}$			4, 6	587°

Sample: M-40

mineral index-number	1	2	3	4	5	6
	GA(3)	CD(3)	BI(4)	GA(2)	CD(1)	BI(2)
SiO_2	37.600	46.920	34.800	37.220	46.400	35.140
TiO_2	0.000	0.000	2.380	0.000	0.000	2.420
Al_2O_3	21.790	32.440	18.670	21.570	32.110	19.280
FeO	35.420	8.910	18.570	37.080	8.370	17.650
MnO	1.460	0.090	0.000	1.880	0.140	0.000
MgO	4.350	7.980	9.420	2.990	8.020	10.350
CaO	0.820	0.000	0.000	0.760	0.000	0.000
K_2O	0.000	0.000	9.480	0.000	0.000	9.830
Total	101.440	96.340	93.320	101.480	95.040	94.670
Si^{4+}	5.939	4.950	5.399	5.938	4.953	5.351
Ti^{4+}	0.000	0.000	0.278	0.000	0.000	0.277
Al	4.056	4.034	3.414	4.056	4.039	3.460
Fe^{2+}	4.679	0.786	2.409	4.944	0.747	2.248
Mn^{2+}	0.196	0.008	0.000	0.255	0.013	0.000
Mg	1.024	1.255	2.178	0.711	1.276	2.349
Ca	0.139	0.000	0.000	0.130	0.000	0.000
K	0.000	0.000	1.876	0.000	0.000	1.910
#of anions	24.000	18.000	22.000	24.000	18.000	22.000

	mineral pair:		mineral pair:	
R ln K_1	1, 2	-8.384	4, 5	-9.568
R ln K_2	1, 2	15.312	4, 5	19.939
P_{HU}	1, 2	3.95 kbar	4, 5	2.85 kbar
$T_{N\text{-}CG}$	1, 2	673°	4, 5	531°
$T_{N\text{-}BG}$	1, 3	652°	4, 6	504°
$T_{F\text{-}BG}$	1, 3	687°	4, 6	499°

Sample: M-47

mineral index-number	1	2	3	4	5	6
	GA(3)	CD(2)	BI(4)	GA(3)	CD(3)	BI(3)
SiO_2	38.000	47.520	35.040	37.720	47.480	35.240
TiO_2	0.000	0.000	3.420	0.000	0.000	2.950
Al_2O_3	21.910	32.690	19.160	21.710	32.510	19.170
FeO	35.620	9.600	19.120	36.980	9.040	18.580
MnO	0.940	0.060	0.000	1.100	0.080	0.000
MgO	4.730	7.610	8.600	3.730	8.090	9.260
CaO	0.970	0.000	0.000	0.980	0.000	0.000
K_2O	0.000	0.000	9.900	0.000	0.000	9.880
Total	102.170	97.480	95.240	102.220	97.200	95.080
Si^{4+}	5.945	4.966	5.345	5.944	4.965	5.367
Ti^{4+}	0.000	0.000	0.392	0.000	0.000	0.338
Al	4.040	4.026	3.445	4.032	4.007	3.441
Fe^{2+}	4.660	0.839	2.439	4.874	0.791	2.367
Mn^{2+}	0.125	0.005	0.000	0.148	0.007	0.000
Mg	1.103	1.185	1.955	0.876	1.261	2.102
Ce	0.163	0.000	0.000	0.165	0.000	0.000
K	0.000	0.000	1.926	0.000	0.000	1.920
#of anions	24.000	18.000	22.000	24.000	18.000	22.000

	mineral pair:		mineral pair:	
R in K_1	1, 2	-7.415	4, 5	-8.804
R in K_2	1, 2	13.884	4, 5	17.221
P_{HU}	1, 2	4.51 kbar	4, 5	3.42 kbar
$T_{N\text{-}CG}$	1, 2	748°	4, 5	610°
$T_{N\text{-}BG}$	1, 3	719°	4, 6	600°
$T_{F\text{-}BG}$	1, 3	750°	4, 6	605°

Sample M-48

mineral index-number	1	2	3	4
	GA(8)	CD(3)	BI(3)	BI(1)
SiO_2	39.010	48.990	36.090	36.490
TiO_2	0.000	0.000	4.500	2.070
Al_2O_3	22.280	33.270	16.920	17.810
FeO	31.950	7.670	17.490	14.550
MnO	0.570	0.060	0.000	0.000
MgO	7.260	8.950	10.200	13.100
CaO	0.990	0.000	0.000	0.000
K_2O	0.000	0.000	9.710	9.430
Total	102.060	98.940	94.910	93.460
Si^{4+}	5.983	4.993	5.480	5.525
Ti^{4+}	0.000	0.000	0.541	0.236
Al	4.027	3.997	3.028	3.178
Fe^{2+}	4.098	0.654	2.221	1.842
Mn^{2+}	0.074	0.005	0.000	0.000
Mg	1.660	1.360	2.309	2.959
Ca	0.163	0.000	0.000	0.000
K	0.000	0.000	1.881	1.821
#of anions	24.000	18.000	22.000	22.000

	mineral pair:		mineral pair:	
R ln K_1	1, 2	-8.905		
R ln K_2	1, 2	10.6		
P_{HU}	1, 2	5.61 kbar		
T_{HU}	1, 2	740°		
$T_{N\text{-}BG}$			1, 4	665°
$T_{F\text{-}BG}$			1, 4	680°

Sample: M-53

mineral index-number	1	2	3	4	5	6
	GA(3)	CD(3)	BI(2)	GA(1)	CD(2)	BI(1)
SiO_2	39.120	48.050	35.400	37.730	48.230	36.580
TiO_2	0.000	0.000	1.950	0.000	0.000	2.270
Al_2O_3	22.490	32.910	18.560	21.550	32.910	18.840
FeO	33.590	8.090	17.320	36.660	8.120	15.950
MnO	0.930	0.050	0.000	1.460	0.060	0.010
MgO	6.200	8.570	10.810	3.420	8.630	11.520
CaO	0.940	0.000	0.000	0.920	0.000	0.000
K_2O	0.000	0.000	9.400	0.000	0.000	9.850
Total	103.270	97.670	93.440	101.740	97.950	95.470
Si^{4+}	5.975	4.975	5.441	5.975	4.979	5.461
Ti^{4+}	0.000	0.000	0.225	0.000	0.000	0.305
Al	4.049	4.016	3.362	4.022	4.005	3.315
Fe^{2+}	4.291	0.700	2.226	4.855	0.701	1.991
Mn^{2+}	0.121	0.004	0.000	0.197	0.005	0.001
Mg	1.411	1.322	2.476	0.807	1.328	2.564
Ca	0.154	0.000	0.000	0.156	0.000	0.000
K	0.000	0.000	1.843	0.000	0.000	1.876
#of anions	24.000	18.000	22.000	24.000	18.000	22.000

	mineral pair:		mineral pair:	
R ln K_1	1, 2	-8.72	4, 5	-10.147
R ln K_2	1, 2	12.123	4, 5	18.868
P_{HU}	1, 2	4.99 kbar	4, 5	3.03 kbar
$T_{N\text{-}CG}$	1, 2	763°	4, 5	541°
$T_{N\text{-}BG}$	1, 3	719°	4, 6	490°
$T_{F\text{-}BG}$			4, 6	483°

Sample: M-54

mineral index-number	1	2	3	4	5	6
	GA(3)	CD(2)	BI(1)	GA(3)	CD(2)	BI(1)
SiO_2	38.560	48.390	35.920	38.230	49.120	36.470
TiO_2	0.000	0.000	3.360	0.000	0.000	3.830
Al_2O_3	22.030	33.000	17.040	21.920	33.490	17.130
FeO	34.470	8.870	17.470	35.620	8.640	15.240
MnO	1.410	0.050	0.000	1.440	0.040	0.000
MgO	4.970	8.450	10.640	4.270	8.720	12.820
CaO	1.100	0.000	0.000	1.090	0.000	0.000
K_2O	0.000	0.000	9.620	0.000	0.000	9.940
Total	102.810	98.760	94.050	102.570	100.010	95.430
Si^{4+}	5.974	4.972	5.502	5.967	4.975	5.452
Ti^{4+}	0.000	0.000	0.387	0.000	0.000	0.431
Al	4.023	3.996	3.076	4.032	3.998	3.018
Fe^{2+}	4.501	0.762	2.238	4.650	0.732	1.905
Mn^{2+}	0.186	0.004	0.000	0.191	0.003	0.000
Mg	1.148	1.294	2.429	0.993	1.317	2.856
Ca	0.183	0.000	0.000	0.182	0.000	0.000
K	0.000	0.000	1.880	0.000	0.000	1.895
#of anions	24.000	18.000	22.000	24.000	18.000	22.000

	mineral pair:		mineral pair:	
R ln K_1	1, 2	-8.395	4, 5	-9.22
R ln K_2	1, 2	14.21	4, 5	16.192
P_{HU}	1, 2	4.29 kbar	4, 5	3.66 kbar
$T_{N\text{-}CG}$	1, 2	706°	4, 5	626°
$T_{N\text{-}BG}$	1, 3	643°	4, 6	512°
$T_{N\text{-}BG}$	1, 3	675°	4, 6	511°

Sample: M-55A

mineral index-number	1	2	3	4
	GA(2)	BI(1)	GA(1)	BI(1)
SiO_2	39.030	36.170	39.010	37.660
TiO_2	0.000	4.310	0.000	2.380
Al_2O_3	21.970	15.070	22.040	15.560
FeO	29.480	13.310	29.860	11.740
MnO	0.450	0.000	0.045	0.000
MgO	8.460	13.370	8.320	15.280
CaO	0.960	0.000	0.950	0.000
K_2O	0.000	9.940	0.000	9.650
Total	100.350	92.170	100.630	92.270
Si^{4+}	6.021	5.570	6.011	5.708
Ti^{4+}	0.000	0.499	0.000	0.271
Al	3.994	2.735	4.003	2.779
Fe^{2+}	3.803	1.714	3.848	1.488
Mn^{2+}	0.059	0.000	0.059	0.000
Mg	1.945	3.069	1.911	3.452
Ca	0.159	0.000	0.157	0.000
K	0.000	1.953	0.000	1.866
#of anions	24.000	22.000	24.000	22.000

	mineral pair:		mineral pair:	
$T_{N\text{-}BG}$	1, 2	707°	3, 4	615°
$T_{F\text{-}BG}$	1, 2	740°	3, 4	620°

Sample: M-57A

mineral index-number	1	2	3	4
	GA(2)	CD(1)	GA(1)	CD(2)
SiO_2	37.900	47.760	37.140	47.520
TiO_2	0.000	0.000	0.000	0.000
Al_2O_3	21.770	32.730	21.430	32.370
FeO	35.560	9.820	37.370	9.510
MnO	1.100	0.090	1.180	0.060
MgO	5.000	7.700	3.220	7.840
CaO	0.610	0.000	0.680	0.000
K_2O	0.000	0.000	0.000	0.000
Total	101.940	98.100	101.000	97.300
Si^{4+}	5.942	4.965	5.945	4.974
Ti^{4+}	0.000	0.000	0.000	0.000
Al	4.023	4.010	4.043	3.994
Fe^{2+}	4.663	0.854	5.003	0.833
Mn^{2+}	0.147	0.008	0.161	0.005
Mg	1.169	1.193	0.768	1.233
Ca	0.102	0.000	0.113	0.000
K	0.000	0.000	0.000	0.000
#of anions	24.000	18.000	24.000	18.000

	mineral pair:		mineral pair:	
R ln K_1	1, 2	-7.304	3, 4	-8.546
R ln K_2	1, 2	13.178	3, 4	18.378
P_{HU}	1, 2	4.80 kbar	3, 4	3.20 kbar
$T_{N\text{-}CG}$	1, 2	776°	3, 4	588°

Sample: M-59

mineral index-number	1	2	3	4	5	6
	GA(9)	CD(7)	BI(2)	GA(3)	CD(5)	BI(3)
SiO_2	37.730	47.570	36.760	37.560	47.470	36.920
TiO_2	0.000	0.000	5.150	0.000	0.000	4.430
Al_2O_3	21.970	33.100	14.980	22.070	33.650	15.880
FeO	34.000	9.210	12.610	35.050	8.410	10.120
MnO	1.050	0.080	0.000	1.160	0.060	0.000
MgO	5.610	7.890	13.750	4.930	8.440	15.740
CaO	0.710	0.000	0.000	0.750	0.000	0.000
K_2O	0.000	0.000	9.860	0.000	0.000	9.870
Total	101.070	97.850	93.110	101.520	98.030	92.960
Si^{4+}	5.928	4.944	5.574	5.908	4.908	5.533
Ti^{4+}	0.000	0.000	0.587	0.000	0.000	0.499
Al	4.068	4.055	2.677	4.091	4.100	2.805
Fe^{2+}	4.468	0.801	1.599	4.610	0.727	1.268
Mn^{2+}	0.141	0.007	0.000	0.155	0.005	0.000
Mg	1.314	1.222	3.108	1.156	1.301	3.516
Ca	0.120	0.000	0.000	0.126	0.000	0.000
K	0.000	0.000	1.907	0.000	0.000	1.887
#of anions	24.000	18.000	22.000	24.000	18.000	22.000

	mineral pair:		mineral pair:	
R ln K_1	1, 2	-7.488	4, 5	-9.026
R ln K_2	1, 2	12.997	4, 5	14.407
P_{HU}	1, 2	4.84 kbar	4, 5	4.16 kbar
$T_{N\text{-}CG}$	1, 2	760° *	4, 5	681°
$T_{N\text{-}BG}$	1, 3	526°	4, 6	420°
$T_{F\text{-}BG}$	1, 3	532°	4, 6	404°

*based on individual mineral analyses, not average analyses.

Sample: M-60A

mineral index-number	1	2	3	4	5	6
	GA(3)	CD(4)	BI(1)	GA(5)	CD(1)	BI(2)
SiO_2	37.920	47.790	37.010	37.660	47.670	37.330
TiO_2	0.000	0.000	4.370	0.000	0.000	3.600
Al_2O_3	22.060	33.040	14.970	21.860	32.850	15.020
FeO	34.690	9.330	13.370	34.180	8.430	10.640
MnO	0.320	0.010	0.000	0.320	0.000	0.000
MgO	5.780	7.970	13.890	5.400	8.560	16.590
CaO	0.670	0.000	0.000	0.630	0.000	0.000
Na_2O	0.000	0.000	0.000	0.000	0.000	0.000
K_2O	0.000	0.000	9.860	0.000	0.000	9.410
Total	101.440	98.140	93.460	100.050	97.510	92.59
Si^{4+}	5.931	4.953	5.607	5.964	4.954	5.615
Ti^{4+}	0.000	0.000	0.498	0.000	0.000	0.407
Al	4.066	4.036	2.673	4.080	4.023	2.663
Fe^{2+}	4.537	0.809	1.694	4.527	0.733	1.338
Mn^{2+}	0.043	0.001	0.000	0.043	0.000	0.000
Mg	1.347	1.231	3.136	1.275	1.326	3.720
Ca	0.112	0.000	0.000	0.107	0.000	0.000
Na	0.000	0.000	0.000	0.000	0.000	0.000
K	0.000	0.000	1.851	0.000	0.000	0.000
#of anions	24.000	18.000	22.000	24.000	18.000	22.000

	mineral pair:		mineral pair:	
R ln K_1	1, 2	-7.624	4, 5	-9.05
R ln K_2	1, 2	11.861	4, 5	13.125
P_{HU}	1, 2	5.29 kbar	4, 5	4.57 kbar
T_{HU}	1, 2	740°	4, 5	719°
$T_{N\text{-}CG}$	1, 3	539°	4, 6	442°
$T_{N\text{-}BG}$	1, 3	560°C	4, 6	431°
$T_{F\text{-}BG}$				

Sample: M-60C

mineral index-number	1	2	3	4	5	6
	GA(4)	CD(1)	BI(2)	GA(4)	CD(1)	BI(1)
SiO_2	37.420	46.530	34.020	37.460	46.650	37.860
TiO_2	0.000	0.000	0.010	0.000	0.000	0.040
Al_2O_3	21.680	31.910	20.700	21.780	32.040	25.240
FeO	37.340	9.040	17.160	38.820	8.440	13.090
MnO	0.470	0.000	0.000	0.660	0.120	0.000
MgO	4.050	7.890	10.530	2.950	8.340	8.840
CaO	0.700	0.000	0.000	0.690	0.000	0.000
K_2O	0.000	0.000	9.730	0.000	0.000	9.820
Total	101.660	95.370	92.150	102.360	95.590	94.890
Si^{4+}	5.925	4.962	5.312	5.931	4.953	5.524
Ti^{4+}	0.000	0.000	0.001	0.000	0.000	0.004
Al	4.046	4.011	3.809	4.064	4.009	4.340
Fe^{2+}	4.944	0.806	2.241	5.140	0.749	1.597
Mn^{2+}	0.063	0.000	0.000	0.089	0.011	0.000
Mg	0.956	1.254	2.451	0.696	1.320	1.922
Ca	0.119	0.000	0.000	0.117	0.000	0.000
Na	0.000	0.000	0.000	0.000	0.000	0.000
K	0.000	0.000	1.938	0.000	0.000	1.828
#of anions	24.000	18.000	22.000	24.000	18.000	22.000

	mineral pair:		mineral pair:	
R ln K_1	1, 2	-8.791	4, 5	-10.251
R ln K_2	1, 2	16.144	4, 5	20.347
P_{HU}	1, 2	3.70 kbar	4, 5	2.76 kbar
$T_{N\text{-}CG}$	1, 2	640°	4, 5	509°
$T_{N\text{-}BG}$	1, 3	564°	4, 5	462°
$T_{F\text{-}BG}$	1, 3	574°	4, 6	449°

Sample: M-63

mineral index-number	1	2	3	4	5	6
	GA(4)	CD(3)	BI(1)	GA(3)	CD(3)	BI(1)
SiO_2	39.010	47.790	36.280	38.280	48.170	37.950
TiO_2	0.000	0.000	3.640	0.000	0.000	3.160
Al_2O_3	22.430	32.740	15.470	21.980	33.080	16.240
FeO	32.080	7.330	13.180	33.160	7.040	11.660
MnO	0.560	0.010	0.000	0.580	0.020	0.000
MgO	7.530	8.790	13.590	6.250	9.080	14.840
CaO	0.910	0.000	0.000	0.000	0.000	0.000
K_2O	0.000	0.000	8.660	0.000	0.000	9.080
Total	102.530	96.660	90.840	101.150	97.410	92.930
Si^{4+}	5.966	4.981	5.613	5.986	4.975	5.679
Ti^{4+}	0.000	0.000	0.424	0.000	0.000	0.366
Al	4.036	4.022	2.821	4.040	4.028	2.864
Fe^{2+}	4.096	0.639	1.705	4.324	0.608	1.468
Mn^{2+}	0.073	0.001	0.000	0.077	0.002	0.000
Mg	1.714	1.366	3.134	1.453	1.399	3.310
Ca	0.149	0.000	0.000	0.154	0.000	0.000
K	0.000	0.000	1.713	0.000	0.000	1.735
#of anions	24.000	18.000	22.000	24.000	18.000	22.000

	mineral pair:		mineral pair:	
R ln K_1	1, 2	-9.027	4, 5	-10.33
R ln K_2	1, 2	10.425	4, 5	12.61
P_{HU}	1, 2	5.66 kbar	4, 5	4.59 kbar
T_{HU}	1, 2	735°		
$T_{N\text{-}CG}$			4, 5	695°
$T_{N\text{-}BG}$	1, 3	633°	4, 6	521°
$T_{F\text{-}BG}$	1, 3	669°	4, 6	525°

Sample: M-65

mineral index-number	1	2	3	4	5
	GA(2)	CD(4)	GA(1)	CD(1)	BI(1)
SiO_2	37.990	47.390	37.680	47.870	34.680
TiO_2	0.000	0.000	0.000	0.000	0.240
Al_2O_3	21.730	32.610	21.990	32.710	22.330
FeO	36.480	9.850	37.450	8.99	18.960
MnO	1.200	0.110	1.330	0.090	0.000
MgO	4.050	7.320	3.620	8.180	8.250
CaO	0.790	0.000	0.750	0.000	0.000
Na_2O	0.000	0.000	0.000	0.000	0.000
K_2O	0.000	0.000	0.000	0.000	9.460
Total	102.240	97.280	102.820	97.840	93.920
Si^{4+}	5.967	4.969	5.915	4.971	5.321
Ti^{4+}	0.000	0.000	0.000	0.000	0.028
Al	4.022	4.030	4.068	4.003	4.038
Fe^{2+}	4.792	0.864	4.916	0.781	2.433
Mn^{2+}	0.161	0.010	0.178	0.008	0.000
Mg	0.948	1.144	0.847	1.266	1.887
Ca	0.133	0.000	0.126	0.000	0.000
Na	0.000	0.000	0.000	0.000	0.000
K	0.000	0.000	0.000	0.000	1.582
#of anions	24.000	18.000	24.000	18.000	22.000

	mineral pair:		mineral pair:	
R ln K_1	1, 2	-7.367	3, 4	-9.027
R ln K_2	1, 2	15.301	3, 4	17.701
P_{HU}	1, 2	4.04 kbar	3, 4	3.31 kbar
$T_{N\text{-}CG}$	1, 2	704°	3, 4	593°
$T_{N\text{-}BG}$			3, 5	626°
$T_{F\text{-}BG}$			3, 5	630°

Sample: M-66

mineral index-number	1	2	3	4	5	6
	GT(3)	CD(1)	BI(1)	GT(1)	CD(2)	BI(2)
SiO_2	39.280	49.850	36.440	38.200	48.430	37.100
TiO_2	0.000	0.000	3.740	0.000	0.000	3.340
Al_2O_3	22.650	33.850	16.580	22.080	32.980	17.070
FeO	36.160	10.540	18.110	36.410	10.450	17.240
MnO	2.490	0.270	0.020	2.570	0.220	0.020
MgO	4.080	7.070	10.430	3.460	7.070	11.530
CaO	0.850	0.000	0.000	0.830	0.000	0.000
Na_2O	0.000	0.000	0.000	0.000	0.000	0.000
K_2O	0.000	0.000	9.730	0.000	0.000	9.910
Total	105.490	101.580	95.030	103.530	99.150	96.210
Si^{4+}	5.969	5.009	5.540	5.950	4.982	5.539
Ti^{4+}	0.000	0.000	0.428	0.000	0.000	0.375
Al	4.057	4.009	2.967	4.060	4.007	3.004
Fe^{2+}	4.596	0.886	2.303	4.743	0.901	2.153
Mn^{2+}	0.322	0.023	0.003	0.341	0.019	0.003
Mg	0.920	1.059	2.364	0.803	1.086	2.566
Ca	0.138	0.000	0.000	0.139	0.000	0.000
Na	0.000	0.000	0.000	0.000	0.000	0.000
K	0.000	0.000	1.887	0.000	0.000	1.888
#of anions	24.000	18.000	22.000	24.000	18.000	22.000

	mineral pair:		mineral pair:	
R ln K_1	1, 2	-6.385	4, 5	-66.89
R ln K_2	1, 2	14.922	4, 5	16.715
P_{HU}	1, 2	4.27 kbar	4, 5	3.68 kbar
$T_{N\text{-}CG}$	1, 2	747°	4, 5	681°
$T_{N\text{-}BG}$	1, 3	590°	4, 6	511°
$T_{F\text{-}BG}$	1, 3	600°	4, 6	510°

Sample: M-67

mineral index-number	1	2	3	4	5
	GA(4)	Plag(1)	Bl(1)	GA(1)	Bl(1)
SiO_2	39.220	58.020	36.880	39.110	37.080
TiO_2	0.000	0.000	3.860	0.000	3.210
Al_2O_3	22.590	26.880	17.900	22.500	18.070
FeO	32.740	0.000	17.400	37.170	16.700
MnO	0.770	0.000	0.000	0.950	0.000
MgO	7.200	0.000	10.740	4.360	11.560
CaO	1.130	8.520	0.000	0.000	0.000
Na_2O	0.000	6.540	0.000	0.000	0.000
K_2O	0.000	0.110	9.550	0.000	9.490
Total	103.650	100.070	96.330	104.090	96.110
Si^{4+}	5.944	10.367	5.487	6.002	5.505
Ti^{4+}	0.000	0.000	0.432	0.000	0.358
Al	4.035	5.660	3.139	4.070	3.162
Fe^{2+}	4.150	0.000	2.165	4.770	2.073
Mn^{2+}	0.099	0.000	0.000	0.124	0.000
Mg	1.627	0.000	2.382	0.997	2.558
Ca	0.184	1.631	0.000	0.000	0.000
Na	0.000	2.266	0.000	0.000	0.000
K	0.000	0.025	1.813	0.000	1.797
#of anions	24.000	32.000	22.000	24.000	22.000

	mineral pair:	
$T_{N\text{-}BG}$	4, 5	553°
$T_{F\text{-}BG}$	4, 5	562°

Sample: M-68

mineral index-number	1	2	3	4
	GA(11)	CD(5)	GA(6)	CD(6)
SiO_2	37.890	47.910	37.630	48.060
TiO_2	0.000	0.000	0.000	0.000
Al_2O_3	21.950	32.880	21.780	33.020
FeO	34.230	8.480	35.230	7.250
MnO	0.560	0.050	0.640	0.030
MgO	6.130	8.680	5.250	9.470
CaO	0.820	0.000	0.870	0.000
Na_2O	0.000	0.000	0.000	0.000
K_2O	0.000	0.000	0.000	0.000
Total	101.580	98.000	101.400	97.830
Si^{4+}	5.916	4.956	5.921	4.952
Ti^{4+}	0.000	0.000	0.000	0.000
Al	4.039	4.008	4.039	4.010
Fe^{2+}	4.470	0.734	4.636	0.625
Mn^{2+}	0.074	0.004	0.086	0.003
Mg	1.427	1.338	1.231	1.454
Ca	0.137	0.000	0.147	0.000
Na	0.000	0.000	0.000	0.000
K	0.000	0.000	0.000	0.000
#of anions	24.000	18.000	24.000	18.000

	mineral pair:		mineral pair:	
R ln K_1	1, 2	-8.674	3, 4	-11.076
R ln K_2	1, 2	12.1	3, 4	14.803
P_{HU}	1, 2	5.00 kbar	3, 4	3.88 kbar
$T_{N\text{-}CG}$	1, 2	765°	3, 4	614°

Sample: M-71

mineral index-number	1	2	3
	GA(7)	CD(2)	BI(3)
SiO_2	37.720	47.730	36.110
TiO_2	0.000	0.000	3.230
Al_2O_3	22.220	33.360	15.610
FeO	36.340	8.150	15.550
MnO	0.810	0.070	0.000
MgO	4.760	8.830	13.140
CaO	0.048	0.000	0.000
K_2O	0.000	0.000	9.460
Total	102.330	98.140	93.100
Si^{4+}	5.901	4.924	5.544
Ti^{4+}	0.000	0.000	0.373
Al	4.097	4.056	2.825
Fe^{2+}	4.754	0.703	1.997
Mn^{2+}	0.108	0.006	0.000
Mg	1.110	1.358	3.007
Ca	0.080	0.000	0.000
K	0.000	0.000	1.853
#of anions	24.000	18.000	22.000

	mineral pair:	
R ln K_1	1, 2	-9.981
R ln K_2	1, 2	15.214
P_{HU}	1, 2	3.85 kbar
$T_{N\text{-}CG}$	1, 2	632°
$T_{N\text{-}BG}$	2, 3	531°
$T_{F\text{-}BG}$	2, 3	535°